

## INFORMATION TO USERS

This manuscript has been reproduced from the microfilm master. UMI films the text directly from the original or copy submitted. Thus, some thesis and dissertation copies are in typewriter face, while others may be from any type of computer printer.

**The quality of this reproduction is dependent upon the quality of the copy submitted.** Broken or indistinct print, colored or poor quality illustrations and photographs, print bleedthrough, substandard margins, and improper alignment can adversely affect reproduction.

In the unlikely event that the author did not send UMI a complete manuscript and there are missing pages, these will be noted. Also, if unauthorized copyright material had to be removed, a note will indicate the deletion.

Oversize materials (e.g., maps, drawings, charts) are reproduced by sectioning the original, beginning at the upper left-hand corner and continuing from left to right in equal sections with small overlaps.

Photographs included in the original manuscript have been reproduced xerographically in this copy. Higher quality 6" x 9" black and white photographic prints are available for any photographs or illustrations appearing in this copy for an additional charge. Contact UMI directly to order.

ProQuest Information and Learning  
300 North Zeeb Road, Ann Arbor, MI 48106-1346 USA  
800-521-0600

**UMI<sup>®</sup>**



University of Alberta

**Single Cell Analysis by Capillary  
Electrophoresis**

by

Zheru Zhang



A thesis submitted to the Faculty of Graduate Studies and research in  
partial fulfillment of the requirements for the degree of Doctor of  
Philosophy

Department of Chemistry  
Edmonton, Alberta

Fall, 2000



National Library  
of Canada

Acquisitions and  
Bibliographic Services

395 Wellington Street  
Ottawa ON K1A 0N4  
Canada

Bibliothèque nationale  
du Canada

Acquisitions et  
services bibliographiques

395, rue Wellington  
Ottawa ON K1A 0N4  
Canada

*Your file* *Votre référence*

*Our file* *Notre référence*

The author has granted a non-exclusive licence allowing the National Library of Canada to reproduce, loan, distribute or sell copies of this thesis in microform, paper or electronic formats.

The author retains ownership of the copyright in this thesis. Neither the thesis nor substantial extracts from it may be printed or otherwise reproduced without the author's permission.

L'auteur a accordé une licence non exclusive permettant à la Bibliothèque nationale du Canada de reproduire, prêter, distribuer ou vendre des copies de cette thèse sous la forme de microfiche/film, de reproduction sur papier ou sur format électronique.

L'auteur conserve la propriété du droit d'auteur qui protège cette thèse. Ni la thèse ni des extraits substantiels de celle-ci ne doivent être imprimés ou autrement reproduits sans son autorisation.

0-612-59703-2

**Canada**

University of Alberta


Library Release Form

Author of thesis: **Zheru Zhang**  
Title of thesis: **Single Cell Analysis by Capillary Electrophoresis**  
Degree: **Doctor of Philosophy**  
Year this Degree Granted: **2000**

Permission is hereby granted to the University of Alberta Library to reproduce single copies of this thesis and to lend or sell such copies for private, scholarly, or scientific research purposes only.

The author reserves all other publication and other rights in association with the copyright in the thesis, and except as hereinbefore provided, neither the thesis nor any substantial portion thereof may be printed or otherwise reproduced in any material form whatever without the author's prior written permission.

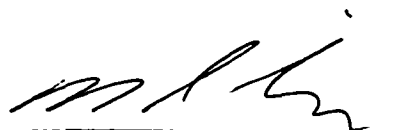
Aug. 25, 2000

  
\_\_\_\_\_  
201-10726 85 AVE  
Edmonton, Alberta  
Canada, T6E 2K8

UNIVERSITY OF ALBERTA

FACULTY OF GRADUATE STUDIES AND RESEARCH

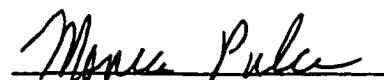
The undersigned certify that they have read, and recommend to the Faculty of Graduate Studies and Research for acceptance, a thesis entitled **Single Cell Analysis by Capillary Electrophoresis** submitted by Zheru Zhang in partial fulfillment of the requirements for the degree of Doctor of Philosophy.




Dr. N. J. Dovichi



Dr. F. F. Cantwell



Dr. M. M. Palcic



Dr. M. T. McDermott



Dr. R. W. Coupland



Dr. R. E. Peter



Dr. D. D. Y. Chen

Date Aug 15, 2000

## **ABSTRACT**

Understanding the molecular mechanisms of many fundamental cell biology processes requires analysis of chemical species within single cell. Development and application of micro-scale analytical techniques such as capillary electrophoresis with laser induced fluorescence detection, and crude cell extract and single cell handling and labeling approaches were presented in this thesis in an effort to address a few of the challenging goals of single cell research.

A single intact cell is injected into the separation capillary. Cellular and organelle membranes are lysed releasing the cellular contents into the separation buffer. High voltage is applied to the injection end of the capillary to separate the contents by electrophoresis.

A simple proteome map was obtained from a HT29 colon adenocarcinoma cell. The protein content was fluorescently labeled with the fluorogenic reagent 3-(2-furoyl)quinoline-2-carboxaldehyde. Several dozen components were resolved. A number of experiments were done to verify that these components were proteins. Protein expression varied significantly between cells, but the average expression was consistent with that observed from a protein extract prepared from  $10^6$  cells. This technique is also correlated cell cycle with oligosaccharide metabolic activity in single cells by measuring DNA ploidy, the uptake of a fluorescent disaccharide, and the amount of metabolic products in a single cell.

Two new approaches to concentrate proteins during the labeling process were discussed in this thesis. The first method combines the concentration of stacking,

reaction efficiency of on-capillary labeling, and the separation efficiency of CZE. The response for selected protein fractions was enhanced through manipulation of sample stacking conditions. The second method presents isotachophoretic stacking of proteins, which is induced by using excess labeling reagent as the leading electrolyte.



**To my Father and in memory of my Mother**

## ACKNOWLEDGEMENTS

The first person I would like to thank is my wife Dinghui, for providing love, moral support, coping with my long working hours during my degree program, and reminding me of the important things in life.

I am deeply grateful to my supervisor, Dr. Norm Dovichi, for introducing me to the world of single cell and the field of separation science, sharing his vast knowledge and never ending enthusiasm. I gained tremendous experience by working under his guidance.

Many thanks to former/present members of Norm's group: Dr. Edgar Arriaga for training me in CE and single cell work. Dr. Sergey Krylov for always being a friend and his carbohydrate work has been crucial to the creation the second chapter of this thesis. There are many other people I must thank for their contributions: Shen Hu for the SDS-CE work, Rob Polakowski and Dawn Richards for the SDS-PAGE and 2D-gel work, Hossein Ahmadzadeh for his tricks for capillary coating. Woei Tan for his experience on yeast cell analysis. Eric Carpenter was incredible resource. Lillian Cook, Xiaoling Puyang and Nora Chan supported the cell lines. Kym Schreiner for her English lessons and editing my papers. Chun-Sheng Liu for the hands-on training on ESI-MS. I would like thank Dr. Liang Li's group members for helping me in MALDI-TOF-MS experiment, especially Jing Zheng, Zheng Ping Wang and Bernd Keller.

I also would like to thank the members of the Machine Shop, the Department Office, Dr. R. Bhatnagar, D. Rutkowsky and J. Wizniak for their technical assistance in confocal microscopy and flow cytometry.

I am deeply indebted to my parents, my brother, for their encouragement and support of my study in Canada.

## TABLE OF CONTENTS

CHAPTER 1: INTRODUCTION.....	1
1.1 Capillary electrophoresis .....	2
1.2 Selected modes of CE operation in this thesis.....	4
1.2.1 Capillary zone electrophoresis (CZE) .....	4
1.2.2 Capillary isotachopheresis (CITP) .....	4
1.2.3 Capillary gel electrophoresis (CGE).....	6
1.2.4 Micellar electrokinetic capillary chromatography (MECC).....	8
1.3 Laser-induced fluorescence detection (LIF) .....	9
1.4 CE of proteins.....	11
1.5 Single-cell analysis by CE.....	13
1.6 Thesis Summary .....	14
1.7 References .....	16
CHAPTER 2: CORRELATING CELL CYCLE WITH METABOLISM IN SINGLE CELLS: THE COMBINATION OF IMAGE AND METABOLIC CYTOMETRY..	19
2.1 Introduction .....	20
2.2 Methods .....	21
2.2.1 Cell culture .....	21
2.2.2 Cell extract.....	21

2.2.3 Image cytometry and cell cycle measurement.....	22
2.2.4 Metabolic cytometry.....	22
2.2.5 Confocal microscopy.....	23
2.2.6 Flow cytometry.....	23
2.3 Results .....	23
2.3.1 Metabolic cytometry.....	23
2.3.2 Image cytometry.....	26
2.3.3 Combined metabolic cytometry and image cytometry.....	29
2.3.3.1 Biosynthesis.....	29
2.3.3.2 Uptake.....	29
2.3.3.3 Biodegradation .....	29
2.3.3.4 Metabolic activity .....	31
2.4 Discussion.....	32
2.5 Conclusions .....	36
2.6 References .....	37
<b>CHAPTER 3: ONE-DIMENSIONAL PROTEOME MAP OF AN HT29 HUMAN COLON ADENOCARCINOMA CELL.....</b>	<b>40</b>
3.1 Introduction .....	41
3.2 MATERIALS AND METHODS .....	42
3.2.1 Capillary electrophoresis/laser-induced fluorescence detection.....	42
3.2.2 Cell culture .....	43
3.2.3 Protein extract.....	43

3.2.4 Proteome analysis from cell extract.....	43
3.2.5 Single-cell proteome analysis.....	43
3.2.6 Protein purification.....	44
3.2.7 Two-dimensional gel electrophoresis.....	44
3.2.8 In-gel digestion of proteins from Silver-stained Polyacrylamide gel.....	45
3.2.8 Sample preparation for MALDI MS .....	46
3.3 RESULTS AND DISCUSSION.....	46
3.3.1 CE separation.....	46
3.3.2 Single-cell proteome maps .....	49
3.3.3 Protein identification. ....	56
3.4 Conclusions .....	63
3.5 References .....	64
<b>CHAPTER 4: PROTEIN FINGERPRINTING OF <i>STAPHYLOCOCCUS</i> SPECIES USING ON-CAPILLARY CONCENTRATING, LABELING, AND ELECTROPHORESIS .....</b>	<b>68</b>
4.1 Introduction .....	69
4.2 Experimental.....	72
4.2.1 Bacterial Isolates.....	72
4.2.2 Instrumentation.....	72
4.2.3 Labeling and capillary electrophoresis .....	73
4.2.4 Phylogenetic analysis .....	73
4.2.5 Safety precautions.....	74

4.3 Results and Discussion .....	74
4.3.1 Bacterial fingerprint with CE .....	74
4.3.2 Field amplification and labeling .....	75
4.3.3 pH focusing effects on field amplification and labeling.....	79
4.3.4 Fingerprinting <i>Staphylococcus</i> species.....	83
4.3.5 Classification of bacteria by cluster analysis.....	84
4.4 References .....	86
CHAPTER 5: ON-CAPILLARY LABELING AND SELF-ISOTACHOPHORETIC PRECONCENTRATION OF PROTEINS IN SUB-MICELLAR SEPARATION OF HUMAN CANCER CELL EXTRACTS .....	89
5.1 Introduction .....	90
5.2 Background.....	93
5.2.1 On-column transient ITP-CZE mode .....	93
5.2.2 ITP/CZE mode.....	95
5.3 Experimental.....	95
5.3.1 Chemical.....	95
5.3.2 Cell extract preparation and protein fraction .....	97
5.3.3 AAEE coated capillary .....	98
5.3.4 Capillary electrophoresis/laser-induced fluorescence detection.....	98
5.4 Results and discussion.....	99
5.4.1 Inlet labeling of protein from HT29 extract .....	99
5.4.2 Sample ITP preconcentration .....	102

5.5 Conclusions .....	109
<b>CHAPTER 6: SEPARATION OF PROTEINS BY SODIUM DODECYL SULFATE- CAPILLARY ELECTROPHORESIS IN HYDROXYPROPYLCELLULOSE SIEVING MATRIX WITH LASER-INDUCED FLUORESCENCE DETECTION</b> .....	113
6.1. Introduction .....	114
6.2 Experimental.....	116
6.2.1 Apparatus.....	116
6.2.2 Reagents .....	116
6.2.3 Capillary coating .....	117
6.2.4 Sieving buffer .....	118
6.2.5 Sample preparation .....	118
6.2.5.1 Model proteins.....	118
6.2.5.2 Cell extract.....	118
6.3 Results and discussion.....	119
6.4 Conclusion.....	127
6.5 References .....	128
<b>CHAPTER 7: CONCLUSIONS AND FUTURE WORK .....</b>	<b>130</b>
7.1 Conclusions .....	131
7.2 Future work .....	134

## LIST OF FIGURES

### CHAPTER 1

Fig. 1.1	Schematic of zone capillary electrophoresis.....	3
Fig. 1.2	Representation of capillary isotachopheresis of ions.....	5
Fig. 1.3	Representation of capillary gel electrophoresis of cations.....	7

### CHAPTER 2

Fig. 2.1	TMR-labeled species from a HT29 cell and HT29 extract.....	24
Fig. 2.2	Single cell metabolic profiles from six cells.....	27
Fig. 2.3	Histogram of DNA content.....	28
Fig. 2.4	Fraction of cells showing biosynthesis.....	30
Fig. 2.5	Correlation of fraction of peak 4 and total substrate uptake...	33
Fig. 2.6	Correlation of metabolic activity and substrate uptake.....	34

### CHAPTER 3

Fig. 3.1	Separation of HT29 extract using an SDS buffer.....	48
Fig. 3.2	Proteome maps from HT29 cells.....	50
Fig. 3.3	Detail of single-cell proteome maps from 5 to 6.5 min.....	51
Fig. 3.4	Detail of single-cell proteome maps from 4.5 to 6 min.....	52
Fig. 3.5	Detail of single-cell proteome maps from 6 to 8.5 min.....	55
Fig. 3.6	Identification of component 10 as a ~100kDa protein.....	60
Fig. 3.7	Verification that most components are high MW proteins.....	61



Fig. 3.8	2D electrophoresis analysis of an HT29 extract.....	62
 CHAPTER 4		
Fig. 4.1A	Illustration of stacking.....	77
Fig. 4.1B	Separation of FQ-labeled extracts of <i>S. lugdunensis</i> .....	78
Fig. 4.2	Schematic illustration of stacking and labeling.....	80
Fig. 4.3	pH effect on the separation of extracts of <i>S. aureus</i> .....	81
Fig. 4.4	Protein fingerprints of six <i>Staphylococcus</i> species.....	82
Fig. 4.5	Phylogenetic tree generated from the data of Fig. 4.4.....	85
 CHAPTER 5		
Fig. 5.1	Illustration of transient ITP-CZE mode.....	94
Fig. 5.2	Illustration of transient ITP/CZE mode.....	96
Fig. 5.3	Schematic representation of experimental procedures.....	101
Fig. 5.4	Effect of ITP/CZE with on-column labeling.....	105
Fig. 5.5A	Effect of an additional plug of cyanide after labeling.....	106
Fig. 5.5B	Illustration of mobility window for ITP/CZE system.....	107
Fig. 5.6	Effect of FQ concentration .....	108
Fig. 5.7	ITP/CZE with fused-silica capillary.....	110
 CHAPTER 6		
Fig. 6.1	Separation using 2% HPC sieving polymer.....	122
Fig. 6.2	Plot of molecular weight vs. migration time.....	123

<b>Fig. 6.3</b>	<b>Separation of HT29 cell extract.....</b>	<b>124</b>
<b>Fig. 6.4</b>	<b>Effect of buffer composition on the separation.....</b>	<b>126</b>

## **LIST OF ABBREVIATIONS**

<b>BGE</b>	<b>background electrolyte</b>
<b>BSA</b>	<b>bovine serum albumin</b>
<b>CE</b>	<b>capillary electrophoresis</b>
<b>CGE</b>	<b>capillary gel electrophoresis</b>
<b>CIEF</b>	<b>capillary isoelectric focusing</b>
<b>CITP</b>	<b>capillary isotachopheresis</b>
<b>CZE</b>	<b>capillary zone electrophoresis</b>
<b>DNA</b>	<b>deoxyribonucleic acid</b>
<b>EMMA</b>	<b>electrophoretically mediated microchemical analysis</b>
<b>EOF</b>	<b>electroosmotic flow</b>
<b>FQ</b>	<b>5-(furoyl)-3-benzoylcarboxyquinoline</b>
<b>HEPES</b>	<b>N-(2-hydroxyethyl)piperazine-N'-ethanesulphonic acid</b>
<b>HPC</b>	<b>hydroxypropylcellulose</b>
<b>HPMC</b>	<b>hydroxypropylmethyl cellulose</b>
<b>i.d.</b>	<b>inner diameter</b>
<b>LIF</b>	<b>laser-induced fluorescence</b>
<b>LPA</b>	<b>linear polyacrylamide</b>
<b>MALDI</b>	<b>matrix-assisted laser desorption and ionization</b>
<b>MECC</b>	<b>micellar electrokinetic chromatography</b>
<b>MES</b>	<b>2-(N-morpholino)ethanesulfonic acid</b>
<b>MS</b>	<b>mass spectrometry</b>
<b>PBS</b>	<b>phosphate buffered saline</b>

<b>Poly-AAEE</b>	poly-acryloylaminoethoxyethanol
<b>RELP</b>	restriction fragment length polymorphism
<b>SDS</b>	sodium dodecyl sulphate
<b>SDS-PAGE</b>	sodium dodecyl sulphate-polyacrylamide gel electrophoresis
<b>SPS</b>	sodium pentanesulfate
<b>TEMED</b>	<i>N, N, N', N'</i> -tetramethylethylenediamine
<b>TMR</b>	tetramethylrhodamine
<b>TOF-MS</b>	time-of-flight mass spectrometry

# **Chapter 1: Introduction**

## 1.1 Capillary electrophoresis

Capillary electrophoresis (CE) is a modern analytical technique derived principally from traditional electrophoresis, but with references to chromatography as well. This combination provides us with possibilities for many modes of operation, and CE has been shown to be applicable to a wide variety of separations, from small inorganic ions to large molecules of biological importance.

The ideas behind CE can be traced back a long way, but capillary zone electrophoresis (CZE) in relatively small capillaries was first performed successfully in the late fifties and sixties (1). The possibilities of the technique were, however, not fully recognised until 1981, when Jorgenson and Lukacs demonstrated high separation efficiencies, using a high field strength in narrow capillaries (2). Since then, there has been a period of rapid growth within CE techniques. Moreover, the development of commercial instruments has made the technique accessible to a large group of analysts.

The most often used modes of CE are capillary zone electrophoresis, micellar electrokinetic capillary chromatography (MEKC), capillary gel electrophoresis (CGE), capillary isoelectric focusing (CIEF), and capillary isotachopheresis (CITP). CZE, MEKC, and CGE are zonal types, whereas CIEF is a focusing technique, and CITP a moving boundary or displacement technique. The versatility of CE is greatly enhanced due to the availability of different modes.

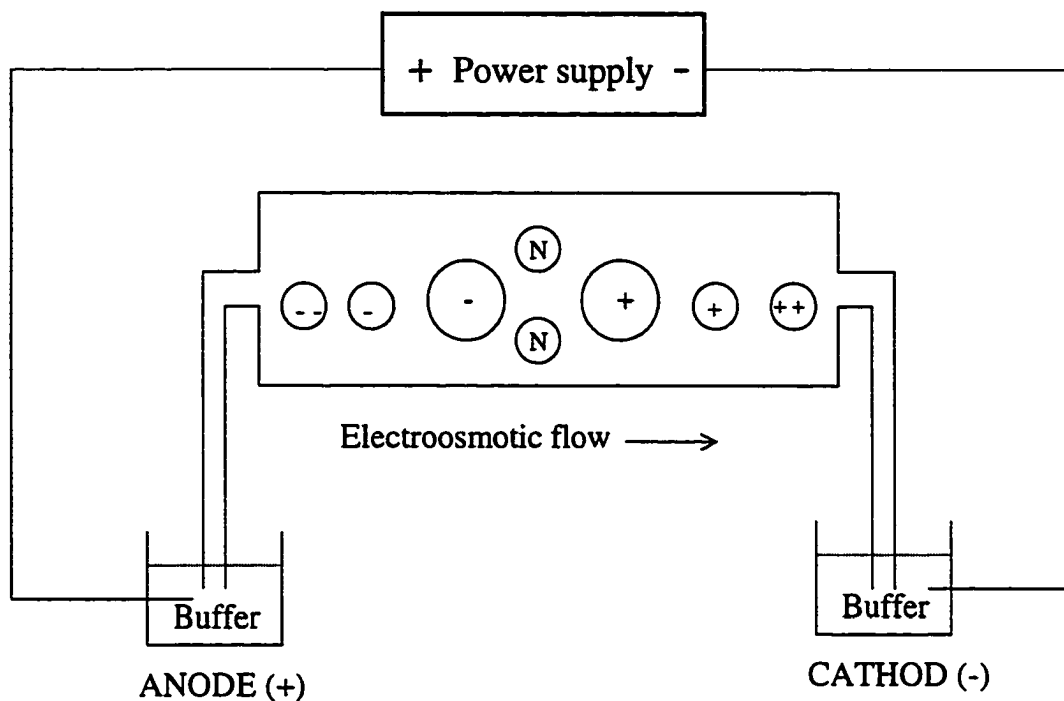


Figure 1.1 Schematic representation of zone capillary electrophoresis. Here the sample mixture was introduced at the anode end of the capillary. The circled +’s, N’s, and -’s represent cationic, neutral, and anionic compounds respectively. The valency of an ion is indicated by the number of +’s or -’s.

## **1.2 Selected modes of CE operation in this thesis**

### **1.2.1 Capillary zone electrophoresis (CZE)**

CZE is fundamentally the simplest form of CE, mainly because the capillary is only filled with buffer. As shown in Figure 1.1, separation occurs because solutes migrate in discrete zones and at different velocities. Separation of both anionic and cationic solutes is possible by CZE due to electroosmotic flow (EOF). Neutral solutes do not migrate and all coelute with the EOF. The separation mechanism is based on differences in the charge-to-mass ratio. Fundamental to CZE is homogeneity of the buffer solution and a constant field strength throughout the length of the capillary.

To date, CZE has been the most popular CE mode, and studies using this technique account for over 60% of the publications in the open literature. Reports have been published regarding the analysis of a wide range of charged simple organic molecules, inorganic ions, peptides, and proteins.

### **1.2.2 Capillary isotachopheresis (CITP)**

Prior to 1981, ITP was the most widely used instrumental capillary electrophoretic technique, although the capillaries were quite wide (250-500 $\mu$ m) by today's standards. ITP relies on zero electroosmotic flow, and the buffer system is heterogeneous. The capillary is filled a leading electrolyte that has a higher mobility than any of the sample compounds to be determined. Then the sample is injected. The mobility of a terminating electrolyte is lower than that of any sample components. Separation will occur in the gap between the leading and terminating electrolytes



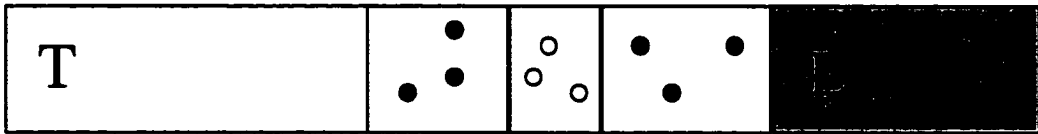


Figure 1.2 Representation of capillary isotachopheresis of ions. A leading buffer is selected which has ions with higher mobility than any sample components. A terminating buffer is selected with ions that have lower mobility than any sample components. When an electric field is applied, the sample components migrate into zones on the basis of their mobilities. The length of each zone is proportional to the amount of component in the zone. After the components migrate into their zones, an equilibrium is established and the buffers and components migrate through the capillary.

based on the individual mobilities of the analytes. As shown in Figure 1. 2, stable zone boundaries form between individual components resulting in highly efficient separations. Both anions and cations could be analyzed, though not in the same run.

IITP has two characteristics, the combination of which is unique amongst electrophoretic methods: all bands move at the same velocity, and the bands are focused. For example, highly mobile bands have high conductivity, and as result, have a lower voltage drop across the band. Since the mobility is the product of the conductivity and the voltage drop, and conductivity and voltage drop are inversely proportional, the individual band velocities are self-normalizing. Focusing is also a consequence of velocity normalization. For example, if a band diffuses into a neighbouring zone, the diffuse part of it will either speeds up or slow down based on the field strength it encounters and rejoin the original band.

### **1.2.3 Capillary gel electrophoresis (CGE)**

CGE, which combines the principles of slab gel electrophoresis with the instrumentation and small diameter capillaries of CZE, was introduced by Cohen and Karger (3). Capillaries dissipate heat better than slab gels, so higher electric field can be used, giving faster separations. In CGE, the capillary is filled with a gel, which is usually either a polyacrylamide/bisacrylamide crosslinked polymer or a linear, noncrosslinked polyacrylamide polymer. Dextran, poly(ethyleneoxide), and agarose gel are also used. There are pores within these gels, and as charged solutes migrate through a gel-filled capillary, they are separated by a molecular sieving mechanism

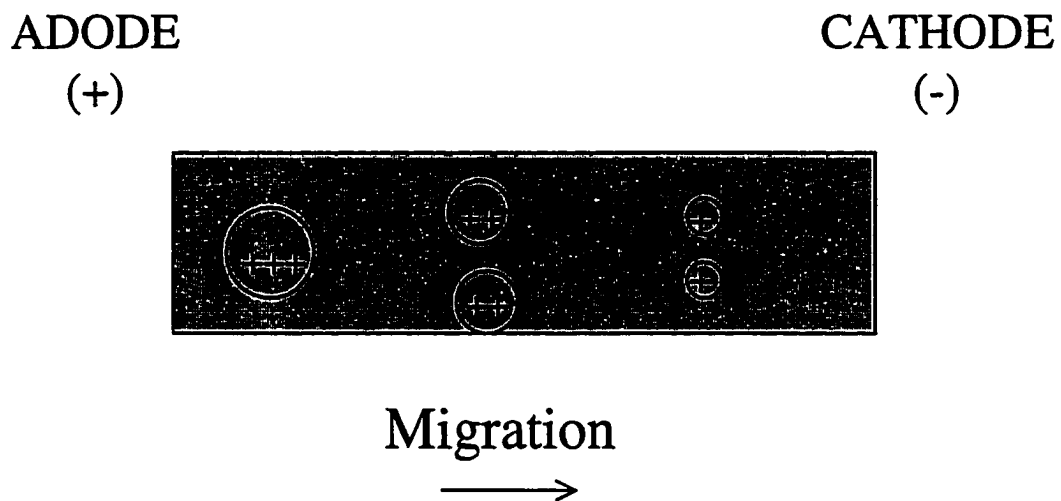


Figure 1.3 Representation of capillary gel electrophoresis of cations. Cations of different sizes and different valences are indicated by the circled +’s. Anions can also be separated by CGE with the polarity reversed. Cations migrate through a gel-filled capillary on the basis of the sizes and charges. When cations have the same charge-to-mass ratio, they elute on the basis of their sizes, with the smallest ones eluting first.

on the basis of their size. Small molecules are able to pass quickly through the pores and elute first, whereas larger molecules are retarded by the gel and elute later. This is represented in Fig. 1. 3. Usually the capillary wall is treated to eliminate EOF so the gel will not be extruded from the capillary. Solutes move through the capillary due to electrophoresis, and are separated by the sieving mechanism of the gel.

In the presence of a reducing agent, SDS causes proteins to dissociate into polypeptides, and the SDS binds to them, producing molecules with similar charge-to-size ratios. Therefore, these solutes are not well separated by CZE; however, they can be separated by CGE.

#### **1.2.4 Micellar electrokinetic capillary chromatography (MECC)**

Perhaps the most intriguing mode for the determination of small molecules is MECC. The use of micelle-forming surfactant solutions can give rise to separations that resemble reverse-phase LC with the benefits of CE. MECC was introduced by Terabe in 1984 (30).

Micelles are amphiphilic aggregates of molecules known as surfactants. They are long chain molecules and are characterized as possessing a long hydrophobic tail and a hydrophilic head group. Normally micelles are formed in aqueous solution with the hydrophobic tails pointing inward and hydrophilic heads pointing outward into the aqueous solution. Above a surfactant concentration known as the critical micelle concentration (CMC) the aggregate is fully formed. SDS is the most widely used surfactant in MECC. It is available in highly purified forms and is inexpensive. Its molecular weight is 288 and CMC is 8 mM. The aggregation number (number of

molecules/micelle) is 62.

Since analytes can partition into and out of the micelle, the requirements for a separation process are at hand. When an analyte is associated with a micelle, its overall migration velocity is slowed. When an uncharged analyte resides in the bulk phase, its migration velocity is that of the EOF. Therefore, analytes that have greater affinity for the micelle have slower migration velocities compared to analytes that spend most of their time in the bulk phase. The separation of neutral species by CE is a compelling example of the general applicability of the technique.

With SDS micelles, the general migration order will be anions, neutrals, and cations. Anions spend more of their time in the bulk phase due to electrostatic repulsions from the micelle. The greater the anionic charge, the more rapid the elution. Neutral molecules are separated exclusively based on hydrophobicity. Cations elute last due to strong electrostatic attraction (e.g. ion-pairing with the micelle). While this is a useful generalization, strong hydrophobic interaction can overcome electrostatic repulsions and attractions. Likewise, the electrophoretic migration of analytes can also affect the elution order.

### **1.3 Laser-induced fluorescence detection (LIF)**

LIF is the most sensitive detection method available for CE. As monochromatic excitation light sources, lasers have made spectacular improvements in detection limits in fluorescence measurements. The high spatial coherence of a laser allows very small sample volumes to be probed with high efficiency. This coherence allows the use of capillaries with very small diameter, as

low as 10  $\mu\text{m}$ . When coupled with efficient collection and detection, minute amounts of analyte may be detected.

In 1985, Zare's group reported the first application of on-column LIF detection in CE (4). Femtomole amounts of dansyl labeled amino acids were detected. This laboratory has achieved detection limits of single molecules using a post-column LIF detector based on a sheath flow cuvette (5-8). The optics are designed to collect as much sample fluorescence as possible and reject as much background light as possible. A comparison with on-column LIF detection demonstrates the advantage of the sheath flow cuvette over other detection methods. In the on-column approaches, the capillary serves as the detection cell. This arrangement is rugged and uncomplicated but the capillary is not an optimal detection cell. The change in refractive index at the capillary/buffer interface produces a large amount of light scatter. The scattered light is responsible for the majority of the noise encountered in on-column detection. The sheath flow cuvette eliminates this source of scattered light by surrounding the capillary eluent with a sheath fluid of equal refractive index. The major source of noise is light scattering from the solvent, which is significantly less than the light scatter found in on-column detection. Although there is still a change in refractive index at the cuvette/sheath fluid interface, this region of light scatter is far away from the analyte fluorescence region and is easily discriminated from the fluorescence using confocal collection optics. For the scatter originating in the same region as the analyte, it has a different wavelength from the analyte fluorescence and it can be removed using a bandpass filter. The filter does pass 1 part in  $10^6$  of light at the wavelengths it is designed to block. This scatter is the main source of noise in the LIF detector. Specifically, the shot noise from the scattered light limits the detection sensitivity.

## **1.4 CE of proteins**

CE as a separation method for the analysis of proteins has made significant progress during the past several years. Different CE modes, such as CZE, CIEF and sieving SDS-CE, are used in proteomic studies. During this period, development and standardization of the method have been the primary activities in the field. Efficient sample preconcentration online together with sensitive detection methods, such as LIF and efficient protein derivatization, have made it possible to analyze ultratrace proteins. Among those techniques, CZE is the most conveniently used one, but each CZE study has to optimize the electrophoretic conditions, including buffer composition to obtain the best resolution for a specific protein mixture, for which a variety of buffer additives has been reported.

### **1.4.1 Sample preconcentration**

There are several methods for concentrating protein online prior to CZE analysis of low-concentration proteins. Sample self-stacking was applied to the analysis of insulin (9) and determination of trace concentrations of recombinant interleukins (10). The approach of a semipermeable hollow fiber between the sample vial and the inlet end of the capillary can lower the detection limit by a factor of  $10^3$ , as demonstrated for a mixture of model proteins (11). Solid phase extraction is another common method used to concentrate peptides and proteins (12).

### **1.4.2 Biologically important protein systems**

Human serum proteins (13) and urine proteins (14) can be separated by CZE into ten peaks and shoulders. The separation is not sufficient to separate the major protein constituents in these samples, but higher sensitivity than agarose gel electrophoresis or cellulose acetate electrophoresis for the detection of monoclonal proteins has been achieved. Soluble proteins in wheat can be separated into 30 to 40 peaks and shoulders by CE in isoelectric buffers (16) or in a phosphate buffer (16), the resolution is at least comparable to that of SDS-gel electrophoresis. CIEF has been employed for the total analysis of human plasma proteins and about sixty protein peaks and shoulders have been separated within 50 min by optimizing the step of chemical mobilization (17). Use of a solution of entangled polymer as a sieving matrix is effective for size separation of SDS-protein complexes, as recently reviewed (18). Cell lysates may contain thousands of proteins and therefore two-dimensional capillary electrophoresis techniques have to be applied. For the comprehensive analysis of a complex protein system, many laboratories must collaborate to obtain integrated information on the system. Then the use of a common technique or comparable techniques for protein separation must be a prerequisite for such collaboration.

At present, proteomic studies imply separation and structural analysis of total proteins in a complex system. CE has been applied to the analysis of the biological functions of a single protein, such as enzyme activity or specific binding with other molecules (19-21).



## 1.5 Single-cell analysis by CE

Chemical analysis of single cells is an area of great interest in the biological and medical sciences. Knowledge of the chemical composition and dynamics of single cells should lead to better understanding of how cells function in complicated cellular environments. It requires the development of analytical techniques capable of monitoring minute amounts of components involved in dynamic cellular processes. CE is well-suited for probing microenvironments due to its typical features, i.e. the compatibility between the dimensions of the capillary (i.d. 2-200  $\mu\text{m}$ ) and the size of most cells (5-500  $\mu\text{m}$ ), much smaller sample requirements than most other analytical methods, extremely high separation efficiency, high analysis speed, and possible on-capillary sample pretreatment.

Ewing's group pioneered research of CE at the single-cell level (22). They successfully introduced subpicoliter cytoplasmic samples from a single neuron in the pond snail *Planorbis corneus* into a capillary by a microinjector with an inner diameter of 5  $\mu\text{m}$ . Analysis of single lymphocytes from human cerebrospinal fluid by CE has led to the discovery of endogenous catecholamines in these cells (23). A significant body of work concerning the analysis of single neurons has also been published by Jorgenson and co-workers (24-26). Their work with bovine adrenal cells and packed microcolumn liquid chromatography represents the first analysis of single mammalian cells using microcolumn separation technology (26). Yeung's group has successfully detected inorganic ions, proteins, enzymes in even smaller human erythrocytes with laser-based detection schemes (27-29).

## **1.6 Thesis Summary**

The next five chapters present CE analysis of proteins and carbohydrates from cell extracts and single cells.

The method presented in Chapter 2 correlated cell cycle with oligosaccharide metabolic activity in single cells. In this chapter, the combination of metabolic cytometry with image cytometry to correlate oligosaccharide metabolic activity with cell cycle was described. This technique is used to measure DNA ploidy, the uptake of a fluorescent disaccharide, and the amount of metabolic products in a single cell. The cells in the G1 phase did not show any biosynthetic activity in respect to the substrate. Several groups of cells with unique biosynthetic patterns were distinguished within G2/M cells.

This is the first report that combined metabolic- and image-cytometry to correlate production of metabolic products with cell cycle. A complete enzymatic cascade is monitored on a cell-by-cell basis and correlated with cell cycle. Chapter 3 presents the first one-dimensional protein electropherograms generated from a single somatic cell. This chemical cytometry method reveals the distribution in protein expression between cells, which is hidden by classic protein analysis performed on cell extracts. Cell labeling and handling techniques and instrumentation for single cell analysis are also discussed.

In this chapter, a single HT29 human colon adenocarcinoma cell was introduced into a fused-silica capillary, lysed, and the protein content was fluorescently labeled with the fluorogenic reagent 3-(2-furoyl)quinoline-2-

carboxaldehyde. The labeled proteins were separated by capillary electrophoresis in a sub-micellar buffer and detected by laser-induced fluorescence in a post-column sheath-flow cuvette. Several dozen components were resolved. A number of experiments were done to verify that these components were proteins. Most components of the single-cell electropherogram had the same mobility as components present in the 30 kDa to 100 kDa fraction of a protein extract prepared from the cell culture. One component was identified as a ~100 kDa protein by co-injecting the sample with purified protein obtained from a SDS-PAGE gel. Protein expression varied significantly between cells, but the average expression was consistent with that observed from a protein extract prepared from  $10^6$  cells.

A highly sensitive and rapid method for the identification of microorganisms is presented in Chapter 4. It is based on on-capillary electrophoretic concentration and labeling. The response for selected protein fractions was enhanced through manipulation of sample stacking conditions.

Chapter 5 presents isotachophoretic stacking of proteins, which is induced by using excess labeling reagent as the leading electrolyte. The method combines protein labeling, ITP stacking and submicellar separation in one capillary. The gain in sensitivity is given by effective focusing of labeled proteins into sharp and concentrated ITP zones.

Chapter 4 and 5 introduce new methods to preconcentrate proteins before and after labeling in a single capillary.

In chapter 6, sodium dodecyl sulfate-capillary electrophoresis (SDS-CE) by using hydroxypropylcellulose (HPC) as the sieving matrix was developed for separation of proteins. Five standard proteins within the molecular weight range of 14000 – 97000 were used to test this method and a calibration curve was obtained between the molecular weight of these proteins and their migration times. This method was also applied to the separation of proteins from HT29 human colon adenocarcinoma cell extracts, and, typically, nearly 30 protein components could be resolved in a 20-min separation. Similar separation patterns were observed for the cell extract proteins when three running buffer systems were employed, indicating that buffer composition did not have much influence on the separation based on HPC sieving.

## 1. 7 References

1. Hjerten, S. *Chromatogr. Rev.* **1967**, 9, 122
2. Jorgenson, J. W.; Lukacs, K. D. *Anal. Chem.* **1981**, 53, 1298
3. Cohen, A. S.; Karger, B. L. *J. Chromatogr.* **1987**, 397, 409-417
4. Gassmann, E.; Kuo, J. E.; R. N. Zare, *Science* **1985**, 230, 813-815
5. Dovichi, N. J. *Trends in Anal. Chem.* **1991**, 3, 55-57
6. Zarrin, F.; Dovichi, N. J. *Anal. Chem.* **1987**, 59, 846-850
7. Chen, D. Y.; Dovichi, N. J. *J. Chromatogr. B* **1994**, 657, 265-269
8. Craig, D. B.; Arriaga, E.; Wong, J.; Lu, H.; Dovichi, N. J. *Anal. Chem.* **1998**, 70, 39A-43A
9. Shihabi, Z. K.; Friedberg, M. *J. Chromatogr. A.* **1998**, 807, 129-133
10. Bergmann, J.; Jaehde, U.; Schunack, W. *Electrophoresis* **1998**, 19, 305-310

11. Wu, X. Z.; Hosaka, A.; Hobo, T. *Anal. Chem.* **1998**, *70*, 2081-2084
12. Figeys, D.; Zhang, Y.; Aebersold, R. *Electrophoresis* **1998**, *19*, 2338-2347
13. Bossuyt, X.; Schiettekatte, G.; Bogaert, A.; Blankaet, N. *Clin. Chem.* **1998**, *44*, 749-759
14. Jenkins, M. A. *Electrophoresis* **1997**, *18*, 1842-1846
15. Capelli, L.; Forlani, F.; Perini, F.; Guerrieri, N.; Cerletti, P.; Righetti, P.G. *Electrophoresis* **1998**, *19*, 311-318
16. Bean, S. R.; Lookhart, G. L. *Electrophoresis* **1998**, *19*, 3190-3198
17. Manabe, T.; Miyamoto, H.; Iwasaki, A. *Electrophoresis* **1997**, *18*, 92-97
18. Takagi, T. *Electrophoresis* **1997**, *18*, 2239-2242
19. Watanabe, T.; Yamamoto, A.; Nagai, S.; Terabe, S. *Electrophoresis* **1998**, *19*, 2331-2337
20. Skeleton, T. P.; Zeng, C.; Nocks, A.; Stamenkovic, I. *J. Cell Biol.* **1998**, *140*, 431-446
21. Guszczynski, T.; Copeland, T. D. *Anal. Biochem.* **1998**, *260*, 212-217
22. Wallingford, R. A.; Ewing, A. G. *Anal. Chem.* **1988**, *60*, 1972-1975
23. Bergquist, J.; Tarkowski, A.; Ekman, R.; Ewing, A. *Proc. Natl. Acad. Sci. USA* **1994**, *91*, 12912-6
24. Kennedy, R. T.; Oates, M. D.; Cooper, B. R.; Nickerson, B.; Jorgenson, J. W. *Science* **1989**, *246*, 57-63
25. Ciolkowski, E. L.; Cooper, B. R.; Jankowski, J. A.; Jorgenson, J. W.; Wightman, R. M. *J. Am. Chem. Soc.* **1992**, *114*, 2815-2821
26. Cooper, B. R.; Jankowski, J. A.; Leszczyszyn, D. J.; Wightman, R. M.; Jorgenson, J. W. *Anal. Chem.* **1992**, *64*, 691-694
27. Hogan, B. L.; Yeung, E. S. *Anal. Chem.* **1992**, *64*, 2841-2845
28. Lee, T. T.; Yeung, E. S. *Anal. Chem.* **1992**, *64*, 3045-3051

29. Xue, Q.; Yeung, E. S. *Anal. Chem.* **1994**, *66*, 1175-1178
30. Terabe, S.; Otsuka, K.; Ichikawa, K.; Tsuchuya, A.; Ando, T. *Anal. Chem.* **1984**, *56*, 111

## **Chapter 2: Correlating cell cycle with metabolism in single cells: the combination of image and metabolic cytometry**

## 2.1 Introduction

Chemical cytometry is this group's term for the analysis of the chemical composition of single cells. In 1953, Edstrom reported the first chemical cytometry analysis, where fine silk fibers were used for the electrophoretic determination of RNA contained within a single cell (1). In 1965, Maholi and Niewisch used a fine agarose fiber to perform gel electrophoresis separation of hemoglobin in single erythrocytes (2). In 1987, Jorgenson lysed a single cell and fluorescently labeled its contents in a miniature reaction vial (3-4). The reaction products were then injected into a capillary chromatography column for analysis. In 1994, Ewing greatly simplified the procedure by injecting the cell directly into the separation capillary, where lysis and labeling were performed on-column (5). Workers have studied single erythrocytes and neurons (6-15). An extension of the single-cell work involves study of exocytosis from single pancreatic cells or neurons (16-23). Recently, there has been interest in mass spectrometric identification of proteins from single cells (24-26). In most cases, chemical cytometry was used to analyze endogenous components within the cell; in one case, a single enzyme's activity was monitored (15).

In earlier work, this group studied cell extracts prepared from  $\sim 10^6$  cells grown in the presence of a tetramethylrhodamine-labeled disaccharide (27). The disaccharide was taken-up by the cells where it acted as a substrate for an enzymatic cascade, forming biosynthetic products corresponding to larger oligosaccharides and biodegradation products corresponding to the monosaccharide and the fluorescently-labeled linker. The fluorescent tag associated with the substrate survived many of the metabolic transformations. When separated with a high-resolution capillary electrophoresis system and detected with a high-sensitivity laser-induced fluorescence



detector, minute amounts of metabolic product were detected in the cellular extracts. This group reported the detection of ~50 molecules ( $\sim 8 \times 10^{-23}$  mole = 80 yoctomole = 80 ymol) of metabolic product (28-29).

The high sensitivity of our fluorescence detector suggests that metabolic products can be detected in single cells. In this chapter, we describe metabolic cytometry, which is the use of capillary electrophoresis/laser-induced fluorescence to analyze the metabolic products within single cells. Five metabolic products were separated and identified from the single cells. This metabolic cytometry is combined with an image cytometry system to provide a hybrid method that monitors cell cycle, substrate uptake, and biosynthetic and biodegradation pathways in single cells.

## **2.2 Methods**

### **2.2.1 Cell culture**

The HT29 cell line (human colon adenocarcinoma) was grown to 80% confluence in Dulbecco's modified Eagle's medium, supplemented with 10% fetal calf serum and 40  $\mu\text{g}/\text{mL}$  gentamycin at 37°C in 5%  $\text{CO}_2$  atmosphere. The cells were then incubated for 18 h with 25  $\mu\text{M}$  tetramethylrhodamine-labeled  $\beta\text{Gal}(1\rightarrow 4)\beta\text{GlcNAc}$  substrate (LacNAc-TMR). After incubation the cells were washed 8 times with phosphate buffered saline (PBS) to remove the residual substrate. The cells were resuspended in PBS.

### **2.2.2 Cell extract**

To prepare cell extracts,  $2 \times 10^6$  cells were homogenized in a micro-tissue grinder on ice with 20 strokes every 15 min over a 1.5 h period. The sample was centrifuged to remove cellular debris. The supernatant was loaded onto a C-18 Sep

Pak cartridge and washed with water. The hydrophobic TMR-labeled compounds were eluted from the cartridge with HPLC grade methanol. The methanol was evaporated and the residue was dissolved in 160  $\mu\text{L}$  of the electrophoresis running buffer.

### **2.2.3 Image cytometry and cell cycle measurement**

A 0.1 mM YOYO-3 stock solution was prepared in water and stored at  $-18\text{ }^{\circ}\text{C}$ . A 1-mg/mL stock solution of Hoechst 33342 was prepared in water and stored at  $4\text{ }^{\circ}\text{C}$ . YOYO-3 and Hoechst 33342 were added to the cell suspension ( $10^6$  cells/mL) to make final concentrations of 1  $\mu\text{M}$  and 10  $\mu\text{g}/\text{mL}$  respectively. Cells were incubated for 1 h at  $37\text{ }^{\circ}\text{C}$  before analysis. A 1- $\mu\text{L}$  aliquot of the cell suspension was diluted with 50  $\mu\text{L}$  of PBS buffer and this diluted suspension was placed on a glass microscope slide. YOYO-3 dye intercalates DNA only in dead cells. We excluded the cells with YOYO-3 fluorescence from further analysis. A live cell was centered in the field of view of the 125 $\times$  objective on a microscope equipped with an R1635-02 photomultiplier tube. The PMT shutter was opened, focusing was adjusted to maximize the signal, and the signal was recorded.

### **2.2.4 Metabolic cytometry**

A 45-cm long, 19- $\mu\text{m}$  ID, and 144- $\mu\text{m}$  OD fused-silica capillary was placed over a cell using micromanipulators and with the aid of an inverted microscope. An 11-kPa partial vacuum was applied to the distal end of the capillary for 1 s, drawing the cell approximately 0.2-mm within the capillary. The capillary tip was placed in a vial containing the SDS - running buffer, which lysed the cell within 20 s. The separation was performed at 18 kV as described earlier (29). Our fluorescence

detector used 1-mW helium-neon laser excitation at 543.5 nm to produce a detection limit of 100 TMR-labeled molecules (30-33).

### **2.2.5 Confocal microscopy**

The fluorescence intensity of 65 cells, chosen at random, was measured by confocal microscopy. Images were obtained with a MultiProbe 2001 confocal laser-scanning microscope (Molecular Dynamics). A 4-mW argon-krypton ion laser at 568 nm was used as the excitation source. The total fluorescence intensity was estimated by imaging 32 sections through the cells and summing the intensity through each cell. A step-size between sections was 0.7  $\mu\text{m}$  to accurately estimate the cell's fluorescence.

### **2.2.6 Flow cytometry**

Conventional flow cytometry data was generated for cells that had been incubated with both LacNAc-TMR and Hoechst 33342. These conditions were chosen to be similar to that used for metabolic cytometry experiments. A Coulter Elite flow-cytometer was used to generate the data.

## **2.3 Results**

### **2.3.1 Metabolic cytometry**

Figure 2.1 presents electropherograms generated from a single HT29 cell, an HT29 cell extract, and a control consisting of the resuspension buffer. Six peaks were observed in the single-cell and cell extract electropherograms, forming the metabolic profile. We were concerned that the metabolic cytometry profile might be biased by injection of fluorescent contaminants in the buffer used to re-suspend the cells.

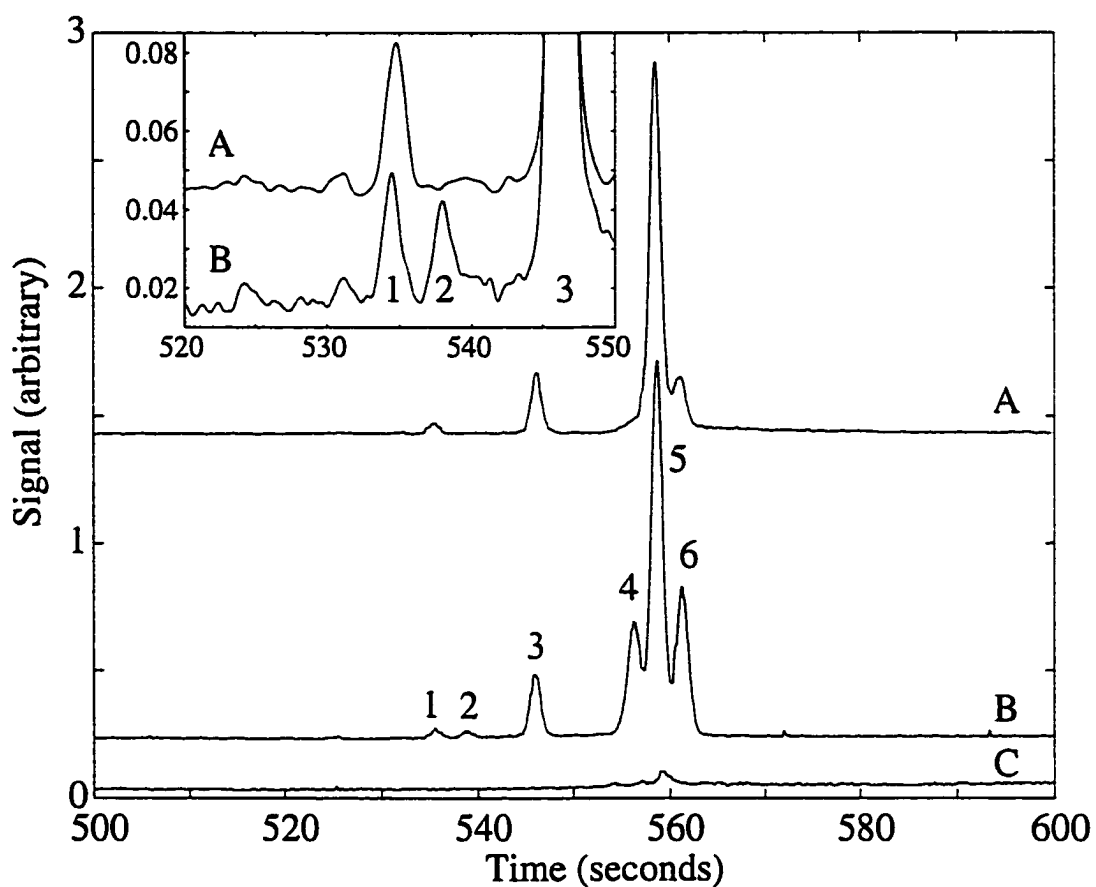


Fig. 2.1 Electropherograms of TMR-labeled species obtained from a single HT29 cell (curve A), an HT29 extract (curve B), and the PBS buffer used to resuspend the cells (curve C). The inset shows peaks 1-2 for the single cell and cell extract.

However, only a very small peak was observed in the control electropherogram; any resuspension buffer injected with a cell makes a minute contribution to the metabolic profile.

Most peaks were identified in the cell extract profile based on co-migration with authentic standards and by enzymatic hydrolysis. Peak 1 was identified as Le<sup>x</sup>,  $\alpha\text{Fuc}(1\rightarrow2)\beta\text{Gal}(1\rightarrow4)[\alpha\text{Fuc}(1\rightarrow3)]\beta\text{GlcNAc-TMR}$ , formed by  $\alpha 1\rightarrow 2$  and  $\alpha 1\rightarrow 3$  fucosylation of the substrate. Peak 2 was Le<sup>s</sup>,  $\beta\text{Gal}(1\rightarrow4)[\alpha\text{Fuc}(1\rightarrow3)]\beta\text{GlcNAc-TMR}$ , formed by addition of fucose to the substrate by  $\alpha 1\rightarrow 3$  fucosyltransferase. Peak 3 was the substrate. Peak 4 does not co-migrate with any of our standards. Peak 5 was  $\beta\text{GlcNAc-TMR}$ , formed by  $\beta$ -galactosidase activity on the substrate. Peak 6 co-migrated with TMR-aglycone,  $(\text{HO}(\text{CH}_2)_4\text{CONH}(\text{CH}_2)_2\text{NH-TMR})$ , which is produced by hydrolysis of the substrate by sequential action of  $\beta$ -galactosidase and hexosaminidases; however, we have not enzymatically confirmed this peak's identity. The protocol for peak identification was described elsewhere (40).

Substrate uptake was measured by both metabolic cytometry and image cytometry. We assume that metabolism neither destroys the fluorescent label nor changes the spectroscopic properties of the label. In metabolic cytometry, substrate uptake was estimated by summing the intensity of all peaks in the electropherogram. The 45% relative standard deviation (n=20) in cell-to-cell intensity from metabolic cytometry was indistinguishable from a 43% relative standard deviation (n=65) in cell-to-cell fluorescence intensity measured by confocal microscopy. Metabolic cytometry and image cytometry provided similar results for substrate uptake.

Conventional cytometric methods are unable to distinguish between metabolic products. In contrast, metabolic cytometry provides a detailed profile of enzymatic

activity for each cell. Six metabolic profiles were chosen to illustrate the range of behaviors, Fig. 2.2 Cell A has low substrate uptake but generates the largest relative amounts of both the aglycone degradation product and the Le' biosynthetic product. In contrast, cells E and F have the largest uptake of the substrate, which is almost completely converted to  $\beta$ GlcNAc-TMR, with virtually no evidence for other biotransformations.

### 2.3.2 Image cytometry

Cells were treated with two DNA intercalating dyes in addition to the LacNAc-TMR substrate. YOYO-3 is permeant only to dead cells and emits red fluorescence upon excitation at 600 nm. Only live cells were chosen for further study.

Hoechst 33342 is permeant to live cells and emits blue fluorescence upon excitation at 350 nm. The intensity of the Hoechst 33342 fluorescence was measured with a photomultiplier tube connected to the microscope. Figure 2.3 presents a frequency histogram for DNA content obtained for 108 randomly chosen cells. The inset shows flow-cytometry data generated from 3,684 cells from the same culture. Both distributions showed two peaks corresponding to cells in the G1 and G2/M phase of the cell cycle. The coefficient of variation in fluorescence signal for the G1 cells was 12% for our image cytometry data and 10% for the commercial flow cytometer.

We used this technique to choose only G1 and G2/M cells for our metabolic cytometry analysis. We applied metabolic cytometry to analyze 20 cells in the G1 phase and 23 cells in the combined G2/M phase.

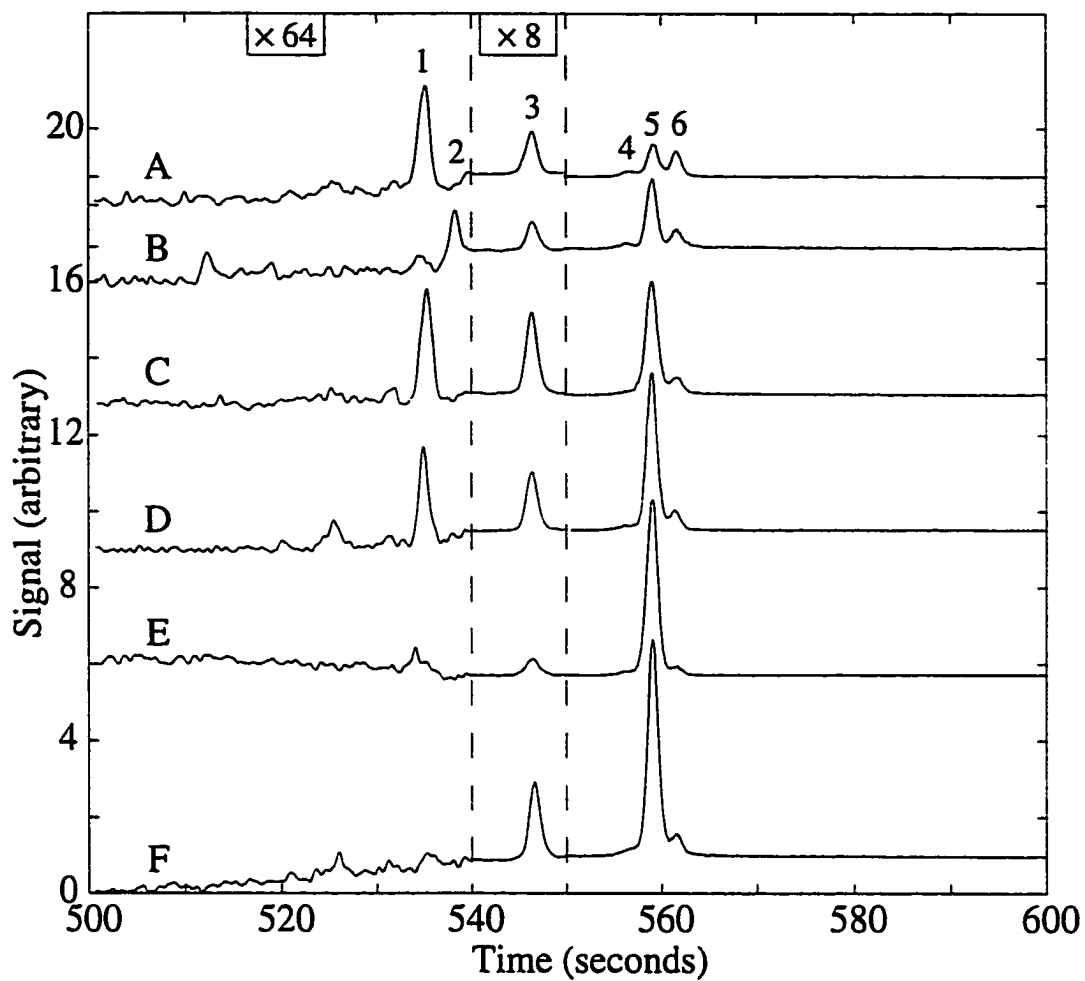


Fig. 2. 2 Single cell metabolic profiles from six cells. The electropherograms are offset for clarity. The region from 540 to 550 seconds was expanded by a factor of eight and the region from 500 to 540 seconds was expanded by a factor of 64.

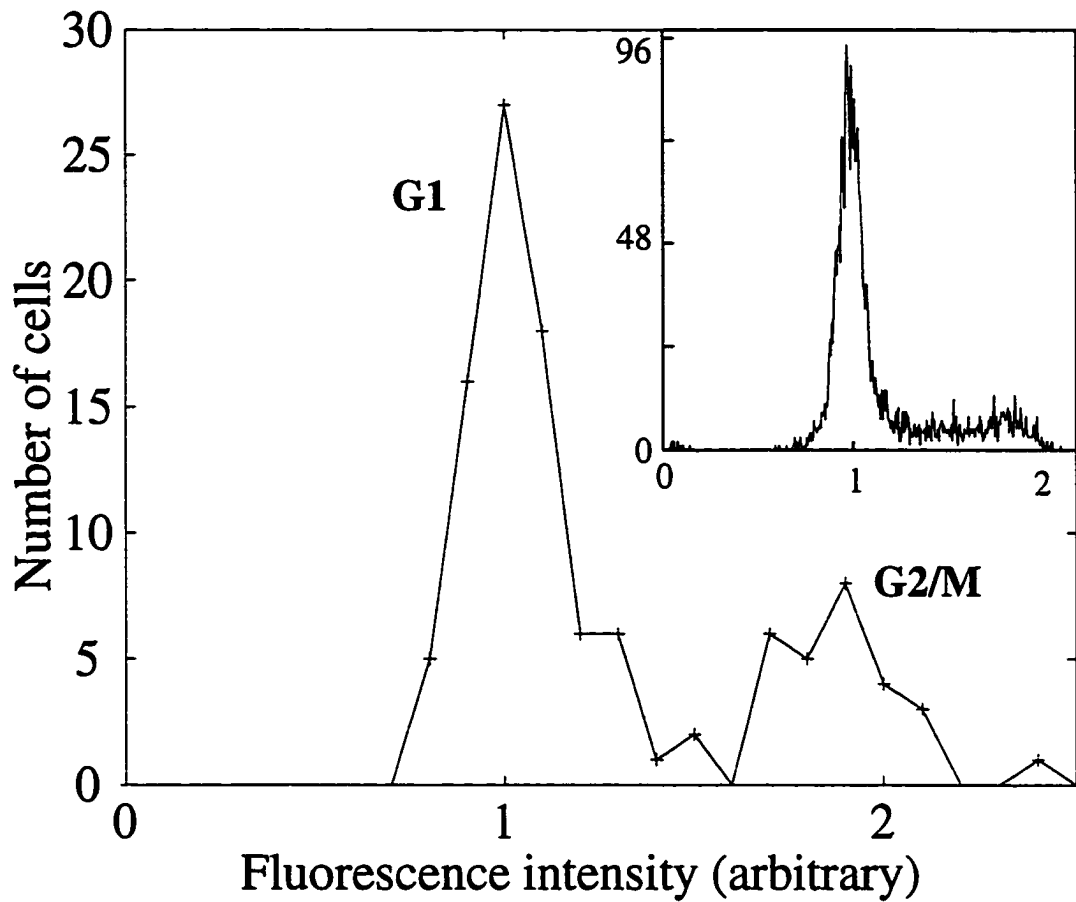


Fig. 2.3 Histogram of DNA content from 108 randomly chosen cells measured with an inverted microscope. The insert shows data generated by a conventional flow cytometer.



### **2.3.3 Combined metabolic cytometry and image cytometry**

#### ***2.3.3.1 Biosynthesis***

No biosynthetic products were observed in the G1 cells, Figure 2. 4. Based on the sensitivity of our instrument, less than 100 molecules of biosynthetic product were present within these cells.

The G2/M cells could be divided into classes based on their biosynthetic activity. No biosynthetic products were observed in about 60% of the G2/M cells. Again, these cells had less than 100 molecules of biosynthetic product.

However, a fraction of the G2/M cells were biosynthetically active. One class generated only  $Le^x$ , another generated  $Le^y$ . No cells in this study generated measurable amounts of both biosynthetic products. About 25% of the G2/M cells generated measurable amounts of  $Le^x$ , about 12% of the G2/M cells generated measurable amounts of  $Le^y$ , and the remainder had no detectable biosynthetic products. The extent of biosynthesis was small, with an average of roughly 3,000 molecules of product in those cells, which accounts for 4% of the fluorescent compounds within the cell. For subsequent analysis, we divided the cells into three classes: G1, biosynthetically inactive G2/M and biosynthetically active G2/M.

#### ***2.3.3.2 Uptake***

Uptake was determined along with cell cycle. Cells in the G1 phase had an average of ~25,000 fluorescent molecules. The biosynthetically inactive cells had an average of ~50,000 fluorescent molecules. The biosynthetically active G2/M cells had an average of ~90,000 fluorescent molecules.

#### ***2.3.3.3 Biodegradation***

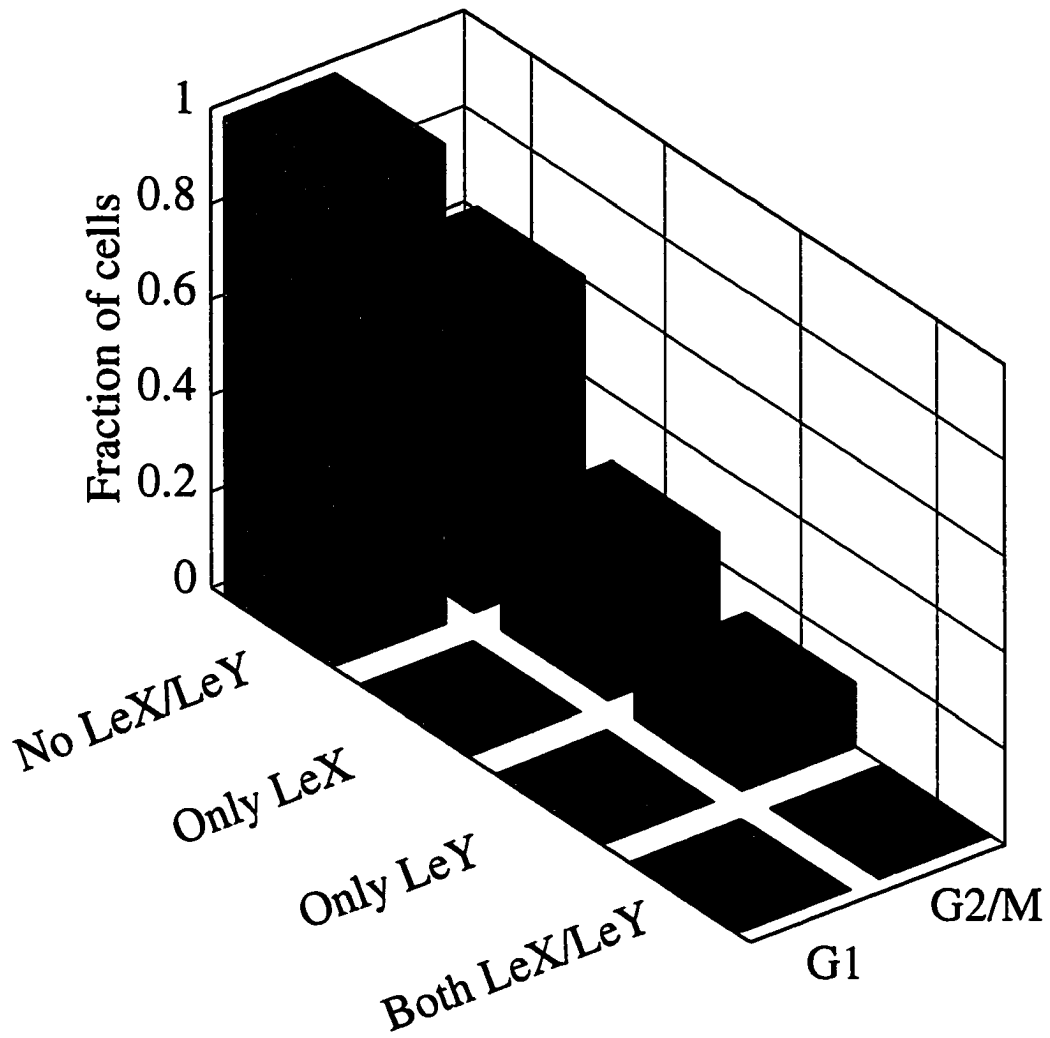


Fig. 2. 4. Fraction of cells showing biosynthesis. G1 cells showed no biosynthesis, whereas ~40% of G2/M cells showed biosynthesis of either  $Le^x$  or  $Le^y$ , but not both.

Biosynthesis made a small contribution to the total metabolism. Instead, biodegradation dominated the metabolic activity for all cells, accounting for ~80% of the fluorescent signal. Biodegradation proceeds through several steps. First,  $\beta$ -galactosidase removes one monosaccharide from the disaccharide substrate, producing the monosaccharide  $\beta$ GlcNAc-TMR. Subsequent degradation by hexosaminidase produces the aglycone, which consists of a linker-arm that is connected to the fluorescent label.

Biodegradation is dominated by the action of  $\beta$ -galactosidase to produce  $\beta$ GlcNAc-TMR, peak 5. On average,  $\beta$ GlcNAc-TMR accounted for about 65% of the fluorescent signal for all cell classes. The aglycone, peak 6, accounted for an additional 15% of the signal for all cell classes.

Peak 4 remains unidentified. Its relative amount was negatively correlated with total substrate uptake ( $r=-0.63$ ,  $n = 43$ ,  $P = 0.6 \times 10^{-4}$ ). However, this negative correlation obscures the behavior of different cell populations, figure 2.5. The peak was present at very low concentration in G2/M phase cells undergoing biosynthesis, accounting for 1% of the fluorescent signal. It was present at higher concentration in the biosynthetically inactive G2/M cells, accounting for 3% of the fluorescent signal. The compound was present at highest concentration in the G1 cells, accounting for 6% of the fluorescent signal.

#### *2.3.3.4 Metabolic activity*

We define metabolic activity as the fraction of fluorescence signal generated by the metabolic products, peaks 1-2 and 4-6. The average metabolic activity was  $0.87 \pm 0.08$  for the G1 cells,  $0.84 \pm 0.08$  for the biosynthetically inactive G2/M cells, and  $0.84 \pm 0.08$  for the biosynthetically active G2/M cells, figure 2.6.

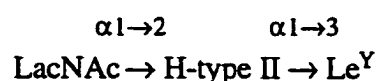
Metabolic activity was uncorrelated with substrate uptake for G1 cells ( $r = 0.05$ ,  $n=20$ ,  $P = 0.83$ ). In contrast, the metabolic activity increased with uptake for metabolically inactive ( $r = 0.61$ ,  $n = 14$ ,  $P = 0.02$ ) G2/M cells and for metabolically active G2/M cells ( $r = 0.84$ ,  $n = 9$ ,  $P = 0.005$ ).

## 2.4 Discussion

Metabolism is the total set of chemical reactions that occur in a cell. While classic analytical tools such as chromatography and electrophoresis can provide detailed information on metabolic pathways (28, 34), they provide no information on the range of activity within a cellular population; differentiation in a population is not discernable in these assays. In contrast, cytometric assays, such as flow or image cytometry, generate a powerful correlation between cell markers and the activity of a single enzyme (35, 36). However, the assays neither provide information on metabolic pathways and fluxes nor do they discriminate between substrate uptake and enzyme activity.

We used metabolic cytometry to study the metabolism of single cells as a function of cell cycle. The biosynthetic and biodegradation behaviour of cells varies during the cell cycle. About 40% of the cells in the G2/M phase actively accumulate the biosynthetic products. The biosynthetically active cells generate either Le<sup>X</sup> or Le<sup>Y</sup>, but not both.

The biosynthesis of Le<sup>X</sup> and Le<sup>Y</sup> from LacNAc is mediated by a set of fucosyltransferases



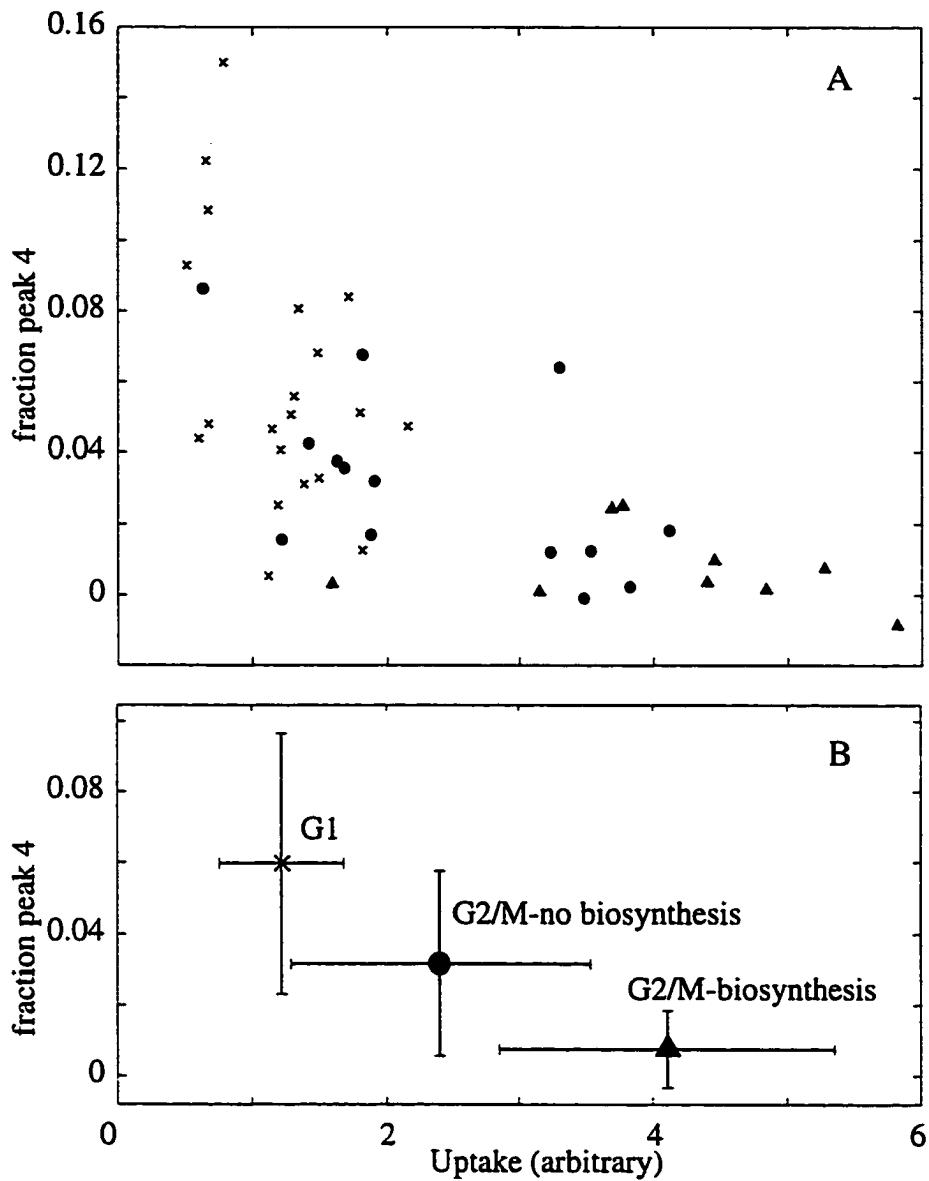


Fig. 2. 5. Correlation of fraction of peak 4 (identified in figure 1) in each cell and total substrate uptake. Cells in the G1 phase are denoted with by ×, metabolically inactive G2/M cells are denoted by ●, metabolically active G2/M cells are denoted by ▲.

A. Scatter plot.

B. Average  $\pm$  one standard deviation.

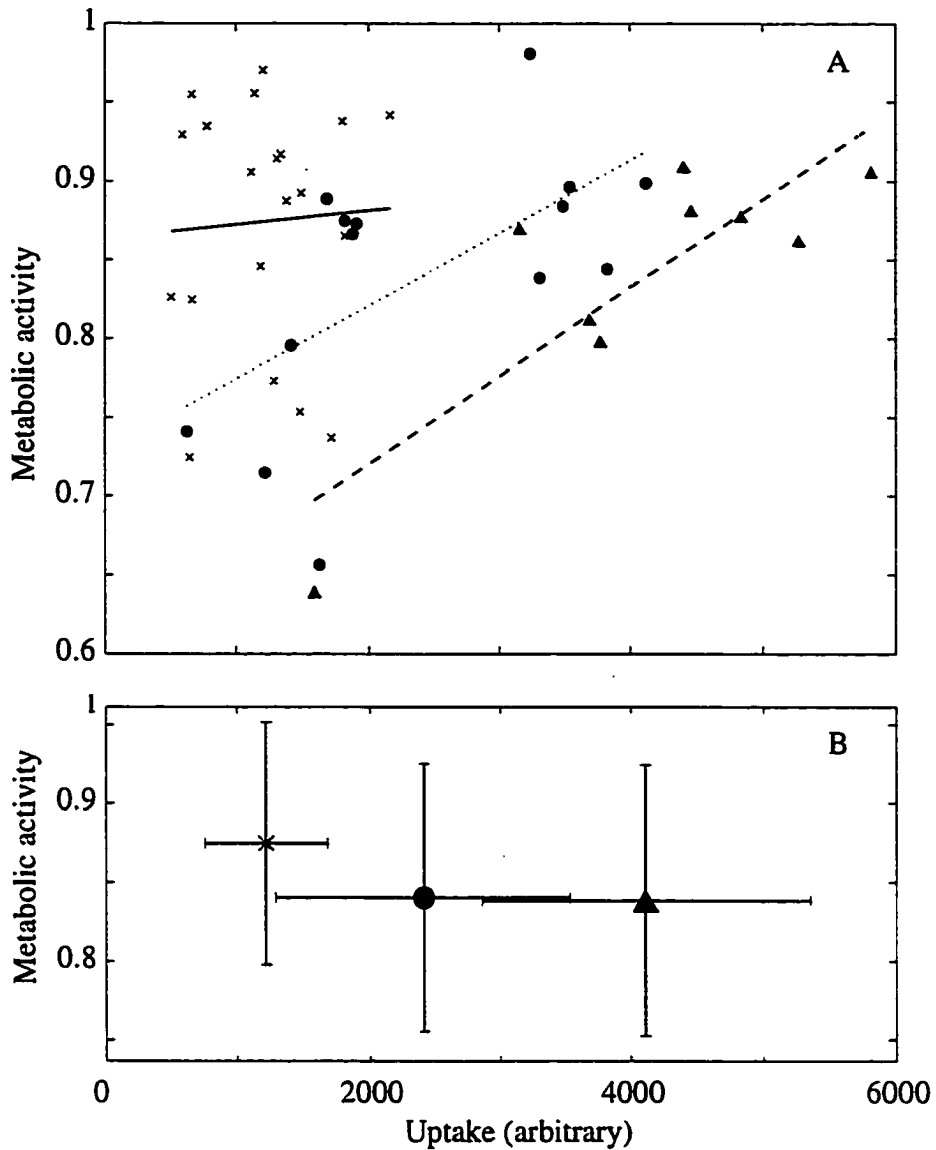


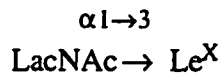
Fig. 2. 6 Correlation of metabolic activity and substrate uptake. Cells in the G1 phase are denoted with by  $\times$ , metabolically inactive G2/M cells are denoted by  $\bullet$ , metabolically active G2/M cells are denoted by  $\blacktriangle$ .

A. Scatter plot. The solid line is the least-squares fit of a line to the G1 data. The dotted line is the least squares fit of a line to the metabolically inactive G2/M cells. The dashed line is the least-squares fit of a line to the metabolically active G2/M cells.

B. Average  $\pm$  one standard deviation.

$\text{Le}^Y$  is formed by sequential action of the  $\alpha 1 \rightarrow 2$  fucosyltransferase to form the intermediate H-type II trisaccharide, followed by the  $\alpha 1 \rightarrow 3$  fucosyltransferase to form  $\text{Le}^Y$ . We saw no evidence for the H-type II intermediate, which suggests that the  $\alpha 1 \rightarrow 3$  fucosylation of H-type II was much faster than the  $\alpha 1 \rightarrow 2$  fucosylation of LacNAc.

The biosynthesis of  $\text{Le}^X$  proceeds by  $\alpha 1 \rightarrow 3$  fucosylation of LacNAc



Once  $\text{Le}^X$  is formed, it can not be converted to  $\text{Le}^Y$  because it is not a substrate for known mammalian  $\alpha 1 \rightarrow 2$  fucosyltransferases. The observation of either  $\text{Le}^X$  or  $\text{Le}^Y$  implies that all biosynthetically active cells contain the  $\alpha 1 \rightarrow 3$  fucosyltransferase. The failure to observe both  $\text{Le}^X$  and  $\text{Le}^Y$  results from the strict specificity of the  $\alpha 1 \rightarrow 2$  fucosyltransferase. Those cells that express this enzyme generate  $\text{Le}^Y$  by way of the H-type II intermediate, whose fleeting existence was not detected in our experiments. Those cells that produce  $\text{Le}^X$  lack  $\alpha 1 \rightarrow 2$  fucosyltransferase or contain much higher levels of  $\alpha 1 \rightarrow 3$  fucosyltransferase.

In contrast, oligosaccharide biosynthesis appears to be shut off during the G1 phase; we observed no biosynthesis in these cells. A higher level of glycosylation activity during the G2/M phase in HT29 cells was earlier demonstrated using bulk analysis of synchronized cells (39). Further studies will be required to determine if  $\text{Le}^X$  or  $\text{Le}^Y$  produced during the G2/M phase is excreted or biodegraded before the cell enters the G1 phase.

## 2.5 Conclusions

We demonstrate the first use of ultrasensitive laser-induced fluorescence with a high-resolution separation by capillary electrophoresis to monitor biosynthetic and biodegradation pathways within single cells. The biotransformations were correlated with cell cycle by measuring DNA ploidy before the electrophoresis analysis.

Cells are divided into several classes. Cells in the G1 phase had the lowest substrate uptake and were biosynthetically inactive. Roughly half the cells in the G2/M phase were biosynthetically active; they had the highest substrate uptake and the highest metabolic activity. Biosynthetically inactive G2/M cells were intermediate in their properties.

These data provide correlations in the activity of different enzymes within the cell, substrate uptake, and cell cycle. The regulation of the molecular machinery associated with oligosaccharide metabolism undoubtedly will change in response to differentiation and environment; the tools presented here can be used to study these changes.

Metabolic cytometry will be useful whenever a cell takes-up a fluorescent enzymatic substrate. For example, we have generated metabolic profiles based on the disaccharide  $\beta\text{Gal}(1\rightarrow3)\beta\text{GlcNAc-TMR}$  metabolism in A431 human epidermoid cancer cells and on the trisaccharide  $\alpha\text{Glc}(1\rightarrow2)\alpha\text{Glc}(1\rightarrow3)\alpha\text{Glc-TMR}$  metabolism in yeast spheroplasts (37). The last example points out one limitation of metabolic cytometry – cells must lyse under the experimental conditions. The cell wall of yeast is robust in our buffer so spheroplasts were prepared to facilitate lysis. However, all mammalian cell lines that we have tested are lysed within one minute.

Metabolic cytometry will be valuable in studying the mechanisms of metabolism. For example, a fluorescent substrate like that used in this report could be



used to study neoplastic transformations, which often have altered glycosyl transferase activity (38).

This technology can be expanded to use any of the dyes employed in image cytometry. For example, labeled antibodies can be used to monitor cell surface marker expression, which can then be correlated with oligosaccharide metabolism. Similarly, other metabolic pathways can be monitored and correlated with cell surface marker expression or phase of cell cycle.

The technique is presently limited by low throughput; about 15 minutes are required to analyze each cell. Although the technology may be improved, the throughput of chemical cytometry is unlikely to approach the throughput of conventional cytometry. However, the high information content of the signal will be of value, particularly when details of enzymatic cascades are to be studied. Rather than averaging response over a cellular population, specific sub-populations can be identified and characterized. The technology will be particularly important in embryogenesis and in fine-needle aspirants, when relatively few cells are available for analysis.

## 2.6 References

1. Edstrom JE. *Nature* **1953**, 172, 908.
2. Maholi GT, Niewisch HB. *Science* **1965**, 150, 1824-1826.
3. Kennedy RT, St. Claire RL, White JG, Jorgenson, J.W. *Mikrochim. Acta* **1987**, II, 37-45.
4. Kennedy RT, Oates MD, Cooper BR, Nickerson B, Jorgenson JW. *Science* **1989**, 246, 57-63.
5. Wallingford RA, Ewing AG. *Anal. Chem.* **1988**, 60, 1972-1975.

6. Kristensen HK, Lau YY, Ewing AG. *J. Neuroscience Methods* **1994**, 51, 183-188.
7. Gilman SD, Ewing AG. *Anal. Chem.* **1995**, 67, 58-64.
8. Colliver TL, Brummel CL, Pacholski ML, Swanek FD, Ewing AG, Winograd N. *Anal. Chem.* **1997**, 69, 2225-2231.
9. Hsieh S, Dreisewerd K, van der Schors RC, Jimenez CR, Stahl-Zeng J, Hillenkamp F, Jorgenson JW, Geraerts WP, Li KW. *Anal. Chem.* **1998**, 70, 1847-1852.
10. Fuller RR, Moroz LL, Gillette R, Sweedler JV. *Neuron* **1998**, 20, 173-181.
11. Chen G, Ewing AG. *Crit. Rev. Neurobiol.* **1997**, 11, 59-90.
12. Lillard SJ, Yeung ES, Lautamo RM, Mao DT. *J. Chromatogr.* **1995**, 718, 397-404.
13. Cheung NH, Yeung ES. *Anal. Chem.* **1994**, 66, 929-936.
14. Lee TT, Yeung ES. *Anal. Chem.* **1992**, 64, 3045-3051.
15. Xue Q, Yeung ES. *J. Chromatogr.* **1996**, 677, 233-240.
16. Huang L, Shen H, Atkinson MA, Kennedy RT. *Proc. Natl. Acad. Sci. (USA)*. **1995**, 92, 9608-9612.
17. Paras CD, Kennedy RT. *Anal. Chem.* **1995**, 67, 3633-3637.
18. Orwar O, Jardemark K, Jacobson I, Moscho A, Fishman HA, Scheller RH, Zare RN. *Science* **1996**, 272, 1779-1782.
19. Chiu DT, Lillard SJ, Scheller RH, Zare RN, Rodriguez-Cruz SE, Williams ER, Orwar O, Sandberg M, Lundqvist JA. *Science* **1998**, 279, 1190-1193.
20. Tong W, Yeung ES. *J. Neurosci. Meth.* **1997**, 76, 193-201.
21. Lillard SJ, Yeung ES. *J. Neurosci. Meth.* **1997**, 75, 103-109.
22. Lillard SJ, Yeung ES, McCloskey MA. *Anal. Chem.* **1996**, 68, 2897-2904.
23. Tong W, Yeung ES. *J. Chromatogr.* **1997**, 689, 321-325

24. Basile F, Beverly MB, Abbas-Hawks C, Mowry CD, Voorhees KJ, Hadfield TL. *Anal. Chem.* **1998**, 70, 1555-62.
25. Easterling ML, Colangelo CM, Scott RA, Amster IJ. *Anal. Chem* **1998**, 70, 2704-2709.
26. Whittal, RM, Keller, BO, Li, L. *Anal. Chem.* **1998**, 70, 5344-5347.
27. Le XC, Zhang Y, Dovichi NJ, Compston CA, Palcic MM, Beever RJ, Hindsgaul O. *J. Chromatogr.* **1997**, 781, 515-522.
28. Zhang Y, Le X, Dovichi NJ, Compston CA, Palcic MM, Diedrich P, Hindsgaul O. *Anal. Biochem.* **1995**, 227, 368-376.
29. Le X, Scaman C, Zhang Y, Zhang J, Dovichi NJ, Hindsgaul O, Palcic MM. *J. Chromatogr.* **1995**, 716, 215-220.
30. Zhao JY, Dovichi NJ, Hindsgaul O, Gosselin S, Palcic MM. *Glycobiology.* **1994**, 4, 239-242.
31. Cheng YF, Dovichi NJ. *Science* **1998**, 242, 562-564.
32. Wu S, Dovichi N.J. *J. Chromatogr.* **1989**, 480, 141-155.
33. Chen DY, Dovichi, NJ *Anal. Chem.* **1996**, 68, 690-696.
34. Sugino Y., Teraoka H., Shimono H.. *J. Biol. Chem.* **1966**, 241, 961-969.
35. Dive C, Workman P, Watson JV. *Cytometry* **1987**, 8, 552-561.
36. Yashphe J, Halvorson OH. *Science* **1976**, 191, 1283-1284.
37. Le XC, Tan W, Scaman C, Szpacenko A, Arriaga E, Zhang Y, Dovichi NJ, Hindsgaul O, Palcic MM. *Glycobiology* in press.
38. Hakomori, S. *Advances in Cancer Research.* **1989**, 52, 257-331.
39. Chou, CF., Omary, M. *J. Biol. Chem.* **1993**, 268, 4465-4472.
40. Chen, N., PhD thesis, 1999, University of Alberta, Canada

## **Chapter 3: One-dimensional proteome map of an HT29 human colon adenocarcinoma cell**

### 3.1 Introduction

The word *proteome* was coined in 1995 to refer to the total protein complement of a genome (40). The human genome encodes roughly 100,000 genes, corresponding to a similar number of proteins. Not all genes are expressed in all tissues; roughly 10,000 proteins are found in any particular cell.

The primary tool of protein analysis is 2-D gel electrophoresis, where isoelectric focusing and SDS-PAGE are performed sequentially to separate protein mixtures. 2-D protein electropherograms from tissues and tumors have been generated over the past few years (2).

This group has coined the term *chemical cytometry* to refer to the chemical analysis of single cells (1). Unlike flow cytometry, which relies on light scatter and several fluorescence spectral channels to monitor a few components within a cell, chemical cytometry relies on miniaturized separation techniques and ultrasensitive detection methods to characterize cells. Jorgenson performed the first chemical cytometry experiment using modern analytical methods in 1987 (4-5). A single cell was lysed and its contents were fluorescently labeled in a miniature reaction vial. The reaction products were then injected into a capillary chromatography column for analysis. Ewing simplified chemical cytometry by injecting the cell directly into the separation capillary, lysing the cell within the capillary, and using electrophoresis for the analysis of the cellular contents (6-9). Subsequent chemical cytometry experiments have relied on capillary electrophoresis and either laser-induced fluorescence or electrochemical detection, primarily to study single erythrocytes and neurons (10-21). Chemical cytometry has also been used to monitor the activity of a single enzyme species in erythrocytes (29-31) and entire enzymatic pathways in human cancer cell lines (1) and in yeast cells (32).

In this paper, we generate a one-dimensional proteome map from a single cell from a human cancer cell line. A typical eukaryotic somatic cell has a 10- $\mu\text{m}$  diameter, 500-fL volume, and 500-pg mass. Assuming the cell is 10% protein by weight and an average protein has a molecular weight of 25,000g/mol, the cell will contain about 2 fmol of protein. About 10,000 proteins are expressed in each cell, with an average of 200 zeptomoles (1 zmol =  $10^{-21}$  mol = 600 copies) per protein. High-sensitivity protein analysis is required for single-cell proteome mapping.

## **3.2 MATERIALS AND METHODS**

### **3.2.1 Capillary electrophoresis/laser-induced fluorescence detection**

Capillary electrophoresis was performed with a locally constructed instrument (33-35). Separation was performed in a 40-cm long, 19- $\mu\text{m}$  ID, and 144- $\mu\text{m}$  OD fused-silica capillary. The separation buffer was 50 mM phosphate, 11 mM sodium pentasulfate (SPS), at pH 6.8. Detection was performed with a locally constructed ultrasensitive laser-induced fluorescence detector, based on a sheath-flow cuvette. The cuvette had a 200- $\mu\text{m}$  square flow chamber and 1-mm thick windows. The flow chamber was held in a stainless-steel fixture, which was held at ground potential during electrophoresis. A 12-mW argon ion laser beam was used for excitation at 488 nm. The beam was focused to a ~15- $\mu\text{m}$  diameter spot about 50- $\mu\text{m}$  downstream from the capillary exit. Fluorescence was collected at right angles with a 60 $\times$ , 0.7 N.A. microscope objective, filtered with a 630DF30 bandpass filter from Omega Optical, imaged onto an iris to block stray light, and detected with a Hamamatsu R1477 photomultiplier tube operated at 1,000 V.

### **3.2.2 Cell culture**

The HT29 cell line (human colon adenocarcinoma) was grown to 80% confluence in Dulbecco's modified Eagle's medium, supplemented with 10% fetal calf serum and 40 µg/mL gentamycin at 37°C in 5% CO<sub>2</sub> atmosphere.

### **3.2.3 Protein extract**

Roughly 10<sup>6</sup> HT29 cells were washed five times with phosphate-buffered saline (PBS) and resuspended in 100 µL of water. The cells were sonicated for 20 min at 4 °C. The suspension was centrifuged at 2500 RPM (600 × g) for 10 min. A 3 µL aliquot of the supernatant was mixed with 3 µL water and 2 µL of 25 mM NaCN.

### **3.2.4 Proteome analysis from cell extract**

A 250-pL plug of the protein extract containing 2.5 mM NaCN was hydrodynamically injected at 11 kPa pressure for 3 s onto the electrophoresis column. A 10 mM aqueous solution of FQ was injected for 1 s. Next, the running buffer was injected electrokinetically at 50 V/cm for 5 s. The solution was incubated at 65 °C for 3 min and then separated at 16 kV.

### **3.2.5 Single-cell proteome analysis**

A cell suspension was prepared in 2.5 mM NaCN in PBS. A drop of this suspension was placed on a microscope slide and observed through an inverted microscope. The capillary was placed over a cell using micromanipulators. An 11 kPa partial vacuum was applied to the distal end of the capillary for 1 s, drawing the cell approximately 0.2 mm within the capillary. A plug of 10 mM FQ solution was injected for 1 s. The capillary tip was placed in a vial containing the SPS running

buffer, and the vial was placed in a 65 °C ultrasound bath for 30 s to lyse the cell. After lysis and reaction, the separation was performed at 16 kV.

### **3.2.6 Protein purification**

One-dimensional SDS-polyacrylamide gel electrophoresis was performed on the protein extract with the BioRad Mini-Protean II system (7 cm × 10 cm minigel). A 10% - 20% TRIS-HCl acrylamide gel of 1 mm thickness was used for the purification. The gel was stained with imidazole and zinc sulfate solution from the BioRad zinc stain kit. The major protein band at ~100 kDa was excised from the gel and purified by the use of a Millipore Ultrafree-DA centrifugal filter. The protein sample was then loaded to hydrated PIERCE Slide-A-Lyzer dialysis cassettes to be dialyzed against CE running buffer that had been diluted 1:10 in water.

### **3.2.7 Two-dimensional gel electrophoresis**

The protein extract was first fractionated by ultrafiltration through 30 kDa and 100 kDa molecular weight cut-off filters. The filters were regenerated cellulose membranes (Amicon Microcon), that had been soaked in a 10% Triton X-100 solution overnight. The ultrafilters were rinsed with deionized water. Next, two 500- $\mu$ L aliquots of deionized water were passed through the devices with the aid of a centrifuge. The filters were inverted and residual water was discarded.

To prepare a 30 kDa to 100 kDa fraction, 350  $\mu$ L of the HT29 protein extract was first passed through the 100 kDa ( $\pm$ 10-20%) molecular weight cut-off filter by centrifuging at 3000  $\times$  G for 10 min. The membranes were inverted and the <100 kDa fraction was recovered by spinning the tube at 1000  $\times$  g for 3 min. The filtrate was then transferred to the 30 kDa ( $\pm$ 10-20%) filter and spun at 14000  $\times$  g for 3 min. The



membrane was inverted and the 30-100 kDa fraction was collected in a new tube by spinning at  $1000 \times g$  for 3 min.

This 30-100 kDa fraction was separated by isoelectric focusing (IEF) by mixing a 15  $\mu\text{L}$  aliquot with 9.5 M urea, 2% Triton X-100, 5%  $\beta$ -mercaptoethanol, 1.6% BioRad 5/7 ampholyte, and 0.4% BioRad 3/10 ampholyte. A 10  $\mu\text{L}$  aliquot of the above mixture was added onto a tube gel (BioRad). A buffer made from 9 M urea, 0.8% BioRad 5/7 ampholyte, 0.2% BioRad 3/10 ampholyte, 0.0025% bromophenol blue was used to overlay the protein/ampholyte solution. The tube gel was run at 500 V for 10 min and then at 750 V for 3 h.

SDS-PAGE was used for the second dimension of the separation. The IEF gel was removed from the tube and covered with a reducing buffer prepared from 0.0625 M Tris-HCl at pH 6.8, 2.3 % SDS, 5%  $\beta$ -mercaptoethanol, 10% glycerol, 0.00125% bromophenol blue. The gel was then placed on an SDS-PAGE gel (12% separating and 5% stacking, prepared the day before). A 10  $\mu\text{L}$  aliquot of a 1:20 dilution of BioRad Silver Stain SDS-PAGE Molecular Weight Standards (Low Range) was added to the standards well. The SDS-PAGE gel was run at 200 V for 46 min in a BioRad Tris/Glycine/SDS buffer. Once the separation was complete, the gel was stained with the BioRad Silver Stain Plus kit.

### **3.2.8 In-gel digestion of proteins from Silver-stained Polyacrylamide gel**

Protein spots were excised from the gel. A “control” experiment was done by cutting a piece of gel from the edge of the gel and processed in parallel with the protein spots. Gel pieces were put into 0.6 mL silicalized plastic vials and rinsed with 100 mM  $\text{NH}_4\text{HCO}_3$  to ensure the pH was about 8.5. This  $\text{NH}_4\text{HCO}_3$  solution was

removed by pipette and replaced with 10  $\mu\text{L}$  of the same solution and 2  $\mu\text{L}$  of 90 mM dithiotreitol (DDT). The gels were smashed using thin 0.25 mL plastic vials and reduced for 30 min at 50 °C. Cooled to ambient temperature, vials were covered by foil and then 2  $\mu\text{L}$  of 200 mM iodoacetamide was added. The gel samples were incubated at room temperature for 30 min, then 1  $\mu\text{L}$  of 0.2  $\mu\text{g}/\mu\text{L}$  trypsin was added. The protein samples were digested at 37 °C for 2 to 5 hours. Extraction of peptides was accomplished with three changes of 20  $\mu\text{L}$  of 75% acetonitrile in 0.25 % trifluoroacetic acid /water with 20 second vortex and 20 min sonication, followed by 10  $\mu\text{L}$  of acetonitrile. The pooled extracts were evaporated to dryness in a vacuum centrifuge.

### **3.2.8 Sample preparation for MALDI MS**

A two-layer method was used for MALDI mass spectrometry analysis. The first layer solution contains 10 mg of matrix ( $\alpha$ -cyano-4-hydroxy-*trans*-cinnamic acid) in 1 mL methanol/acetone (1:4 v/v). The second layer was a saturated solution of matrix in 40 % methanol / water. 5  $\mu\text{L}$  of second layer was added to each vial containing dried sample and vortex to dissolve well. 2  $\mu\text{L}$  of first layer was deposited onto a probe tip, quickly spread and evaporated to form a thin matrix layer. Then 0.5 to 1.5  $\mu\text{L}$  of sample was deposited onto the first layer, allowed to dry, and washed three times with water.

## **3.3 RESULTS AND DISCUSSION**

### **3.3.1 CE separation**

There are several issues that complicate high-sensitivity proteome analysis by laser-induced fluorescence. While native fluorescence can be used to detect minute

amounts of proteins that are rich in tryptophan, the UV lasers necessary to excite fluorescence tend to be expensive, require frequent alignment, and have a relatively short lifetime.

Rather than detecting native fluorescence, we use the fluorogenic reagent 3-(2-furoyl)quinoline-2-carboxaldehyde (FQ) to fluorescently label proteins. This reagent is non-fluorescent until it reacts with a primary amine in the presence of cyanide anion. The fluorescent product is excited with a low power argon-ion laser operating at 488 nm. These hard-sealed, fixed-wavelength, air-cooled lasers are commonly used in DNA sequencers, flow cytometers, and photolithography devices; they are reliable, simple to operate, and relatively inexpensive.

We have reported that FQ can be used to label proteins that are lower than  $10^{-12}$  M in concentration (36-37). These labeled proteins can be separated by capillary electrophoresis and detected by high sensitivity laser-induced fluorescence.

Unfortunately, fluorescent labeling does not go to completion for most proteins. Only a fraction of the available lysine residues is accessible to the reagent and the reaction produces a large number of products. If there are  $n$  possible labeling sites, then there are  $2^n - 1$  possible fluorescent products; a protein with 10 primary amines can generate 1023 different fluorescent products (38). The FQ labeling reaction converts cationic lysine residues to neutral products, which changes the size-to-charge ratio of the product. Each of the products has a different electrophoretic mobility, which leads to broad electrophoresis peaks with poor resolution (39).

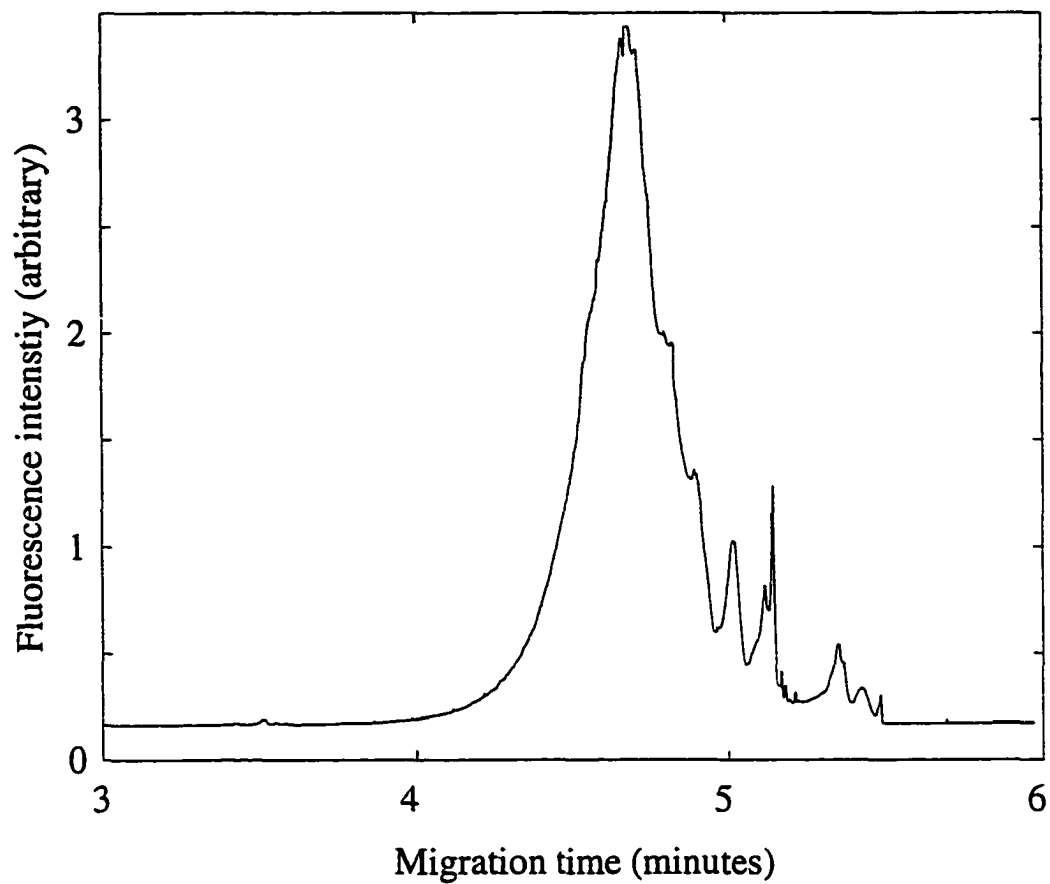


Figure 3.1 Separation of HT29 protein extract using an SDS buffer.

We have reported that the use of sub-micellar concentrations of SDS in the separation buffer eliminates multiple labeling artifacts in FQ-labeled proteins (34-35). We believe that the anionic surfactant ion-pairs with the unlabeled lysine residues, neutralizing the charge on the cationic lysine residues and resulting in a similar mobility to proteins that had that site fluorescently labeled with FQ.

Figure 3.1 presents the separation of the protein extract prepared from roughly  $10^6$  HT29 human colon adenocarcinoma cells using the SDS buffer of reference 36. Although this buffer system produces high theoretical plate counts for standard proteins, the HT29 proteome is very poorly resolved. Unfortunately, SDS also strongly binds to other residues on the protein, which leads to a constant size-to-charge ratio for the protein and generates an electropherogram with a very narrow separation window.

We have replaced SDS with sodium pentanesulfonate (SPS) as a buffer additive, Figure 3.2. SPS, like SDS, collapses the multiple-labeling envelope to a single, sharp peak. More importantly, there are many more components resolved in this separation than were observed with the SDS buffer in Figure 3.1. SPS appears to have a much lower affinity for neutral amino acid residues, and appears to primarily interact with the  $\epsilon$ -amine lysine residues. The use of this surfactant at low concentrations does not produce a constant charge-to-size ratio for proteins but instead results in a relatively large separation window.

### **3.3.2 Single-cell proteome maps**

Figure 3.2 also presents electropherograms generated from two single cells. Each cell was introduced into the capillary using a simple vacuum system and lysed.

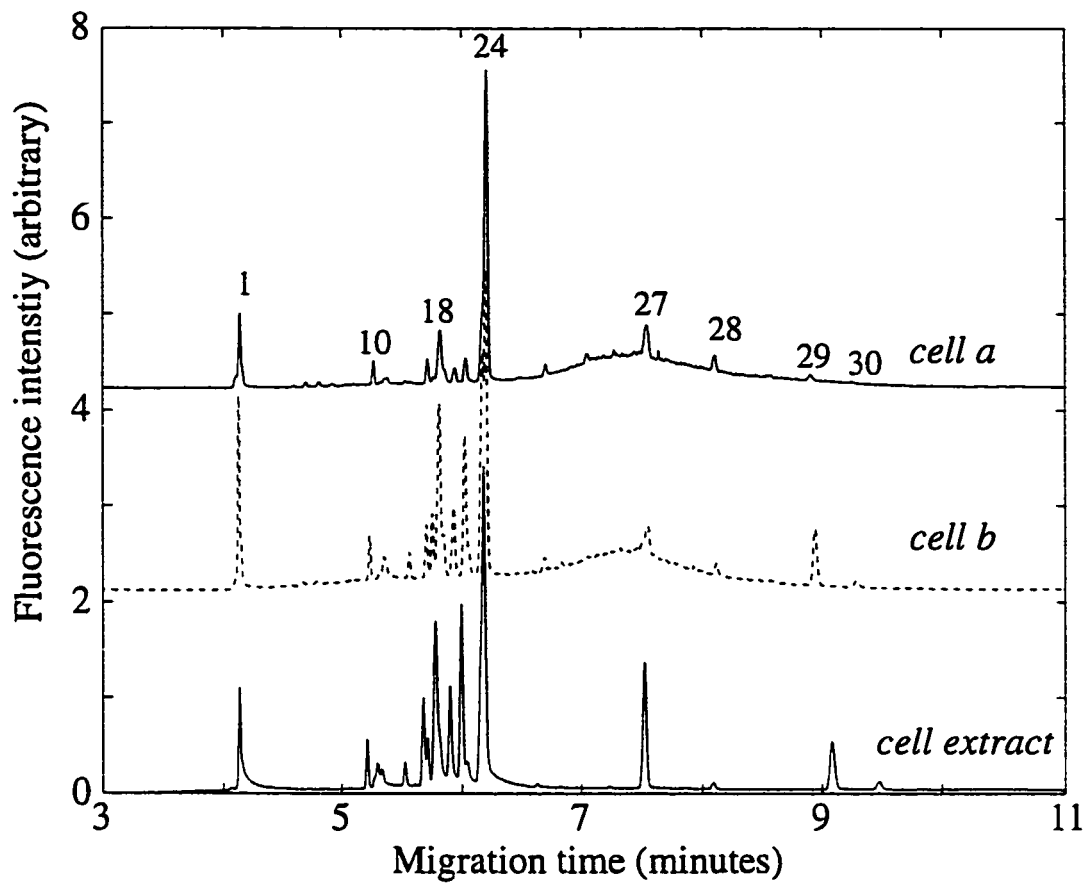


Figure 3. 2 Free-solution electrophoresis proteome analysis from HT29 cells. The cell extract was generated from roughly  $10^6$  cells. Individual HT29 cells were used to generate the single-cell curves. An SPS buffer was used for the separations.

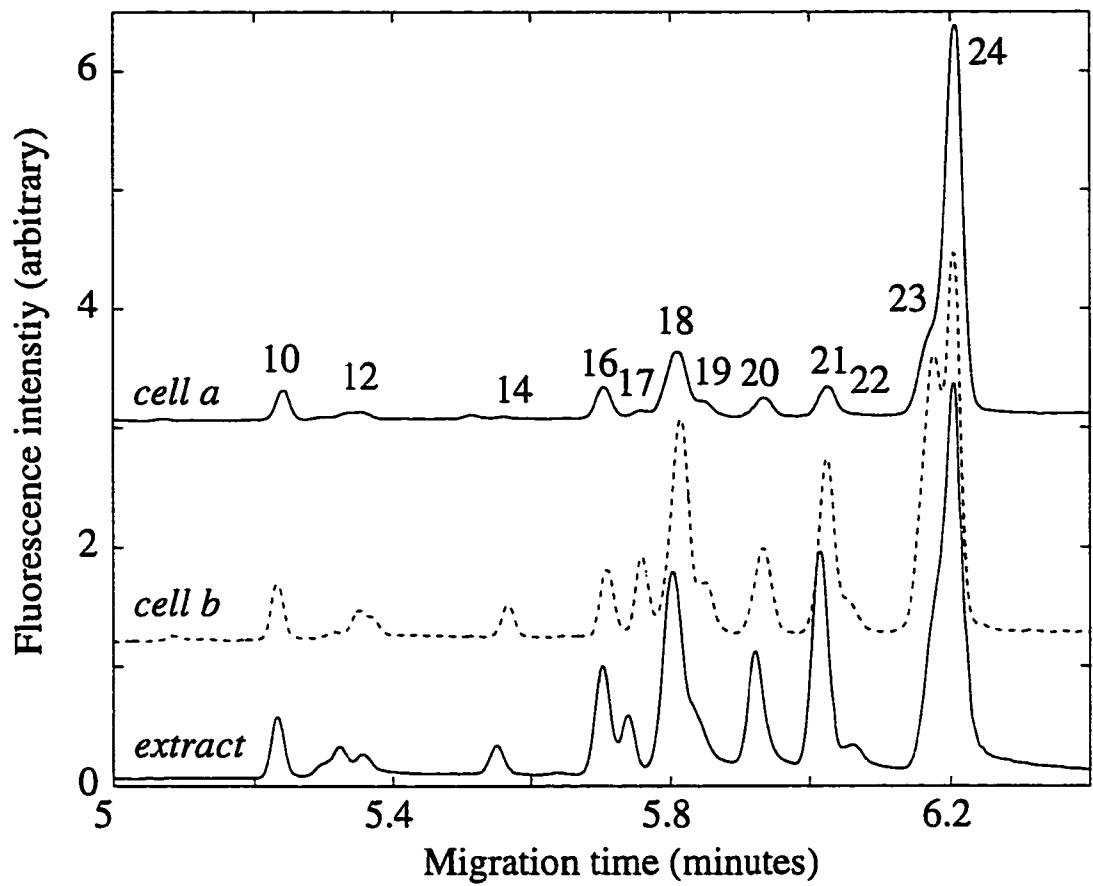


Figure 3.3 Detail of the single-cell proteome maps.

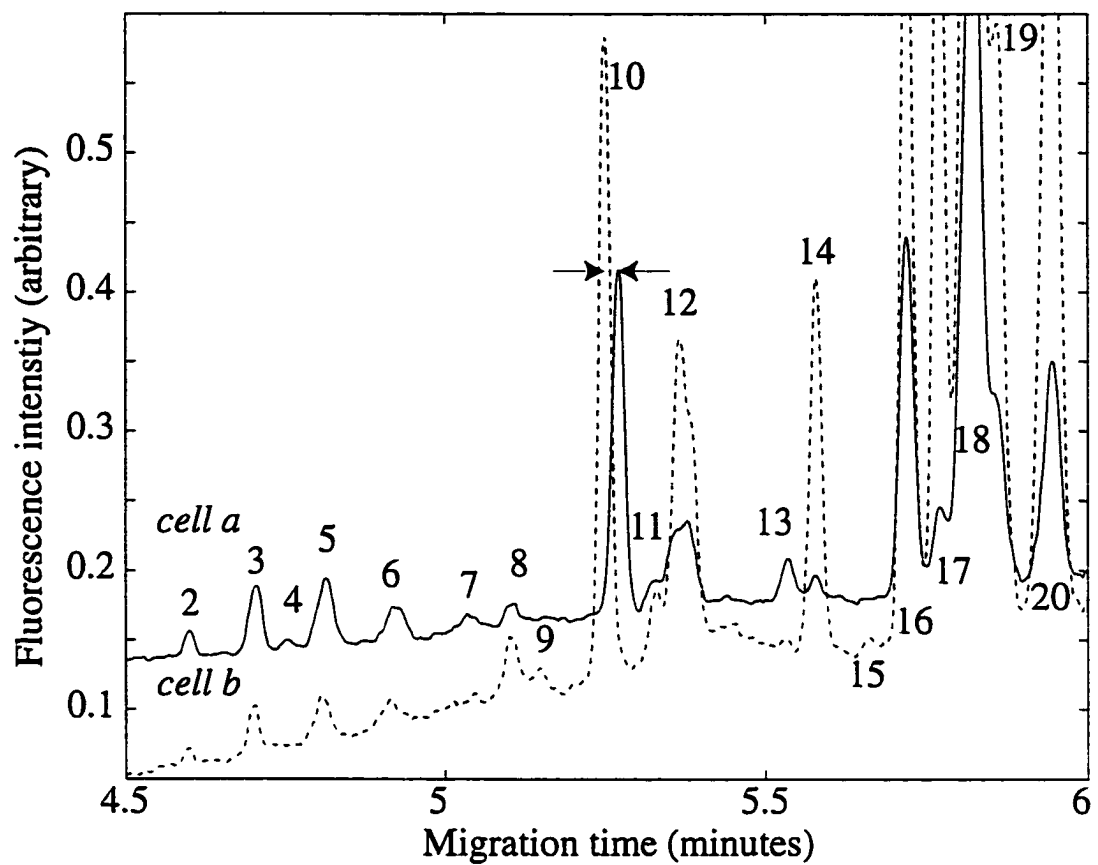


Figure 3.4 Detail of the single-cell proteome maps.



The liberated proteins were fluorescently labeled by reaction with FQ, separated by capillary electrophoresis, and detected by laser-induced fluorescence. The protein electropherogram from a single cell was similar, but not identical, to that generated by the cell extract.

Figures 3.3 and 3.4 compare the middle portion of the protein electropherogram for the two cells. In all cases, plate counts are quite high, approaching 400,000. There was a noticeable variation in protein expression between the two cells. For example, peaks 14 and 17 were barely detected and peaks 12, 19 and 22 were under-expressed in *cell a*. Peaks 23 and 24 were resolved into two roughly equal components in *cell b*, whereas peak 23 appeared as a low shoulder on peak 24 in *cell a*. The cell extract electropherogram was a rough average of the two single-cell electropherograms. Peak 10, shown in detail in Figure 3.4, shifted to a slightly longer migration time for *cell a* (solid curve). This shift could be due to the disappearance of component 10 in *cell b* and the appearance of another component in *cell a*, where the latter component serendipitously has a similar migration time as peak 10. However, a more intriguing interpretation of the data is that peak 10 is generated by a protein and that the mobility shift represents a post-translational modification of that protein. For example, the mobility shift could have been due to the addition of a single phosphate group to the protein in *cell b*, producing a slightly longer migration time.

There was a set of small peaks in the 4.5-5 minute range. Most of these components were present in both cells. The minor components 9 and 15 were two of the few components present in *cell b* but not in *cell a*.

There was a broad peak at 7 to 8 min in the single-cell protein electropherograms that was not observed in the cell-extract electropherogram, Figure 3.5. We believe that this broad peak is an envelope generated by hydrophobic proteins that were lost during the preparation of the cell extract. In the single-cell experiment, the cell was lysed within the capillary and hydrophobic proteins were solubilized by the SPS in the separation buffer. The broad peak is poorly resolved because the components interact with the capillary wall. Some components interact strongly with the capillary wall. These components generate a large fluorescent peak when the capillary is flushed with a sodium hydroxide solution after a single-cell assay. The cell extract preparation did not use a surfactant; most hydrophobic proteins were lost on the glassware used to prepare the extract and the broad peak was not observed in the cell extract electropherogram.

There was a significant variation in protein expression from cell to cell. We analyzed five cells and compared the protein expression for 10 of the major components. The results are summarized in Table 3.1. Most components had a large range in expression level, which reflects the complex biology of this cell line. These cells are likely found in different stages of the cell cycle, leading to differences in the expression of cell-cycle dependent proteins. The cells also have experienced different levels of confluence; those cells growing in close proximity to their neighbors will presumably express different levels of structural proteins. Although there is a wide variation in protein expression between cells, the average expression level is consistent with the expression level obtained from cell extracts at the 95% confidence level.

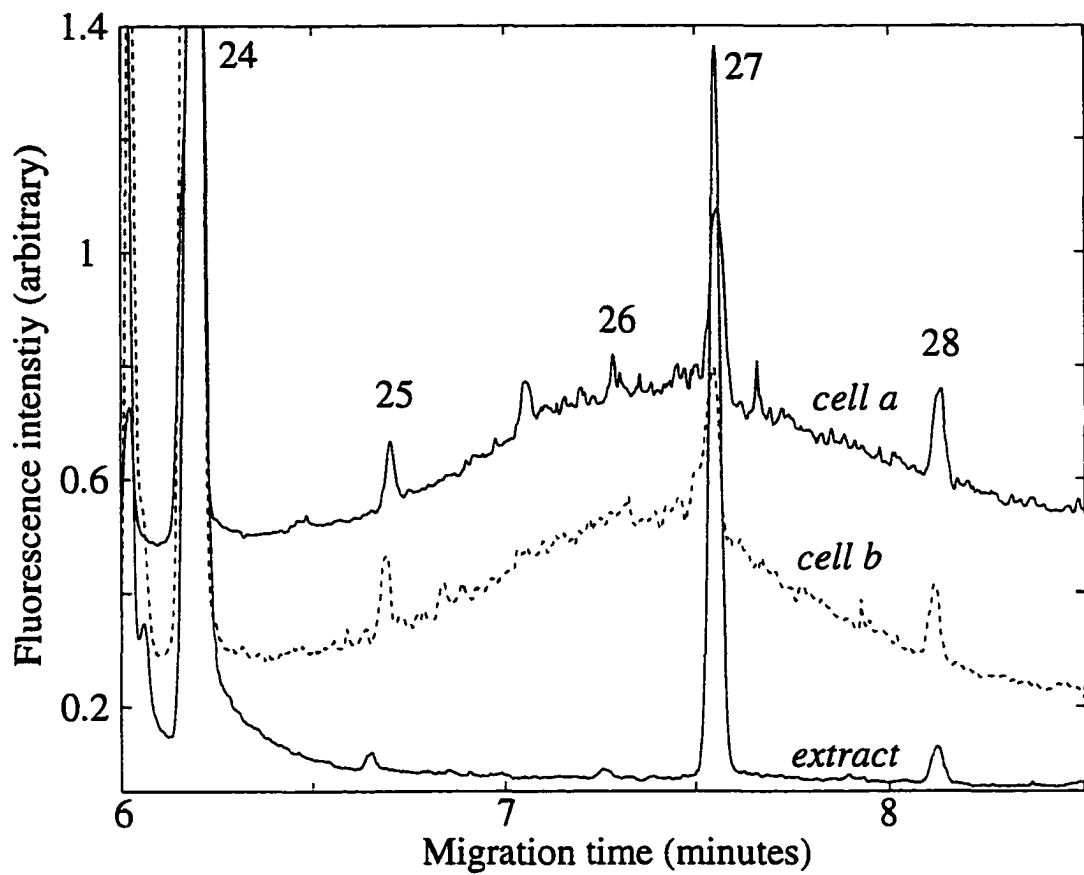


Figure 3.5 Detail of the single-cell proteome maps.

### **3.3.3 Protein identification.**

This group is in the process of identifying the components detected by the single-cell proteome analysis. To test if the peaks were due to proteins or amino acids, I mixed the protein extract with amino acid standards to generate a  $10^{-7}$  M solution and repeated the experiment. None of the amino acids generated detectable peaks in the cell extract signal. This result is not surprising. Under our experimental conditions, FQ reacts much more readily with the  $\epsilon$ -amine of lysine than with the  $\alpha$ -amine group of amino acids. The reaction discriminates against the labeling of biogenic amines and instead favors the labeling of proteins. This result is in contrast with the results obtained by Jorgenson, who used a fluorogenic reagent that appears to react more efficiently with small amines contained within single neurons (4).

To characterize the proteins responsible for these peaks, a cell extract was separated using classic SDS-PAGE and detected by zinc-ion staining. The major component had an apparent molecular weight of 100 kDa. This protein was isolated from the gel and was used to spike the cell extract, Figure 3.6. This spiked component co-migrated with peak 24 in the free-solution electropherogram.

To verify that the other components were not small biogenic amines, we passed the protein extract through a series of ultrafilters to collect the fraction with molecular weight between 30-kDa and 100-kDa. This sample was then fluorescently labeled and analyzed by capillary electrophoresis, Figure 3.7. This experiment used a slightly longer capillary than was used in the earlier experiments. Once scaled by an appropriate factor, the electropherogram is quite similar to that observed in the cell extract of Figure 3.2.

**Table 3.1****Relative protein expression for extract and single-cell analysis**

	Cell extract	Single cell data <sup>*</sup>
Peak number	protein expression	protein expression
1	0.088	0.125 ± 0.047
2	0.041	0.039 ± 0.005
3	0.022	0.024 ± 0.009
4	0.022	0.015 ± 0.007
5	0.075	0.051 ± 0.013
7	0.139	0.123 ± 0.043
8	0.085	0.077 ± 0.031
9	0.154	0.081 ± 0.042
10	0.268	0.359 ± 0.17
11	0.106	0.106 ± 0.091

<sup>\*</sup> n = 5; mean ± standard deviation

Total protein expression is determined by summing the peak heights from the major components. Peak 6 was not included in the analysis because its height was difficult to determine accurately. Relative protein expression is determined by dividing the peak height by the total protein expression. Data from five single-cell electropherograms was used. The relative precision in protein expression from a cell extract is about 5%.

Components 19 and 23 were underrepresented and component 15 and 17 were over represented in the fractionated sample. The other components were present in roughly similar proportion as was observed in the cell extract. Most of the components in the single-cell electropherogram are generated by proteins with molecular weight ranging from 30 to 100 kDa.

MALDI MS was used to identify this protein from two-dimensional gel electrophoresis (3.3.4). After submitting the m/z data to SwissProt database, the data 58% matches a 94,300 Da protein called Heat shock 70 KD protein 4, as Table 3.2.

#### **3.3.4 Two-dimensional gel electrophoresis analysis of HT29 proteins.**

It is worth comparing the performance of our one-dimensional proteome mapping with a conventional two-dimensional separation. Figure 3.8 presents a classic IEF/SDS-PAGE gel electropherogram from the 30- to 100-kDa fraction of the HT29 extract. The first dimension separation was based on IEF while the second dimension was based on SDS-PAGE. The proteins were visualized by treatment with silver-stain. Proteins with molecular weight above 70 kDa did not migrate on this gel. The major component with molecular weight ~100 kDa was not observed.

In general, each dimension of the separation resolved about 30-50 components. The combination of the two separation techniques could resolve nearly a thousand components. Many more components were present within the sample. Some were present at too low a concentration to be detected. Others had extreme isoelectric focusing points and were lost from the first dimension separation. Others had a molecular weight that caused them to be lost during sample pretreatment.

**Table 3.2**

**Protein identification by MALDI MS**

M/Z submitted	MH+ matched	Delta Da
951.3000	949.5219	1.7781
1117.5000	1117.6469	-0.1469
1117.5000	1117.5927	-0.0927
1117.5000	1116.5611	0.9389
1149.4000	1149.554	-0.1540
1316.4000	1315.6932	0.7068
1320.4000	1321.7116	-1.3116
1320.4000	1319.6807	0.7193
1347.4000	1347.6942	-0.2942
1347.4000	1348.7146	-1.3146
1383.3000	1382.6448	0.6552
1449.6000	1449.8066	-0.2066
1793.1000	1792.9090	0.1910
2011.0000	2009.0820	1.9180

10/17 matches (58%). 94300.5 Da, pI = 5.18. Swissprot. Acc. # P34932

Human heat shock 70 KD protein 4 ( heat shock 70-related protein APG-2)  
(HSP70RY)

7 unmatched masses: 1229.5000, 1235.7000, 1643.7000, 1701.6000,  
1919.8000, 1948.4000, 1970.6000

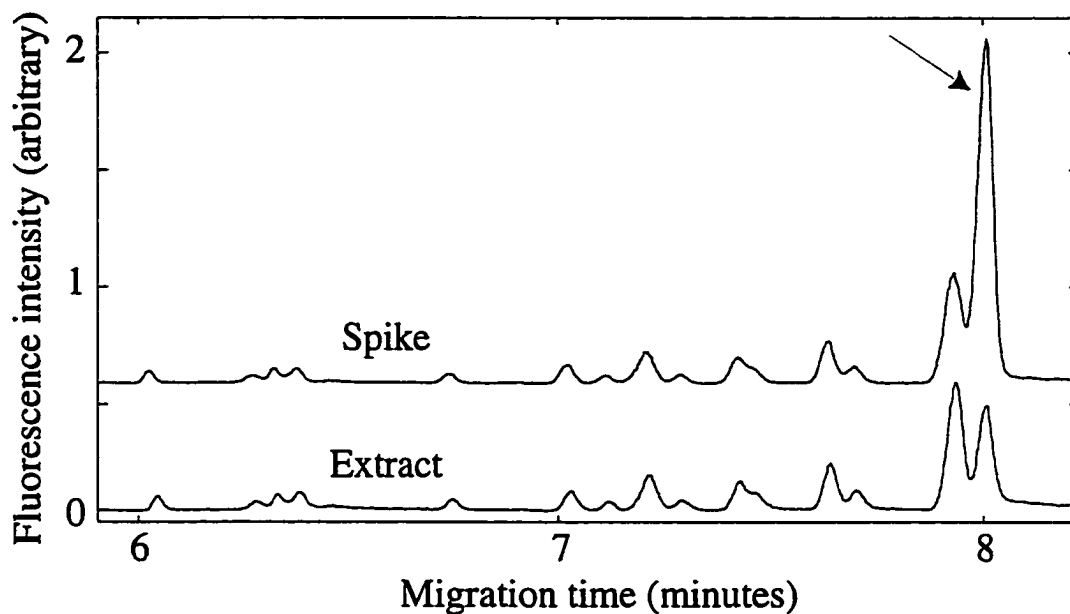


Figure 3.6 Identification of component 10 as a ~100 kDa protein. The entire HT29 cell extract was separated by SDS-PAGE. The gel was treated with a zinc stain, and the main component was excised from the gel, purified, and used to spike the cell extract. The bottom electropherogram was obtained from the cell extract and the top electropherogram was obtained from the spiked cell extract. The spiked-component is marked with the arrow and co-migrated with component 24.



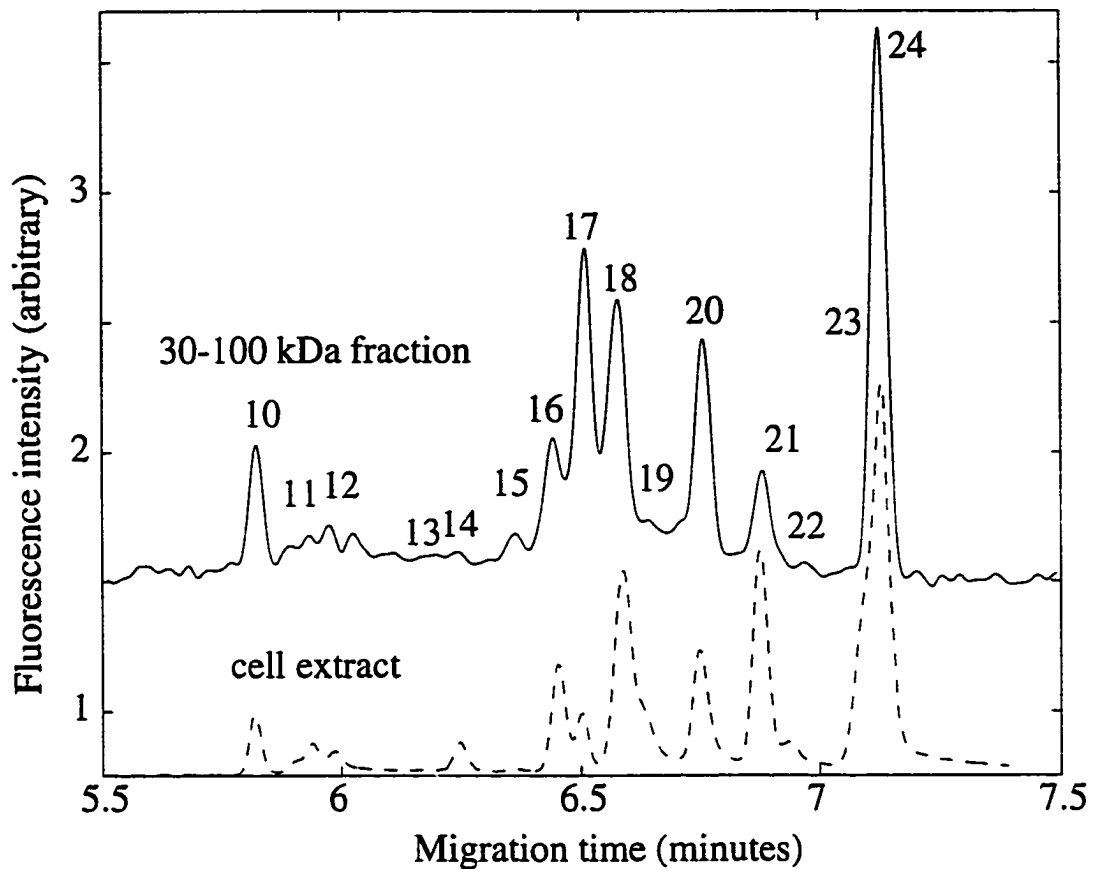
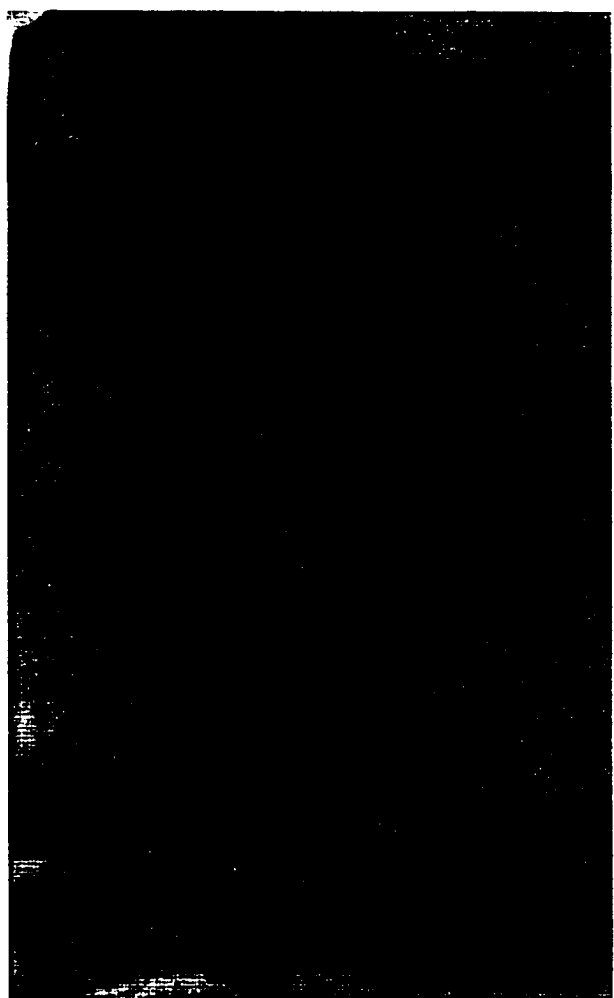


Figure 3.7 Verification that most components are high molecular weight proteins. The cell extract of Figures 2-5 was passed through a series of ultrafilters, and the 30-100 kDa fraction was isolated. A slightly longer capillary was used to generate this electropherogram compared to earlier experiments. The time-axis of the Figure 3 data was scaled to match the migration time of the fractionated sample; this electropherogram was added to the figure to compare the fractionated and entire cell-extract electropherograms.

9

IEF  
(pI)

4



21 (kDa) 66  
SDS/PAGE

Figure 3.8 Two-dimensional electrophoresis analysis of an HT29 protein extract. The first dimension separation was based on isoelectric focusing and the second dimension was based on SDS-PAGE, which separates proteins based on their size. The proteins were visualized by treating the gel with a silver stain. A size marker was also run at the bottom side of the gel; the molecular weight of the standards is shown.

### 3.4 Conclusions

The word *proteome* was coined to refer to the total protein complement of a genome (40). The portion of the proteome that is expressed by an organism varies in time, between tissues, and in response to environmental factors.

Analytical chemists, interested in protein analysis from single cells, have used mass spectrometry to identify peptides in single giant snail neurons and hemoglobin in single erythrocytes (41-47). However, the sensitivity of mass spectrometry is not yet sufficient to study proteins present in typical somatic cells (47). There have been several reports of the use of capillary-based separations and fluorescence detection for the analysis of proteins from single cells (3, 12-13); these analyses were only able to detect a few major components within the cell. There have also been a number of reports of the analysis of amino acids and biogenic amines from single cells (5, 8, 16, 24).

This chapter presents the first one-dimensional proteome map from a single somatic cell. The separation resolves roughly 12 major and 20 minor proteins, most with molecular weight between 30 kDa and 100 kDa. There was a large variation in protein expression between cells, but the average expression level was consistent with the protein expression observed in a cell extract prepared from  $10^6$  cells. Single cell proteome mapping reveals cell-to-cell heterogeneity in protein expression that is obscured in the analysis of cell extracts.

The peak capacity of the one-dimensional proteome map is similar to that observed for one-dimensional IEF or one-dimensional SDS-PAGE. Many more components are resolved in the two-dimensional IEF/SDS-PAGE separation. Clearly, a second separation method (48) must be combined with sub-micellar electrophoresis to match the peak capacity produced by IEF/SDS-PAGE.

Although the one-dimensional electrophoresis technique produces lower peak capacity than conventional two-dimensional electrophoresis, the analysis is performed on a single cell, which represents roughly a million-fold improvement in the amount of sample compared with conventional two-dimensional electrophoresis (49-50). This chemical cytometry method reveals the distribution in protein expression between cells, which is hidden by classic proteome analyses performed on cell extracts.

### 3.5 References

1. Krylov, S.N.; Zhang, Z.; Chan, N.W. C.; Arriaga, E.; Palčić, M.M.; Dovichi, N.J. *Cytometry*, 1999, 37, 15-20.
2. Wimmer, K.; Kuick, R.; Thoraval, D.; Hanash, S. M. *Electrophoresis* 1996, 17, 1741-51.
3. Maholi, G.T.; Niewisch, H.B. *Science* 1965, 150, 1824-1826.
4. Kennedy, R.T.; St. Claire, R.L.; White, J.G.; Jorgenson, J.W. *Mikrochim. Acta* 1987, II, 37-45.
5. Kennedy, R.T.; Oates, M.D.; Cooper, B.R.; Nickerson, B.; Jorgenson, J.W. *Science* 1989, 246, 57-63.
6. Wallingford, R.A.; Ewing, A.G. *Anal. Chem.* 1988, 60, 1972-1975.

7. Kristensen, H.K.; Lau, Y.Y.; Ewing, A.G. *J. Neuroscience Methods* **1994**, *51*, 183-188.
8. Gilman, S.D.; Ewing, A.G. *Anal. Chem.* **1995**, *67*, 58-64.
9. Chen, G.; Ewing, A.G. *Crit. Rev. Neurobiol.* **1997**, *11*, 59-90.
10. Hogan, B.L.; Yeung, E.S. *Anal. Chem.* **1992**, *64*, 2841-2845.
11. Lee, T.T.; Yeung, E.S. *Anal. Chem.* **1992**, *64*, 3045-3051.
12. Xue, Q.; Yeung, E.S. *J. Chromatogr.* **1994**, *661*, 287-295.
13. Cheung, N.H.; Yeung, E.S. *Anal. Chem.* **1994**, *66*, 929-936.
14. Lillard, S.J.; Yeung, E.S.; Lautamo, R.M.; Mao, D.T. *J. Chromatogr.* **1995**, *718*, 397-404.
15. Tan, W.; Parpura, V.; Haydon, P.G.; Yeung, E.S. *Anal. Chem.* **1995**, *67*, 2575-2579.
16. Chang, H.T.; Yeung, E.S. *Anal. Chem.* **1995**, *67*, 1079-1083.
17. Fuller, R.R.; Moroz, L.L.; Gillette, R.; Sweedler, J.V. *Neuron* **1998**, *20*, 173-181.
18. Lillard, S.J.; Yeung, E.S. *J. Chromatogr.* **1996**, *687*, 363-369.
19. Tong, W.; Yeung, E.S. *J. Chromatogr.* **1996**, *685*, 35-40.
20. Wang, Z.; Yeung, E.S. *J. Chromatogr.* **1997**, *695*, 59-65.
21. Fuller, R.R.; Moroz, L.L.; Gillette, R.; Sweedler, J.V. *Neuron* **1998**; *20*:173-181.
22. Huang, L.; Shen, H.; Atkinson, M.A.; Kennedy, R.T. *Proc. Natl. Acad. Sci. (USA)* **1995**, *92*, 9608-9612.
23. Paras, C.D.; Kennedy, R.T. *Anal. Chem.* **1995**, *67*, 3633-3637.
24. Orwar, O.; Jardemark, K.; Jacobson, I.; Moscho, A.; Fishman, F.A.; Scheller, R.H.; Zare, R.N. *Science* **1996**, *272*, 1779-1782.

25. Chiu, D.T.; Lillard, S.J.; Scheller, R.H.; Zare, R.N.; Rodriguez-Cruz, S.E.; Williams, E.R.; Orwar, O.; Sandberg, M.; Lundqvist, J.A. *Science* **1998**, *279*, 1190-1193.
26. Lillard, S.J.; Yeung, E.S.; McCloskey, M.A. *Anal. Chem.* **1996**, *68*, 2897-2904.
27. Lillard, S.J.; Yeung, E.S. *J. Neurosci. Meth.* **1997**, *75*, 103-109.
28. Tong, W.; Yeung, E.S. *J. Neurosci. Meth.* **1997**, *76*, 193-201.
29. Xue, Q.; Yeung, E.S. *J. Chromatogr.* **1996**, *677*, 233-240.
30. Tan, W.; Yeung, E.S. *Anal. Biochem.* **1995**, *226*, 74-79.
31. Xue, Q.; Yeung, E.S. *Anal. Chem.* **1994**, *66*, 1175-1178.
32. Le, X.C.; Tan, W.; Scaman, C.; Szpacenko, A.; Arriaga, E.; Zhang, Y.; Dovichi, N.J.; Hindsgaul, O.; Palcic, M.M., *Glycobiology* **1999**, *9*, 219-225.
33. Cheng, Y.F.; Dovichi, N.J. *Science* **1988**, *242*, 562-564.
34. Cheng, Y.F.; Wu, S.; Chen, D.Y.; Dovichi, N.J. *Anal. Chem.* **1990**, *62*, 496-503.
35. Wu, S.; Dovichi, N.J., *J. Chromatogr.* **1989**, *480*, 141-155.
36. Pinto, D.M.; Arriaga, E.A.; Craig, D.; Angelova, J.; Sharma, N.; Ahmadzadeh, H.; Dovichi, N.J.; Boulet, C.A. *Anal. Chem.* **1997**, *69*, 3015-3021.
37. Lee, I.H.; Pinto, D.; Arriaga, E.A.; Zhang, Z.; Dovichi, N.J. *Anal. Chem.* **1998**, *70*, 4546-4548.
38. Zhao, J.Y.; Waldron, K.C.; Miller, J.; Zhang, J.Z.; Harke, H.R.; Dovichi, N.J. *J. Chromatogr.* **1992**, *608*, 239-242.
39. Craig, D.B.; Dovichi, N.J. *Anal. Chem.* **1998**, *70*, 2493-2494.

40. Wasinger, V.C.; Cordwell, S.J.; Cerpa-Poljak, A.; Yan, J.X.; Gooley, A.A.; Wilkins, M.R.; Duncan, M.W.; Harris, R.; Williams, K.L.; Humphery-Smith, I. *Electrophoresis* **1995**, *16*, 1090-1094.
41. Colliver, T.L.; Brummel, C.L.; Pacholski, M.L.; Swanek, F.D.; Ewing, A.G.; Winograd, N. *Anal. Chem.* **1997**, *69*, 2225-2231.
42. Redeker, V.; Toullec, J.Y.; Vinh, J.; Rossier, J.; Soye, D. *Anal. Chem.* **1998**, *70*, 1805-1811.
43. Hsieh, S.; Dreisewerd, K.; van der Schors, R.C.; Jimenez, C.R.; Stahl-Zeng, J.; Hillenkamp, F.; Jorgenson, J.W.; Geraerts, W.P.; Li, K.W. *Anal. Chem.* **1998**, *70*, 1847-1852.
44. Hofstadler, S.A.; Swanek, F.D.; Gale, D.C.; Ewing, A.G.; Smith, R.D. *Anal. Chem.* **1995**, *67*, 1477-1480.
45. Jimenez, C.R.; Li, K.W.; Dreisewerd, K.; Spijker, S.; Kingston, R.; Bateman, R.H.; Burlingame, A.L.; Smit, A.B.; van Minnen, J.; Geraerts, W.P. *Biochemistry* **1998**, *37*, 2070-2076.
46. Garden, R.W.; Moroz, L.L.; Moroz, T.P.; Shippy, S.A.; Sweedler, J.V. *J. Mass Spectrometry* **1996**, *31*, 1126-1130.
47. Whittall, R.M.; Keller, B.O.; Li, L. *Anal. Chem.* **1998**, *70*, 5344-5347.
48. Bushey, M.M.; Jorgenson, J.W. *Anal. Chem.* **1990**, *62*, 161-167.
49. Muller, E.C.; Thiede, B.; Zimny-Arndt, U.; Scheler, C.; Prehm, J.; Muller-Werdan, U.; Wittmann-Liebold, B.; Otto, A.; Jungblut, P. *Electrophoresis* **1996**, *17*, 1700-1712.
50. Franzen, B.; Hirano, T.; Okuzawa, K.; Uryu, K.; Alaiya, A.A.; Linder, S.; Auer, G. *Electrophoresis* **1995**, *16*, 1087-1089.

**Chapter 4: Protein Fingerprinting of  
*Staphylococcus* Species Using On-Capillary  
Concentrating, Labeling, and Electrophoresis**



## 4.1 Introduction

Most bacterial species are unknown. Consequently, our knowledge about bacterial ecology is poor and bacterial identification is a growing field of interest within microbiology (1). Current microbiological identification relies on bacterial culture in specific media and growing conditions. These methods, while inexpensive and reliable for the identification of common bacteria species, are slow, require highly trained technicians, and don't always distinguish bacterial strains (2).

In addition to bacterial culture techniques, two other general approaches are used to identify bacteria. In probing techniques, the bacteria are treated with a panel of DNA or antibody probes (3-4). These probes are relatively specific, although antibody probes can suffer from cross-reaction with closely related species. Probing techniques require relatively little sample work-up, since the specific probe is usually not affected by complex matrices, such as human serum. However, novel organisms are not recognized by probing technology; a positive signal is observed only if a probe is used that recognizes the target organism. Also, probing technologies require a large number of reagents, which can be difficult and expensive to stockpile.

In another approach, a chemical fingerprint is obtained from the organism, which is compared with a database for identification. Chemical fingerprinting techniques require many fewer reagents than probing techniques. However, they tend to require greater sample work-up to eliminate contaminating components found in the sample matrix. When presented with a novel organism, fingerprinting techniques can provide valuable phylogenetic information based on similarity to the fingerprint of known organisms. Chemical fingerprints have been developed based on a large number of components and properties, including enzymes (5), fatty acids (6),

polyamines (7), carbohydrates (8), mixed dye staining (9), proteome analysis (1), and genomic sequencing (10).

The genome sequence, which is the ultimate chemical fingerprint, uniquely defines an organism. However, complete DNA sequencing suffers from practical difficulties. While the bacterial DNA can be randomly sheared, cloned into a vector, grown, and sequenced, this time-consuming procedure is currently impractical for rapid identification of bacterial species (10).

More commonly, the polymerase chain reaction is used to amplify a portion of the genome for subsequent sequence determination. To limit the number of primers required, a single highly conserved gene is usually selected for analysis; examples include several rRNA genes (11), sigma70 factors (12), type II DNA topoisomerase (13), recA genes (14) and heat-shock proteins (15). Unfortunately, DNA sequences from these conserved genes are not always unique. For example, the sequence of a portion of the 16S rRNA from three strains of *Vibrio cholerae* and one strain of *V. mimicus* were identical, except for one point mutation (16).

Another genomic fingerprint is based on restriction fragment length polymorphism (RFLP) maps of genomic DNA (17). However, the analysis does not always identify bacterial species or strains. For example, several strains of *Salmonella paratyphi* and *S. java* were analyzed by RFLP of 16S rRNA; the same profile was shared by the majority of strains (18).

Probably the most common chemical fingerprinting method is based on protein content. For example, gel electrophoresis of proteins is commonly used in

taxonomy (1, 19), where two-dimensional gel patterns are used to identify an organism. Instrumental methods are based on mass spectrometric analysis of proteins or pyrolysis patterns (20-21), including mass spectrometric analysis of whole bacterial cells (22). Capillary electrophoresis has been used to study the outer membrane protein from four strains of the *Enterobacteriaceae* family (23). Peptides and proteins of microorganisms have been examined by capillary electrophoresis (24-26). However, we are unaware of the use of capillary electrophoresis for the identification of bacteria based on a protein fingerprint.

In this chapter, I report the use of capillary electrophoresis/laser-induced fluorescence to generate protein fingerprints from six *Staphylococci* species. Proteins were labeled on-column with the fluorogenic reagent 3-(2-furoyl)quinoline-2-carboxaldehyde (FQ), separated with sub-micellar electrophoresis, and detected by laser-induced fluorescence. A phylogenetic tree was constructed from the data.

On-column labeling usually induces stacking on the analyte. Burgi and Chien introduced field-amplified stacking of charged analytes for capillary zone electrophoresis (26-27). Stacking based on the pH of the sample has been described by Aebersold (28). The stacking concept has also been applied to micellar capillary electrophoresis for neutral analytes (29). In this paper, we demonstrate that the labeling of protein fractions can be manipulated by adjustment of sample stacking conditions.

## 4.2 Experimental

### 4.2.1 Bacterial Isolates

Six *Staphylococcus* species were kindly donated by Dr. Anthony Chow, Department of Medicine, Division of Infectious Disease, University of British Columbia. The species and strains were *Staphylococcus aureus* 8325-4, *S. epidermidis* 9759, *S. haemolyticus* ATCC 29970, *S. lugdunensis* CRSN 850412, *S. saprophyticus* KL122, and *S. schleiferi* ATCC 43808. Bacteria were grown for 24 h in nutrient broth at 37 °C and then pelleted by centrifugation at 10,000 × g for 10 min. The pellets were washed 5 times in physiological saline solution, re-suspended in an equivalent volume of distilled water, and then disrupted on ice by ultrasonication (3 × 60 s with a 30 s cooling period between each burst) at 4°C. The crude sonicates were centrifuged at 10,000 × g for 20 min, and then the supernatant was removed and stored at -20°C. Protein concentrations were estimated by the method of Lowry.

### 4.2.2 Instrumentation

Capillary electrophoresis was performed with a locally constructed instrument (30). Separation was performed in a 35 or 40-cm long, 50- $\mu$ m ID, and 150- $\mu$ m OD fused-silica capillary at 400 V/cm. The separation buffer was 50 mM phosphate, 11 mM sodium pentasulfate (SPS), at pH 6.9. Detection was performed with a locally constructed ultrasensitive laser-induced fluorescence detector, based on a sheath-flow cuvette. The cuvette had a 200- $\mu$ m square flow chamber and 1-mm thick windows. The flow chamber was held in a stainless-steel fixture, which was kept at ground potential. A 12-mW argon-ion laser beam was used for excitation at 488 nm. The beam was focused to a ~15- $\mu$ m diameter spot about 50- $\mu$ m downstream from the capillary exit. Fluorescence was collected at right angles with a 60×, 0.7 N.A.

microscope objective, filtered with a 630DF30 bandpass filter from Omega Optical, imaged onto an iris to block stray light, and detected with a Hamamatsu R1477 photomultiplier tube operated at 900 V. Hydrostatic injection was under 5 kPa negative pressure.

#### **4.2.3 Labeling and capillary electrophoresis**

The electrophoresis separation buffer consisted of 50 mM phosphate and 15 mM SPS, pH 7.0. The protein extract concentration ranged from  $10^{-7}$  to  $10^{-9}$  M and was prepared in a 5 mM CN<sup>-</sup> solution that was buffered as described in the text. In the pH stacking mode, the pH of the sample solution was raised to the desired pH by the addition of small volumes of NaOH. A solution of 5 mM FQ was prepared in running buffer. Solutions were injected as described in the text. Once the solutions were injected, the capillary tip was immersed in a vial of fresh separation buffer that had been heated to 65 °C in a dry bath incubator. After a 30-s reaction, the capillary was immersed in a vial of separation buffer at room temperature and electrophoresis was carried out.

#### **4.2.4 Phylogenetic analysis**

The portions of the electropherograms between 3 and 10 min were used for the cluster analysis. The similarity between each of the 15 pairs of electropherograms was estimated by calculating the Fisher z-transform of the Pearson product-moment correlation coefficient between the two data sets (31). This method of comparison was selected in part because its result is invariant under linear transformations of the data sets. This property is important because it allows variations in the data due to differing amounts of cellular material being injected into the capillary and differences in the baseline of the electropherogram to be ignored. The similarity between clusters

was taken to be the mean similarity of all pairs of elements between the clusters (UPGMA) (31). After the cluster analysis was performed, the Fisher correlations were converted into Pearson product-moment correlation coefficients. All calculations were performed with IGOR Pro using macros and functions for automation.

#### **4.2.5 Safety precautions**

Potassium cyanide is highly poisonous and reacts readily with acids to form lethal HCN gas. Stock solutions should be made in a basic buffer, neutralization of waste containing KCN should be made by addition of 1% NaOH (50  $\mu\text{L/g}$  of cyanide) solution followed by slow addition of bleach (70  $\mu\text{L/g}$  of cyanide).

Several of the *Staphylococcus* strains require level 2 biological containment and should be cultured and manipulated under appropriate biohazard protocols.

### **4.3 Results and Discussion**

#### **4.3.1 Bacterial fingerprint with CE**

Six species of the genus *Staphylococcus* were used in our study; three are of major medical importance: *S. aureus*, *S. epidermidis*, and *S. saprophyticus*. They are now regarded as the principal cause of nosocomial bacteremia in the United States, and their identification is of clinical importance (32-33). I also studied *S. lugdunensis*, *S. schleiferi*, and *S. haemolyticus*. I investigated protein fingerprinting of these organisms by means of capillary electrophoresis and laser-induced fluorescence.

Rather than using expensive ultraviolet lasers to generate native fluorescence from the separated proteins, I rely on relatively inexpensive visible lasers to generate fluorescence from labeled proteins. I used the fluorogenic reagent 3-(2-furoyl)quinoline-2-carboxaldehyde (FQ) to label proteins and other biogenic amines

(34). This reaction does not go to completion for many proteins (35), creating a population of fluorescently labeled products for each protein. Normally, these products have different mobilities, which results in broad, poorly resolved electrophoresis peaks. However, this group reported that the multiple-labeling envelope collapses to a single sharp peak for each protein when separation is performed with a sub-micellar SDS buffer (34). We observed a rather narrow separation windows when SDS was used in the buffer. In this study, I replaced SDS with sodium pentanesulfonate (SPS). SPS, like SDS, collapses the multiple-labeling envelope to a single, sharp peak while generating a relatively large separation window.

This group reported a method for the analysis of protein using on-column labeling (35). The labeling conditions must be adjusted based on the relative mobilities of the neutral FQ, the cyanide anion, and the proteins. While it is relatively simple to optimize the reaction for a few standard proteins, the wide range of protein mobilities in whole-cell protein extracts complicates the mixing process and labeling reaction.

#### **4.3.2 Field amplification and labeling**

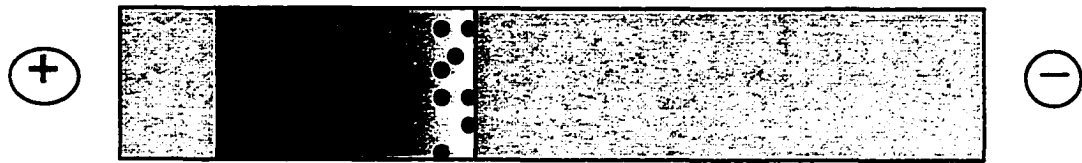
In this chapter, I investigated the use of on-column stacking to enhance the labeling reaction for selected fractions of the protein mixture. A plug, consisting of soluble proteins and cyanide in a relatively low conductivity matrix, was first hydrostatically injected into the capillary. At pH 7, the basic proteins were positively charged while acidic proteins and cyanide were negatively charged. A plug of FQ was then electrokinetically injected for 4 s. Next, a plug of separation buffer was electrokinetically injected for 5 s. During the 2<sup>nd</sup> and 3<sup>rd</sup> injections, there was a greater voltage drop across the sample plug, and ions at the plug moved with a greater

velocity through the sample plug under the influence of this amplified field. When proteins reached the sample/separation buffer interface or the sample/FQ interface, the proteins encountered a much lower electric field and their velocity was dramatically decreased. The stacking mechanism occurs for both charged proteins and cyanide. Cyanide and negatively charged proteins stack in the back of the sample plug and positively charged proteins tend to stack in the front of the sample plug, Fig. 4.1A. Of course, diffusion counteracts stacking, helping to mix components.

Fig. 4.1B presents electropherograms for labeling reactions with and without stacking. In the absence of stacking, the ionic strength of the sample was the same as both the FQ and separation buffer. Electrical field was uniform along the capillary, and the mixing of components was dominated by diffusion within the plugs. Because of this inefficient mixing, a relatively small fraction of the proteins reacted with the labeling reagent, even though the sample was hydrodynamically injected for 8 s.

In the case of stacking, the ionic strength of the sample was about 1/3 of that of the separation buffer and the sample was hydrodynamically injected for 4 s. The higher electric field in the sample plug drove cyanide and negatively charged proteins towards the FQ plug, where stacking occurred, mixing was efficient, and a large fraction of the protein was labeled. In contrast, cationic proteins migrated away from the FQ plug, and their reaction was suppressed. In this electropherogram, the intensities of anionic proteins with lower mobilities (~10 min) increased about 2.5-fold, while intensities of cationic proteins with higher mobilities (~4 min) decreased about 2-fold. Stacking dominated over diffusion in controlling the reaction with different classes of proteins.





□ cyanide      ■ FQ      ● protein

buffer

Figure 4.1.A. Illustration of stacking.

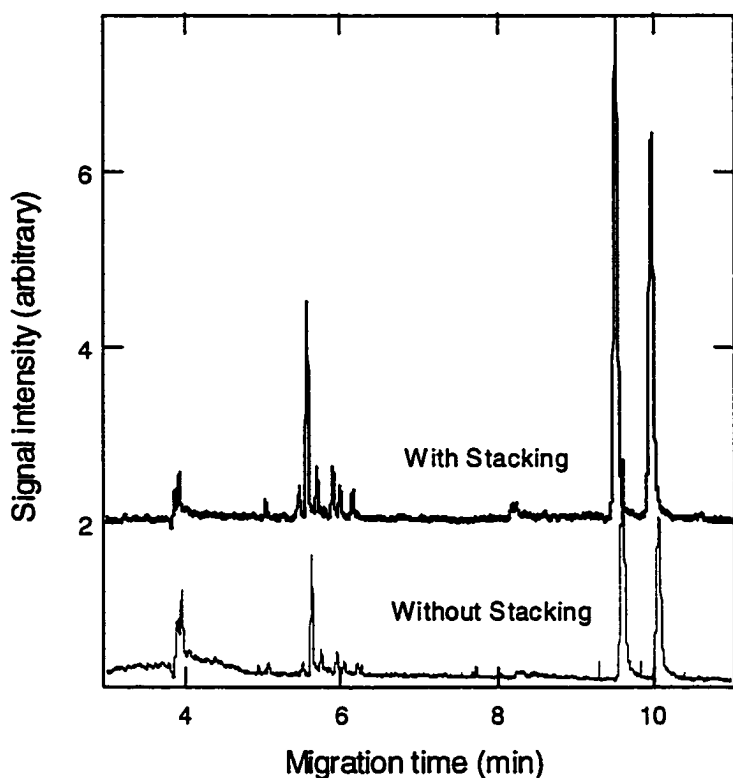


Figure 4.1.B. Separation of FQ-labeled extracts of *S. lugdunensis*. Protein concentration was estimated as  $10^{-8}$  M by means of the Lowry method. The water soluble protein extract was injected hydrodynamically. For the *without stacking* electropherogram, injection of the sample was for 8 s. The sample used for the *with stacking* had been prepared in a buffer with half the ionic strength of the without stacking sample; this sample was injected for 4-s. Next, the FQ reagent was injected for 5 s at 100 V/cm, followed by a plug of pH 7 buffer for 5 s at 100 V/cm. The labeling reaction was incubated for 20 s at 65 °C. Separation was performed with a pH 7 buffer and at 400 V/cm in the 38-cm long capillary.

### 4.3.3 pH focusing effects on field amplification and labeling

The selectivity of the labeling reaction can be manipulated by adjusting the sample pH in field amplification, Fig. 4.2. The pH of the sample was raised well above the isoelectric point (pI) of most proteins. The protein-cyanide mixture in a pH 10.5 buffer was hydrostatically injected into the capillary filled with neutral separation buffer, Fig. 4.2A. After sample introduction, a plug of FQ in neutral buffer was electrokinetically injected. This procedure resulted in a pH-step gradient at both interfaces of the sample plug. Application of an electric field initiated the movement of ions. Cyanide and proteins with  $\text{pH}_{\text{sample}} > \text{pI}$  migrated towards the positive electrode, Fig. 4.2B. For proteins with  $\text{pH}_{\text{sample}} > \text{pI} > 7$ , the electrophoretic migration direction was reversed as soon as the proteins entered the neutral FQ region; these proteins were focused at the interface. Proteins with  $\text{pI} = 7$  became neutral as soon as they entered the FQ region. Proteins with  $\text{pI} < 7$  slowed as they passed the boundary region. Proteins with  $\text{pI} > \text{pH}_{\text{sample}}$  moved away from the cyanide and were not efficiently labeled, Fig. 4.2C.

Fig. 4.3 presents electropherograms of *S. aureus* at basic pH. At pH 10.5, anionic proteins mixed efficiently with the labeling reagents; slow moving, low mobility proteins generated higher signals than did the faster moving cationic proteins. Fig. 3 also shows the electropherogram generated when the sample plug was adjusted to a higher pH. Most proteins gained a negative charge at this pH and moved towards the FQ plug as soon as the voltage was applied. The fluorescent intensity of the fastest moving proteins was greater than in the pH 10.5 electropherogram.

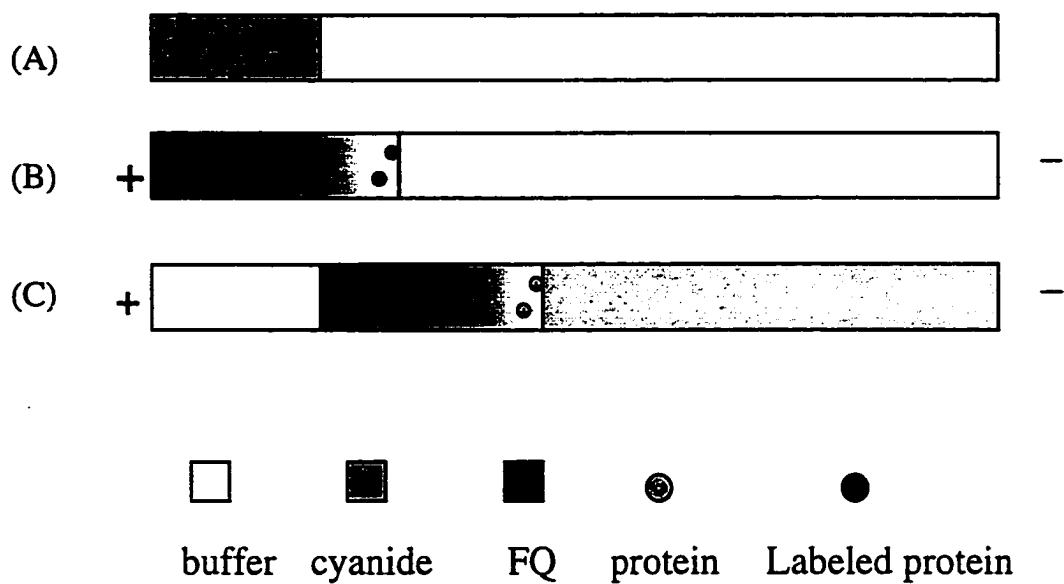


Figure 4.2 Schematic illustration of stacking and labeling. (A) Sample with CN<sup>-</sup> was hydrostatically injected the capillary in a basic solution. (B) FQ was electrokinetically injected to the capillary and stacking occurred. (C) After dissipation of the pH gradient, FQ mixed with proteins and CN<sup>-</sup>.

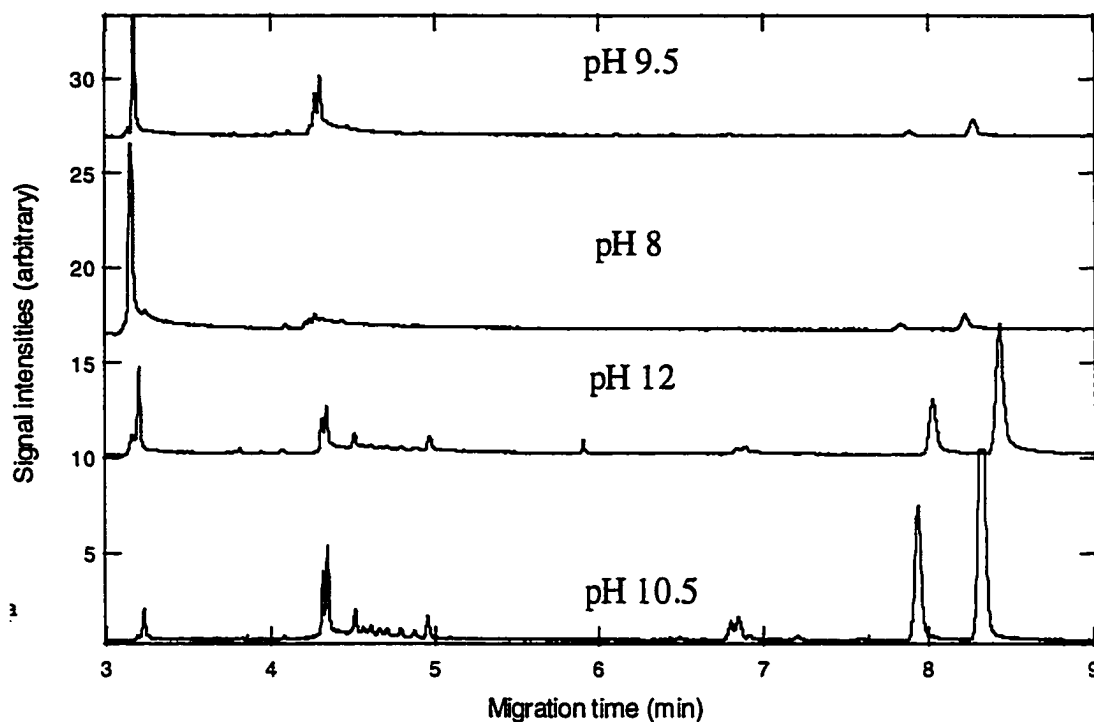


Figure 4.3 pH effect on the separation of extract from *S. aureus*. The bottom trace was generated by injecting a protein/cyanide solution buffered at pH 10.5 followed by a plug of FQ at neutral pH. The second trace was generated by injecting a protein/cyanide solution buffered at pH 12.5 followed by a plug of FQ at neutral pH. The next trace was generated by first injecting the FQ plug and then the protein/cyanide mixture buffered at pH 8. The top trace was generated by first injecting the FQ plug and then the protein/cyanide mixture buffered at pH 9.5.

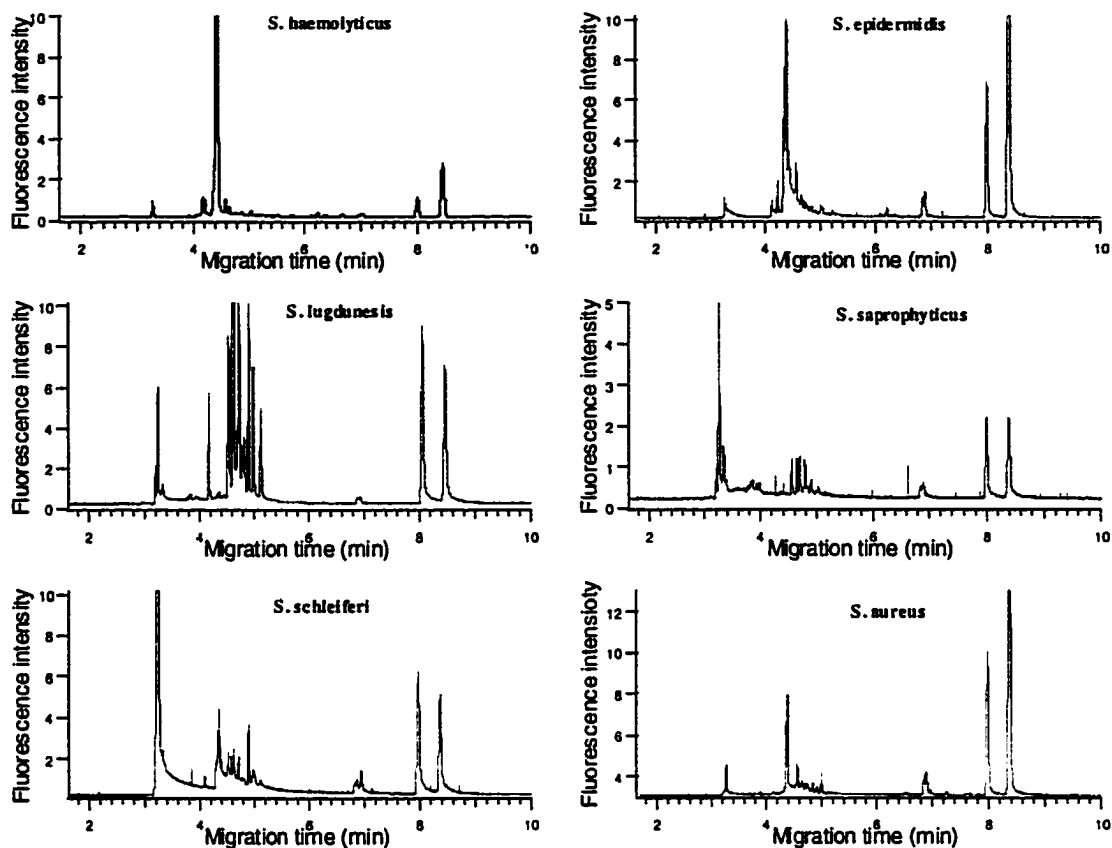


Figure 4.4 Protein fingerprints of six *Staphylococcus* species. Protein concentration was  $10^{-8}$  M in a pH 10.5 buffer. Sample was injected hydrodynamically for 5 s, followed by FQ injection for 5 s at 100 V/cm and running buffer for 5 s at 100 V/cm. Labeling was performed for 30 s at 65 °C. Separation was performed in a pH 7 buffer and at 400 V/cm in the 35 cm long capillary.

The lowest mobility proteins also showed a decrease in mobility at pH 12 compared with pH 10.5. Their migration time was longer because they moved to the back of the FQ plug before starting to undergo electrophoresis.

Positively charged proteins could be selectively labeled by changing the order of sample and FQ introduction. In the top two traces of Fig. 4.3, the FQ plug was introduced first. Then a sample plug, mixed with cyanide and buffered at pH 8 or 9.5, was hydrostatically injected. Then high voltage was applied for 3 s to stack the ions in the sample. In this experiment, positively charged proteins were stacked adjacent to FQ, enhancing their labeling. At pH 8, more proteins were positively charged and efficiently labeled compared with proteins labeled at pH 9.5.

#### **4.3.4 Fingerprinting *Staphylococcus* species**

Fig. 4.4 shows the electropherograms of the water-soluble proteins obtained from the six *Staphylococcus* species. Each electropherogram was comprised of 20-30 peaks. In some regions, the relative intensity varied more than migration time. Peaks tended to cluster in four regions: 3.1 to 3.5 min, 4.1 to 5.3 min, 6.1 to 7.1 min, and 8.0 to 8.5 min. In the first and third regions, some of the species have a distinctive peak pattern. The second region is a rich fingerprint showing large difference between those six species. In the last region, there are two peaks with different intensities, but having almost identical migration times in all electropherograms.

#### 4.3.5 Classification of bacteria by cluster analysis

The relative peak mobilities and intensities were used to generate a phylogenetic tree for these *Staphylococcus* species, Fig. 4.5. The Pearson product-moment correlation coefficient was used to measure the similarity between each pair of electropherograms. Phylogenetic trees are valuable because they can classify new and unknown isolates by comparing data with database library. In this study, the six *Staphylococcus* species were allotted to 4 groups on the basis of protein fingerprints: group 1 consisting of 4 species.

Other phylogenetic trees are available for these species based on HSP60 DNA and protein sequence, 16S rRNA DNA sequence, and DNA-DNA hybridization (15). The species are quite closely related, and the genetic differences between the species are not large. Our phylogenetic tree is similar to those in reference 15, except that our tree shows much greater relationship between *S. saprophyticus* and *S. schleiferi* than is shown by the other trees. The genomic sequence will be required to determine the correct relationship between these organisms.



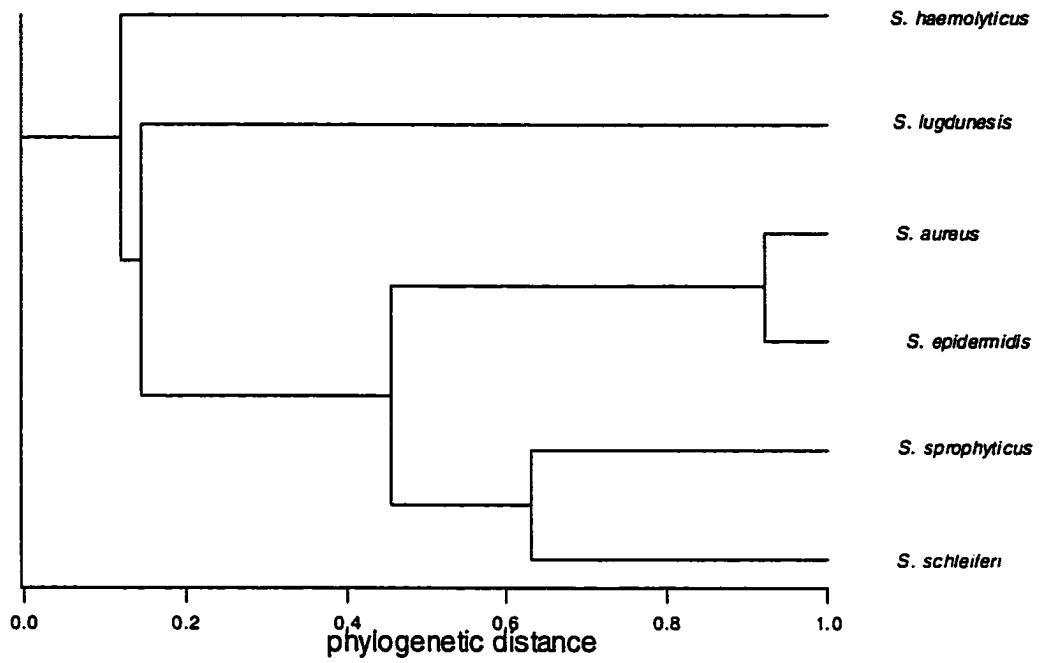


Figure 4.5 Phylogenetic tree generated from the data of Figure 4.4.

#### 4.4 References

1. Busse, H.; Denner, E.; Lubitz, W. *J. Biotechnol.* **1996**, *47*, 3-38.
2. Tilton, R.C. *Ann. Rev. Microbiol.* **1982**, *36*, 467-493.
3. Ratcliff, R.M.; Mirelli, C.; Moran, E.; O'Leary, D.; White, R. *Antimicrob. Agents Chemother.* **1981**, *19*, 508-512.
4. Vanechoutte, M.; Van Eldere, J. *J. Med. Microbiol.* **46**, 188-194 (1997).
5. Miller, K.J.; Lytle, F.E. *Anal. Chem.* **1994**, *66*, 2420-2423.
6. Gharaibeh, A.A.; Voorhees, K.J. *Anal. Chem.* **1996**, *68*, 2805-2810.
7. Hamana, K.; Matsuzaki, S. *Can. J. Microbiol.* **1991**, *37*, 885-888.
8. Iwami, M.; Kiyoto, S.; Nishikawa, M.; Terano H.; Kohsaka, M.; Aoki, H.; Imanaka, H. *J. Antibiot.* **1985**, *38*, 835-839.
9. Shelly, D.C.; Warner, I.M.; Quarles, J.M. *Clin. Chem.* **1983**, *29*, 290-296.
10. Bult, C.J.; White, O.; Olsen, G.J.; Zhou, L.; Fleischmann, R.D.; Sutton, G.G.; Blake, J.A.; FitzGerald, L.M.; Clayton, R.A.; Gocayne, J.D.; Kerlavage, A.R.; Dougherty, B.A.; Tomb, J.F.; Adams, M.D.; Reich, C.I.; Overbeek, R.; Kirkness, E.F.; Weinstock, K.G.; Merrick, J.M.; Glodek, A.; Scott, J.L.; Geoghagen, N.S.M.; Venter, J.C. *Science* **1996**, *273*, 1058-1073.
11. Ludwig, W.; Schleifer, K.H. *FEMS Microbio. Rev.* **1994**, *15*, 155-173.
12. Gruber, T.M.; Bryant D.A. *J. Bacteriol.* **1997**, *179*, 1734-1747.
13. Huang, W.M. *Ann. Rev. Gen.* **1996**, *30*, 79-107.
14. Karlin, S.; Weinstock, G.M.; Brendel, V. *J. Bacteriol.* **1995**, *177*, 6881-6893.
15. Kwok, A.Y.C.; Su, S.C.; Reynolds, R.P.; Bay, S.J.; Av-Guy, Y.; Dovichi, N.J.; Chow, A.W. *Int. J. Syst. Bacteriol.* **1999**, *49*, 1181-1192.
16. Coelho, A.; Momen, H.; Vicente, A.C.; Salles, C.A. *Res. Microbiol.* **1994**, *145*, 151-156.

17. Tenover, F.C.; Arbeit, R.D.; Goering, R.V.; Mickelsen, P.A.; Murray, B.E.; Persing, D.H.; Swaminathan, B. *J. Clin. Microbiol.* **1995**, *33*, 2233-2239.
18. Stanley, J.; Baquar N. *Int. J. Food Microbiol.* **1994**, *21*, 79-87.
19. Ferreira, A.C.; Morais, P.V.; Gomes, C.; da Costa, M.S. *J. Appl. Bacteriol.* **1996**, *80*, 479-486.
20. Krishnamurthy, T.; Ross, P.L.; Rajamani, U. *Rapid Commun. Mass Spectrom.* **1996**, *10*, 883-888.
21. Magee, J.T. *Zentralbl. Bakteriologie* **1997**, *285*, 182-194.
22. Hollard, R.D.; Duffy, C.R.; Rafil, F.; Sutherland, J.B.; Heinze, T.M.; Holder, C.L.; Voorhees, K.J.L. Lay, J.O. *Anal. Chem.* **1999**, *71*, 3226-3230.
23. Kustos, I.; Kocsis, B.; Kerepesi, I.; Kilar, F. *Electrophoresis* **1998**, *19*, 2324-2330.
24. Kustos, I.; Kocsis, B.; Kerepesi, I.; Kilar, F. *Electrophoresis* **1998**, *19*, 2317-2323.
25. Xing, J.Z.; Richards, R.M. *J. Chromatogr. A* **1996**, *740*, 273-278.
26. Chien, R. L.; Burgi, D. S. *J. Chromatogr.* **1991**, *559*, 141.
27. Burgi, D.S. *Anal. Chem.* **1993**, *65*, 3726-3729.
28. Aebersold, R.; Morrison, H.D. *J. Chromatogr.* **1990**, *516*, 79-88.
29. Palmer, J.; Munro, N.J.; Landers, J. P. *Anal. Chem.* **1999**, *71*, 1679-1687.
30. Wu, S.; Dovichi, N.J. *J. Chromatogr.* **1989**, *480*, 141-155.
31. Sneath, P.H.A.; Sokal, R.R. "Numerical Taxonomy: The Principles and Practice of Numerical Classification." Freeman, San Francisco, 1973.
32. Kloos, W.E. *Ecology of human skin*, in *Coagulase-negative Staphylococci*. P. A. Mardh and K. H. Schleifer (ed.), Almquist and Wiksell International, Stockholm **1986**, p. 37-50.
33. Archer, G. L. *J. Antimicrob. Chemother.* **1988**, *21* (Suppl. C), 133-138.

34. Pinto, D.M.; Arriaga, E.A.; Craig, D.; Angelova, J.; Sharma, N.; Ahmadzadeh, H.; Dovichi, N.J.; Boulet, C.A. *Anal. Chem.* **1997**, *69*, 3015-3021.
35. Lee, I.H.; Pinto, D.; Arriaga, E.A.; Zhang, Z.; Dovichi, N.J. *Anal. Chem.* **1998**, *70*, 4546-4548.

**Chapter 5: On-capillary labeling and self-isotachophoretic preconcentration of proteins in sub-micellar separation of human cancer cell extracts**

## 5.1 Introduction

Capillary electrophoresis is a powerful separation tool for proteins, especially when used with laser induced fluorescence, which can provide highly sensitive detection of very low concentrations of native and labeled proteins(1-3). Native fluorescence detection usually requires the use of expensive and temperamental lasers that operate in the ultraviolet portion of the spectrum. Labeled proteins can be detected with relatively inexpensive air-cooled argon ion or helium-neon lasers. Protein labeling may be carried out in pre-column, on-column and post-column approaches. This group has developed pre-capillary and on-capillary labeling approaches (3, 17).

The on-column approach is an attractive one since it uses the separation capillary itself as a reactor and minimizes external sample manipulating steps. It is especially suitable for the determination of analytes present in extremely small sample volumes. Dilution is limited by the size of the capillary bore and the reaction time. Virtually the only source of dilution is longitudinal diffusion of the analytes along the capillary. Various on-column reactions have been demonstrated in capillary zone electrophoretic systems (4, 5). However, on-column labeling processes usually cause labeled products to have a broader zone than the original sample zone, especially when more than one labeling reagent is under electrophoretic mixing and when high temperature is required. The proteins reach the detector at a time dependent on their mobilities, the capillary length and the voltage applied. When no additional effects (e.g. stacking) are involved, the concentration of a protein in its zone passing the detector is always lower than that in the injected zone due to dispersive effects (22).

There is a need for efficient preconcentration techniques applicable for minute-volumes of labeled proteins. For example, physiological samples often contain proteins at extremely low concentrations, challenging even CE-LIF analysis. Coupling CZE with concentrating techniques has been shown to separate protein mixtures with a remarkable resolving power based on the differences in the charge/mass ratio of the analytes. Concentration procedures, such as solid-phase extraction and liquid-liquid extraction are easy and effective but laborious and time consuming. Chromatographic preconcentration with packed columns in an on-line mode has achieved a signal enhancement of up to a factor of 100 (6,7). Sieving techniques using a gel and a membrane were introduced by Hjerten and coworkers to concentrate proteins (8,9).

It is possible to apply a longer sample plug and still have good separation efficiency by sharpening the starting zone prior to the analysis step. There are both chromatographic and electrophoretic strategies (10,11) to achieve this sample preconcentration. By introducing or dissolving the sample in an electrolyte (or pure water), which has a lower conductivity than the background electrolyte (BGE), zone sharpening can be accomplished, i.e. the well-known stacking principle (12). When the conductivity is lower in the sample zone, the electric field will accordingly be higher than in the BGE and the velocity of the analytes will be high. When the sample ions cross the border into the BGE, which has a lower electric field, they will slow down and a stacking effect is produced. Utilizing this technique, I have evolved a strategy to identify bacteria species with on-column labeling of proteins from crude extract (see chapter 4).

More effective focusing of sample zones can be achieved by employing isotachopheresis (ITP). An on-line combination of ITP prior to capillary zone electrophoresis (CZE) has been developed to enhance the loadability and improve detection limits (19). In ITP preconcentration the buffer system is discontinuous. All species in the sample are lined up in a “train” without gaps according to their electrophoretic mobilities between a leading and a terminating ion. By choosing the proper conditions the analyte ions in a large sample plug can be stacked to a width of only a fraction of a millimeter. The drawback of this on-line version is the use of two coupled capillaries, which is not part of most commercial instruments. This problem can be overcome by performing the entire procedure in a single-column mode (20). Single capillary ITP-CZE can be performed with a distinct transition from ITP to CZE or a gradual change. It has been referred to as on-column transient ITP preconcentration (20). Other papers describe methods whereby the terminating electrolyte is removed before the CZE step is started by using backpressure programming, giving a more distinct transition (23). Hjerten *et al.* (8) have described several automated on-line methods, including ITP, for concentration of peptides and proteins based on principles suitable for such amphoteric compounds.

In this chapter I used the simple way to label proteins on-column at the very beginning of a poly-acryloylaminoethoxyethanol (poly-AAEE) coated capillary inlet. A protein fraction above 30 kDa MW extracted from the human cancer cell line HT29 was labeled by the fluorescent dye 3-(2-furoyl) quinoline-2-carboxaldehyde (FQ) in the presence of cyanide. I first combined on-column labeling, ITP and CZE in a single capillary by using the excess cyanide ions from the labeling reagents as the leading electrolyte instead of adding higher mobility ions to induce ITP concentration. ITP features the focusing and separation of labeled proteins into small and highly



concentrated zones, offering a good starting point for a following separation in a sub-micellar buffer system. The ITP concentration effect is demonstrated with the excess reagent in on-column labeling of proteins.

## **5.2 Background**

### **5.2.1 On-column transient ITP-CZE mode**

The most common way to preconcentrate a sample with ITP in a single capillary is on-column transient ITP-CZE (19, 20). If the BGE can serve as the leading zone, then after introducing the sample zone, a pulse of a suitable terminating electrolyte is introduced. An ITP system is created temporarily that focuses the sample zones. The terminating zone is then gradually penetrated by the BGE, resulting in destacking of the sample zones and finishing their separation in the CZE mode, as in Fig. 5.1a. A single BGE can be used for both ITP preconcentration and CZE separation. In this case, shown in Fig. 5.1b, two requirements must be met. First, the mobility of the BGE must be low during the transient ITP step so that it can serve as the terminating ion. Secondly, the sample must contain additional ions with high mobility which can serve as the leading zone during transient ITP migration. Real biological samples usually contain salts which can potentially serve as source of leading ions. Fig. 5.1c shows the concentration profiles of the different zones.

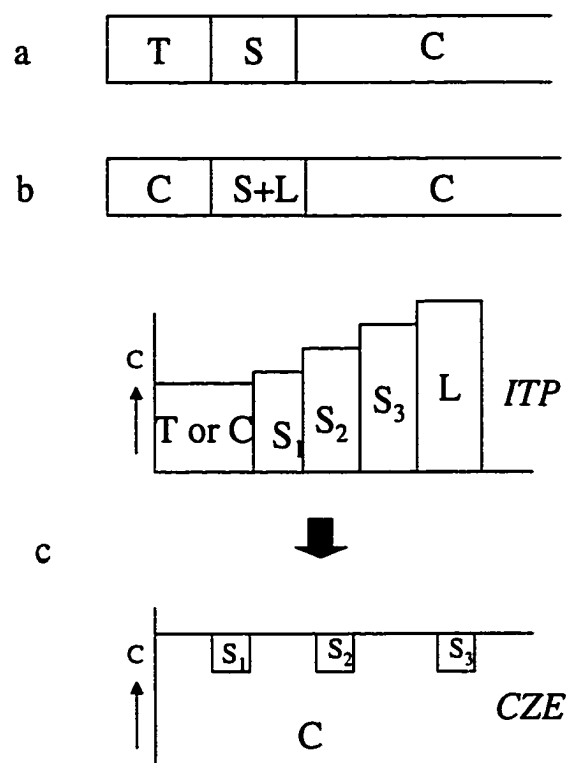


Fig. 5.1 Illustration of transient ITP-CZE mode. (a) The background electrolyte C has a mobility higher than those of the sample components S and thus serves as the leading ion. The analysis starts with the sample injection and then a suitable terminating electrolyte T is introduced to allow the sample to isotachophoretically preconcentrate. Next, the terminating electrolyte is replaced with background electrolyte C, and separation proceeds in the zone electrophoretic mode. (b) When the mobility of background electrolyte C is lower than that of the sample ions, a suitable leading ion L must be added to the sample. The separation starts in the isotachophoretic mode. As the concentration of the leading zone gradually decreases owing to its electromigration dispersion (21), the migration mode converts into zone electrophoresis. (c) Schematic representation of concentration profiles of ITP-CZE mode.

### **5.2.2 ITP/CZE mode**

The basis of ITP/CZE is somewhat different from the on-column transient in CZE and the use of discontinuous buffer system in CZE. It can be found in the 2L-ITP system (17), where some components of a sample migrate in the ITP mode and others in the CZE mode, depending on the concentrations of the leading ions and the mobilities of the concerning ionic species. In the system a leading electrolyte is used with two leading ions whereas the terminating electrolyte contains only that with lowest effective mobility. The leading ion with the lowest effective mobility, L2, remains partially behind the leading ion with the highest mobility, L1, and creates a terminating L2 zone. The mathematical model for this system has been described (24). In fact, an ITP system is created superimposed on a zone electrophoretic system of L2 ions and the counter ions, as Fig.5.2.

## **5.3 Experimental**

### **5.3.1 Chemical**

Sodium tetraborate (Borax) and sodium dodecyl sulfate (SDS) were from BDH (Toronto, ON, Canada). All buffers were made with Milli-Q deionized water and were passed through a 0.2  $\mu\text{m}$  filter.

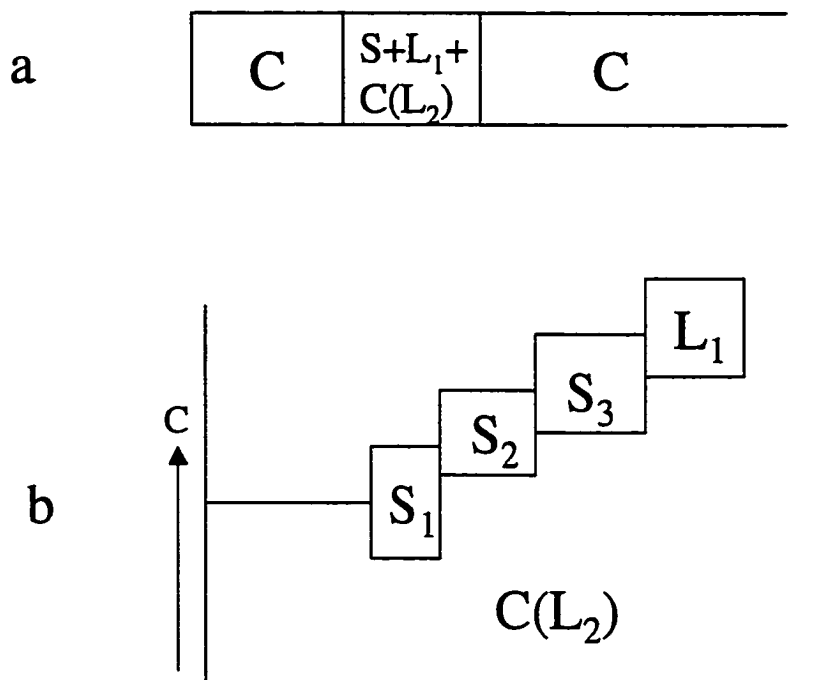


Fig 5. 2 (a) In ITP/CZE mode, leading ions with the highest mobility,  $L_1$ , act as the leading ions in the ITP system and the leading ions with the lowest mobility,  $L_2$ , create the terminating zone and act as the BGE of the CZE system. (b) The concentration profile of sample zones migrating in consecutive electrolyte in the ITP mode superimposed on a background electrolyte of  $L_2$ .

Derivatizing reagents, 3-(2-furoyl)quinoline-2-carboxaldehyde (FQ) and potassium cyanide, were from Molecular Probes (Eugene, OR). KCN was dissolved in water (100 mM). FQ solutions were dried before storage. A stock solution of 100 mM FQ was prepared in methanol, 10  $\mu$ L aliquots were placed into 500  $\mu$ L microcentrifuge tubes, and the solvent was removed under vacuum using a Speed Vac (Savant Instruments Inc., Farmingdale, NY). The dried FQ aliquots were stored at -20°C. The dried FQ was dissolved in running buffer to a final concentration of 5 mM on the day of the experiment and stored on ice.

Phosphate-buffered saline (PBS) solution was prepared by mixing 8 g of NaCl, 0.2 g of  $\text{KH}_2\text{PO}_4$ , 0.46 g  $\text{Na}_2\text{HPO}_4$ , and 0.2 g of KCl and diluting to 1.00 L in distilled water.

### **5.3.2 Cell extract preparation and protein fraction**

Roughly  $10^6$  HT29 human colon adenocarcinoma cells (American Type Culture Collection, ATCC No. HTB-38) were washed five times with PBS and resuspended in 100  $\mu$ L of water. The cells were sonicated for 20 minutes at 4°C. The suspension was centrifuged at 2500 RPM (600  $\times$  g) for 10 minutes. The supernatant was fractionated by ultrafiltration through 30 kD molecular weight cut-off filters.

These filters were regenerated cellulose membranes (Amicon Microcon), that had been soaked in a 10% Triton X-100 solution overnight. The ultrafilters were rinsed with deionized water. Next, two 500  $\mu$ L aliquots of deionized water were passed through the devices with the aid of a centrifuge. The filters were inverted and residual water was discarded.

To prepare a fraction, 350  $\mu\text{L}$  of the HT29 protein extract was first passed through the 30 kDa ( $\pm 10\text{-}20\%$ ) molecular weight cut-off filter by centrifuging at  $14,000 \times g$  for 3 min. The membrane was inverted and the 30+ kDa fraction was collected in a new tube by spinning at  $1000 \times g$  for 3 minutes.

### **5.3.3 AAEE coated capillary**

The experiments were performed in a  $36 \text{ cm} \times 50 \mu\text{m I.D.} \times 150 \mu\text{m O.D.}$  fused-silica capillary. The capillary was Grignard coated with poly-AAEE as described elsewhere (24).

### **5.3.4 Capillary electrophoresis/laser-induced fluorescence detection**

Capillary electrophoresis was performed with a locally constructed instrument (26). The separation buffer was 10 mM borate and 1 mM SDS, at pH 9, unless specified. Detection was performed with a locally constructed ultrasensitive laser-induced fluorescence detector, based on a sheath-flow cuvette. The cuvette had a  $200 \mu\text{m}$  square flow chamber and 1 mm thick windows. The flow chamber was held in a stainless-steel fixture, which was held at ground potential during electrophoresis. A 12 mW argon ion laser beam was used for excitation at 488 nm. The beam was focused to approximately a  $15 \mu\text{m}$  diameter spot about  $50 \mu\text{m}$  downstream from the capillary exit. Fluorescence was collected at a right angle to the excitation beam with a  $60\times$ , 0.7 N.A. microscope objective, filtered with a 630DF30 bandpass filter (Omega Optical), imaged onto an iris to block stray light, and detected with a Hamamatsu R1477 photomultiplier tube operated at a bias of 1,000 V.

## 5.4 Results and discussion

### 5.4.1 Inlet labeling of protein from HT29 extract

The latest development in derivatization procedures for CE is the use of the on-column approach. When reactions with expensive reagents are involved, the costs are reduced with the reduction of the reaction cell volume. However, its chemistry can suffer not only from interference due to excess labeling reagent but also from complex electropherograms generated by multiple reaction products due to incomplete labeling of all possible sites on the protein (14,15). Some fluorigenic reagents have proven useful for protein analysis (16). These reagents are not fluorescent until they react with a primary amine; they generate low background signals compared to traditional fluorescent labeling reagents. This group has exploited (FQ) to generate highly fluorescent proteins that are separated efficiently when used with a submicellar buffer system, without noticeable band-broadening due to multiple labeling (3). We reported a method for the analysis of protein using on-column labeling (17). In this chapter I used a form of electrophoretically mediated microanalysis (EMMA). The reagents and the sample were injected in different plugs based on their mobilities, and they usually traveled a certain distance before mixing (zone overlap) in the capillary. A simple example in a fused-silica capillary is when two plugs of reagents and proteins were injected. The time for the two plugs to complete mixing can be estimated as following:

$$T_{\text{mix}} = L/(\Delta\mu E)$$

L: Distance between leading edges or tailing edges of the two plugs,  
whichever is shorter

$\Delta\mu$ : Difference in electrophoretic mobilities of the two plugs

E: applied electric field

The electric field was stopped after the electric field had been applied for  $T_{\text{mix}}$ , and then the tip of the capillary was heated at 65 °C. Calculation and experiment were used to obtain the optimum mixing time. For the plug which has molecules with very different electrophoretic mobilities, the time interval  $\Delta t$  during total mixing should be controlled very precisely. The electroosmotic flow (EOF) might also be modified by the proteins in real samples and complicated by the experimental conditions. A polyAAEE-coated capillary was used in our experiment. The measured EOF value was  $1 \times 10^{-6} \text{ cm}^2/\text{Vs}$ . In our simple on-column labeling approach, the first plug of neutral FQ was hydrostatically introduced into a capillary filled with separation buffer. A second plug, consisting of proteins and cyanide, was electrokinetically injected into the capillary. Only the portion of proteins with  $\text{pI} < \text{pH}_{\text{buffer}}$  entered the capillary in the second injection, while the FQ plug almost did not move. Since the length of the second plug was less than the first one, all cyanide anions and protein anions were located inside of the zone of FQ molecules. The mixing of the reacting species is done in a very controlled way. The capillary tip was heated at 65 °C for one minute to allow labeling reaction. (Fig 5.3 A-C)

An increase in zone broadening was observed for on-column labeling compared to pre-column labeling. In particular, this effect was more significant for the hydrophobic proteins. The zone broadening partially originates from the mixing of the two plugs and is partially due to a contribution from the submicelles. The higher labeling temperature may also contribute to band broadening.



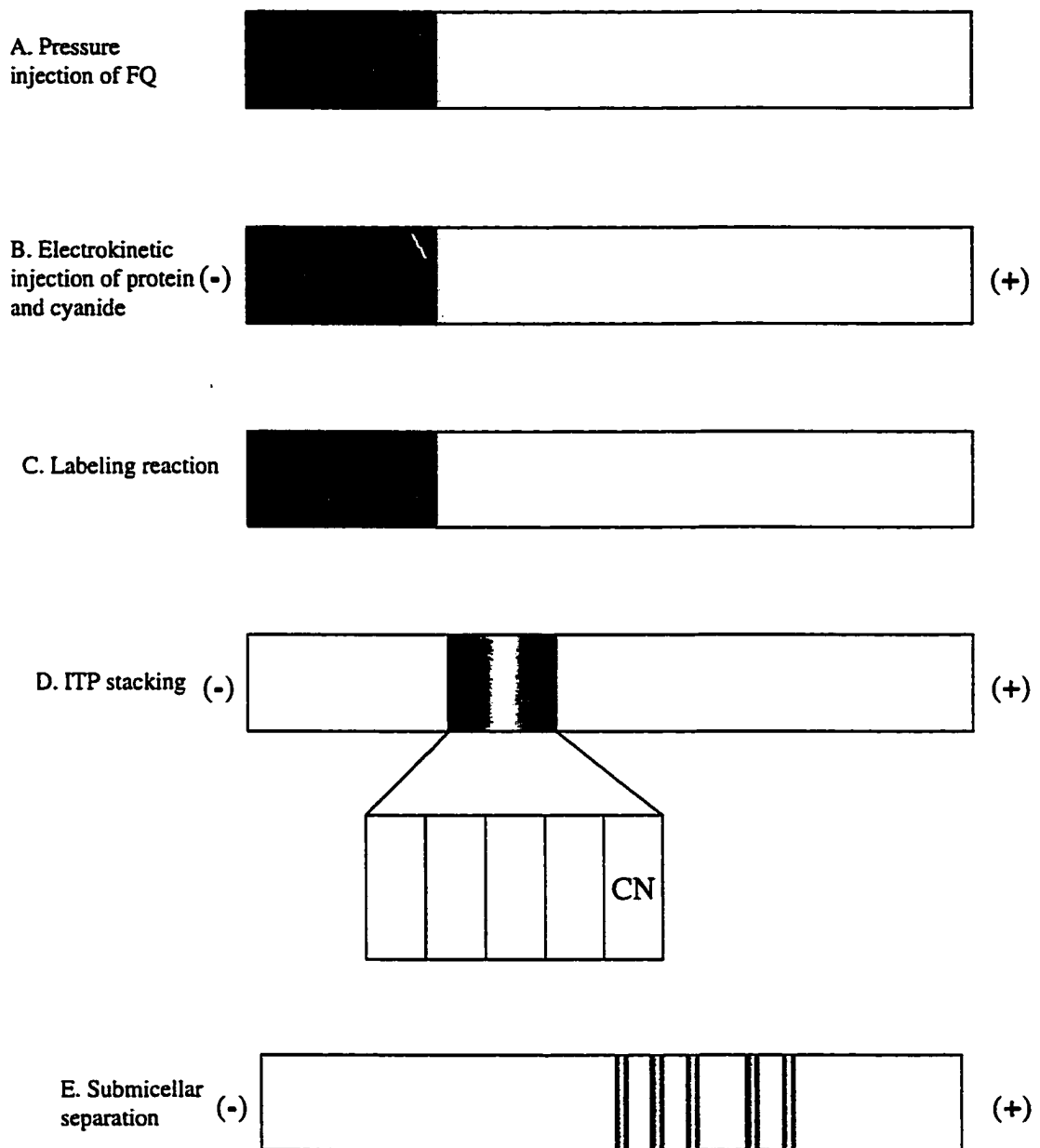


Fig. 5.3 Schematic representation of procedures of protein analysis: on-capillary labeling, isotachophoretic preconcentration and separation

#### 5.4.2 Sample ITP preconcentration

In on-column transient ITP-CZE mode, the components present in excess in a sample and concentrated to a high concentration in the ITP system can disturb the CZE system (18). Also, the narrow bands formed in the ITP mode at a high concentration broaden very quickly in the CZE mode due to diffusion and electrodispersion. So I chose ITP/ CZE mode, that is applying ITP with two leading ions (2L-ITP system), as in Fig. 5.2 . In this system ITP may superimposed on CZE (18) instead of only conversion of ITP to CZE.

In my method, after the on-column reaction the labeled protein zone consists of the excess labeling reagents FQ and cyanide, as well as BGE borate. The leading ions L1, cyanide anions, with the highest mobility acts as the leading ions in the ITP system and the leading ions L2, borate anions, with the lowest mobility creates the terminating zone and acts as the co-ions of the CZE system. We did not add any additional leading electrolyte.

When the ITP has reached the steady state all ions of the same charge as the leading ion are lined up in a continuous “train” according to their electrophoretic mobility. The concentrations of the labeled proteins, migrating in the ITP mode, are adapted that of the leading ion with the highest mobility, L1. The concentration ( $C_i$ ) in each band is dependent on the mobility of the ion ( $\mu_i$ ), the concentration ( $C_{L1}$ ) and mobility of the leading ion ( $\mu_{L1}$ ), and the mobility of the counter ion ( $\mu_r$ ) according to the following expression derived from the Kohlrausch regulating function:

$$C_i = C_{L1} \mu_i (\mu_{L1} + \mu_r) / \mu_{L1} (\mu_i + \mu_r)$$

In order to accomplish a preconcentration, cyanide must have a higher concentration than any of the analytes. In our system the mobility of cyanide is  $78 \times 10^5 \text{ cm}^2/\text{Vs}$ . The mobility of borate can be estimated as about  $26 \times 10^5 \text{ cm}^2/\text{Vs}$  (27), and the mobility of SDS is  $24 \times 10^5 \text{ cm}^2/\text{Vs}$ . However the concentration of SDS is 10 times less than borate in the BGE. Submicellar SDS is used to improve the separation of proteins (3,17).

As a rule of thumb the injection volume is kept below 1% of the total capillary volume to avoid significant loss in efficiency. Up to 10% of the total capillary volume was used in our experiment.

The concentration of cyanide plays an important role in the ITP/CZE process. When 0.5 mM cyanide is in the second plug, broad peaks were observed in the electropherogram (Fig. 5.4a). When the concentration of cyanide was increased to 10 mM, such a concentration of cyanide in the system may effectively concentrate the labeled proteins during the ITP/CZE, the results are illustrated in Fig. 5.4b. Because originally cyanide is one of the reactants for the labeling reaction, I had to make sure the stacking effect here is due to cyanide as a leading ions L1. Chloride ions was chosen as a replacement for cyanide as L1, since the mobility of chloride ion is  $76 \text{ cm}^2/\text{Vs}$  at 25 °C, which is almost the same as for cyanide ion. For Fig. 5.4c 0.5 mM cyanide and 10 mM chloride were in the second plug. Stacking effects as in Fig.5.4b were observed. When the concentration of cyanide was further decreased to 0.01mM, the labeling efficiency was greatly decreased. The interesting result in Fig. 5.4a is the first a couple of peaks were much sharper than the later peaks. The low concentration

of cyanide may still have a very narrow mobility window to cover those proteins with higher mobilities (18).

Together with some fluorescent dyes, cyanide is used as nucleophile to label the amine group in amino acids or proteins. Our approach makes on-column labeling more attractive in a CE system. Biological samples with high concentrations of chloride (for example urine) is another good field of application.

This system can also be applied to the relatively larger on-column reaction zone. Fig. 5.5A illustrated the effects of an additional plug of cyanide introduced after the labeling of the protein. The cyanide concentration of the second plug was 1 mM. The mixing zone for labeling was around 10% of the capillary volume. After 8 minutes for the labeling reaction, another plug of the cyanide was hydrostatically injected into the capillary. The total concentration of cyanide was 2 mM in (a), 4 mM in (b) and 6 mM in (c). There were more effects on the proteins with higher mobilities than those with lower mobilities. The mobility window is reduced with decreasing the concentration of L1 cyanide. So proteins with higher mobilities were easily within the window while proteins with lower mobilities maybe only partially inside the window (Fig. 5.5B).

Although FQ is the labeling reagent, it seems not effect the ITP/CZE process (Fig. 5.6). High concentration of FQ in the capillary may react with cyanide and form fluorescent impurities that interfere in the analysis of very low concentration proteins.

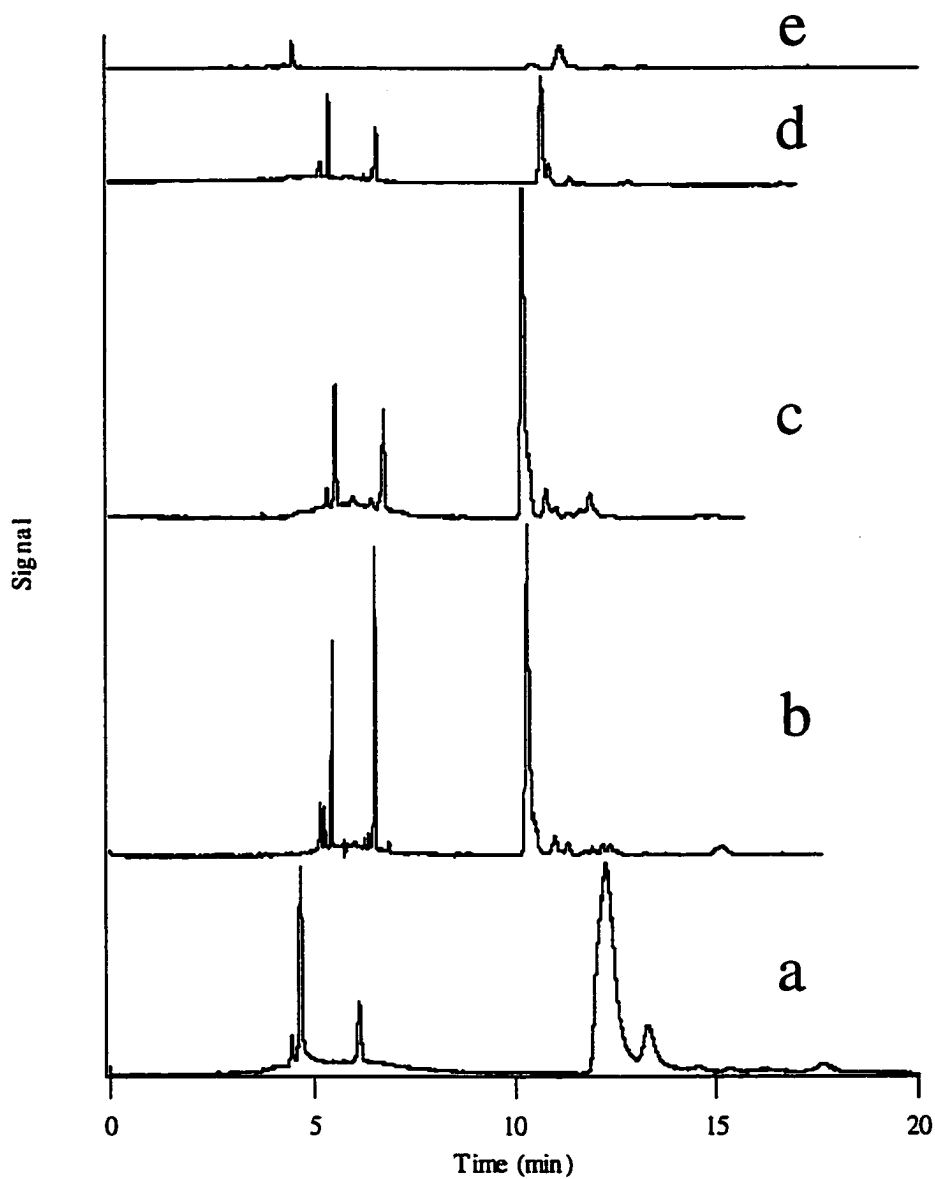


Fig. 5.4 Effects of ITP/CZE with the conditions of on-column reaction at 65°C for 5 minutes. [FQ]=2 mM. Separation buffer: 10 mM borate and 1 mM SDS.

a. [CN<sup>-</sup>] = 0.5 mM, b. [CN<sup>-</sup>] = 10 mM, c. [CN<sup>-</sup>] = 0.5 mM, [Cl<sup>-</sup>] = 10 mM, d. [CN<sup>-</sup>] = 0.1 mM, [Cl<sup>-</sup>] = 10 mM, e. [CN<sup>-</sup>] = 0.01 mM, [Cl<sup>-</sup>] = 10 mM.

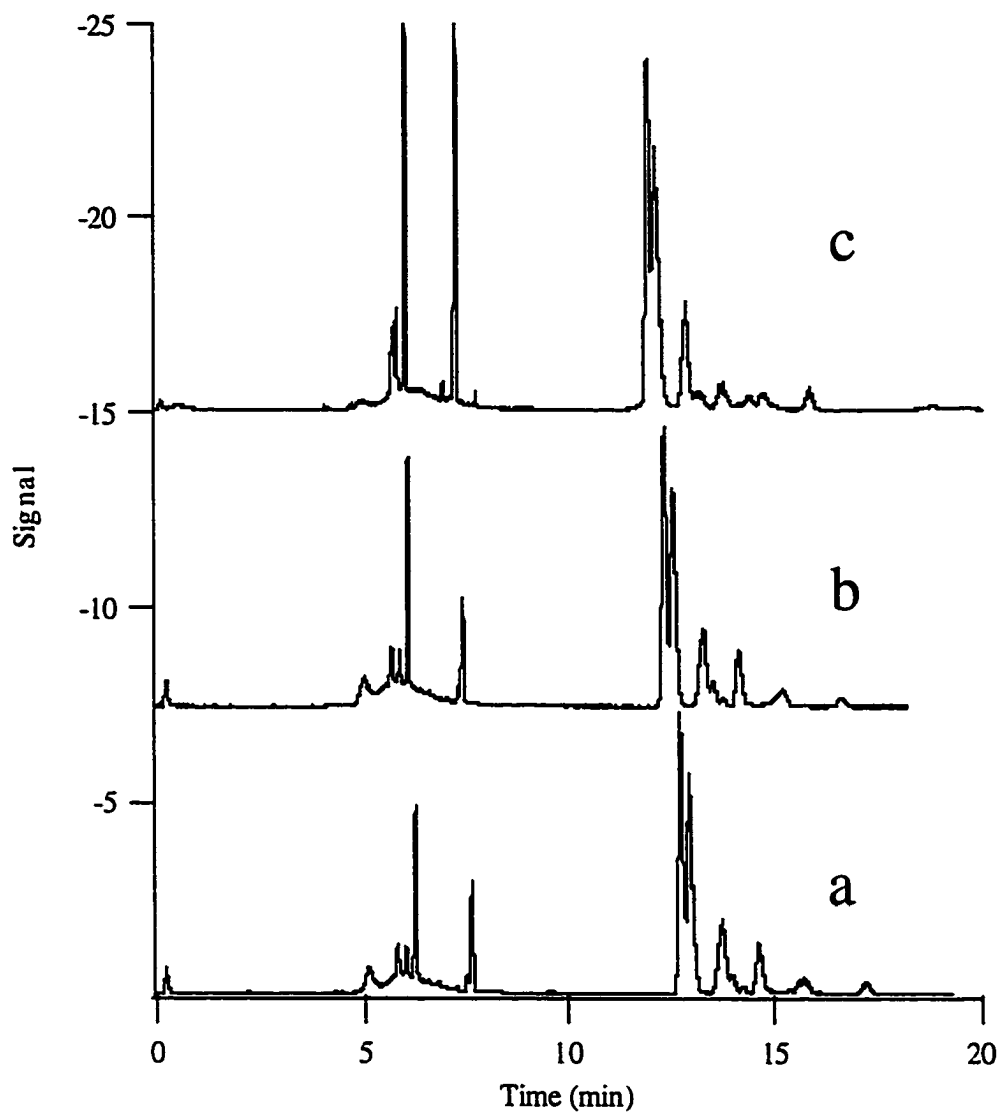


Fig. 5.5A Effects of introducing an additional plug of CN after labeling the proteins with 1 mM CN at 65°C.

a.  $[\text{CN}]_{\text{total}} = 2 \text{ mM}$ , b.  $[\text{CN}]_{\text{total}} = 4 \text{ mM}$ , c.  $[\text{CN}]_{\text{total}} = 6 \text{ mM}$ .

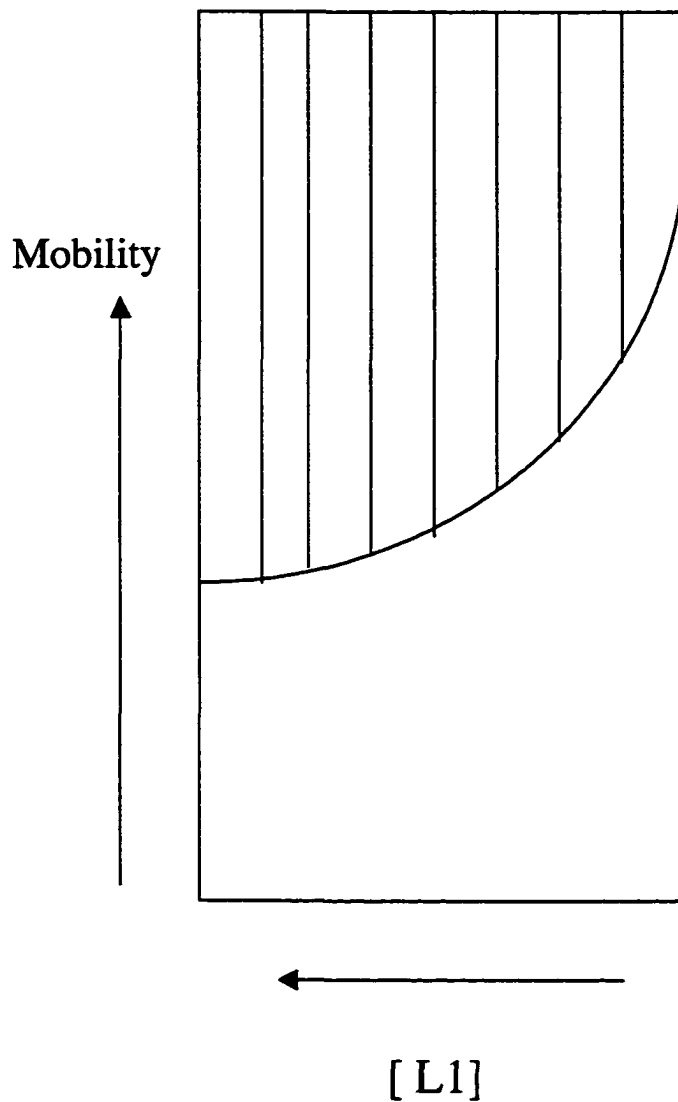


Fig. 5.5B Illustration of mobility window for ITP/CZE system. The window width is reduced if [L1] is decreased (18).

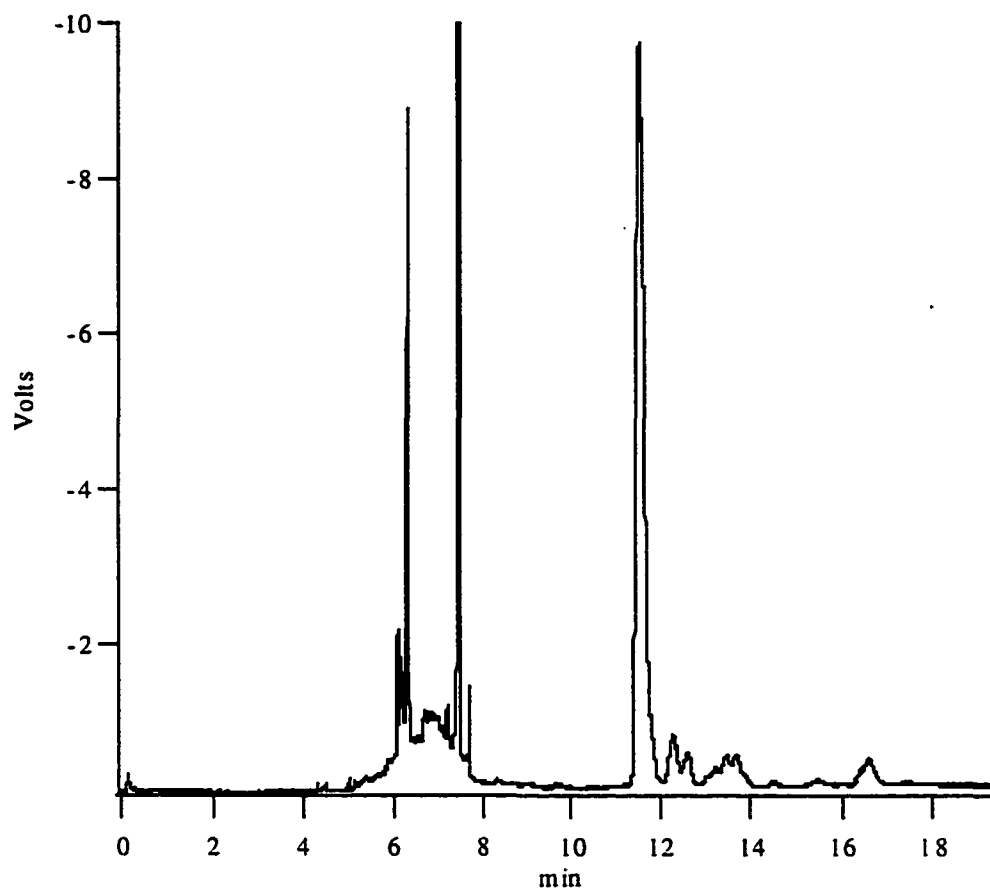


Fig. 5.6 Effect of FQ concentration on ITP/CZE. Same experimental condition as Fig. 4b except [FQ] = 20 mM.



The prerequisite for the existence of ITP in CZE is the presence of a component in the system that can play the role of either the leading or the terminating ion for the other species present in the system consisting of a sample and a BGE. To fulfill this, a component of adequate mobility has to be present in this system with its amount above a certain critical value in order to be effective, and the background ion has always to play the other role, i.e. of the terminator or of the leading ion (13). A similar system was also applied in fused silica capillary, as in Fig. 5.7.

## **5.5 Conclusions**

The anions with high mobilities which are existing for labeling (cyanide) or as an additive (chloride) in my on-column labeling system induced ITP concentration in the submicellar separation of proteins in human cancer cell extract. The described procedure combines labeling, ITP stacking and submicellar separation inside one capillary. The gain in sensitivity is given by effective focusing of the labeled proteins into sharp concentrated ITP zones. The use of ITP concentration would appear to be very promising especially when the sample is not dissolved in pure water or diluted buffer but also contains other ions which increase its conductivity. Labeled proteins from an on-column reaction is a good example of this.

Single capillary labeling-ITP-CZE is less complicated and is easy to automate. Moreover, no additional hardware modifications are necessary in most systems. This technique has great potential in real sample analysis.

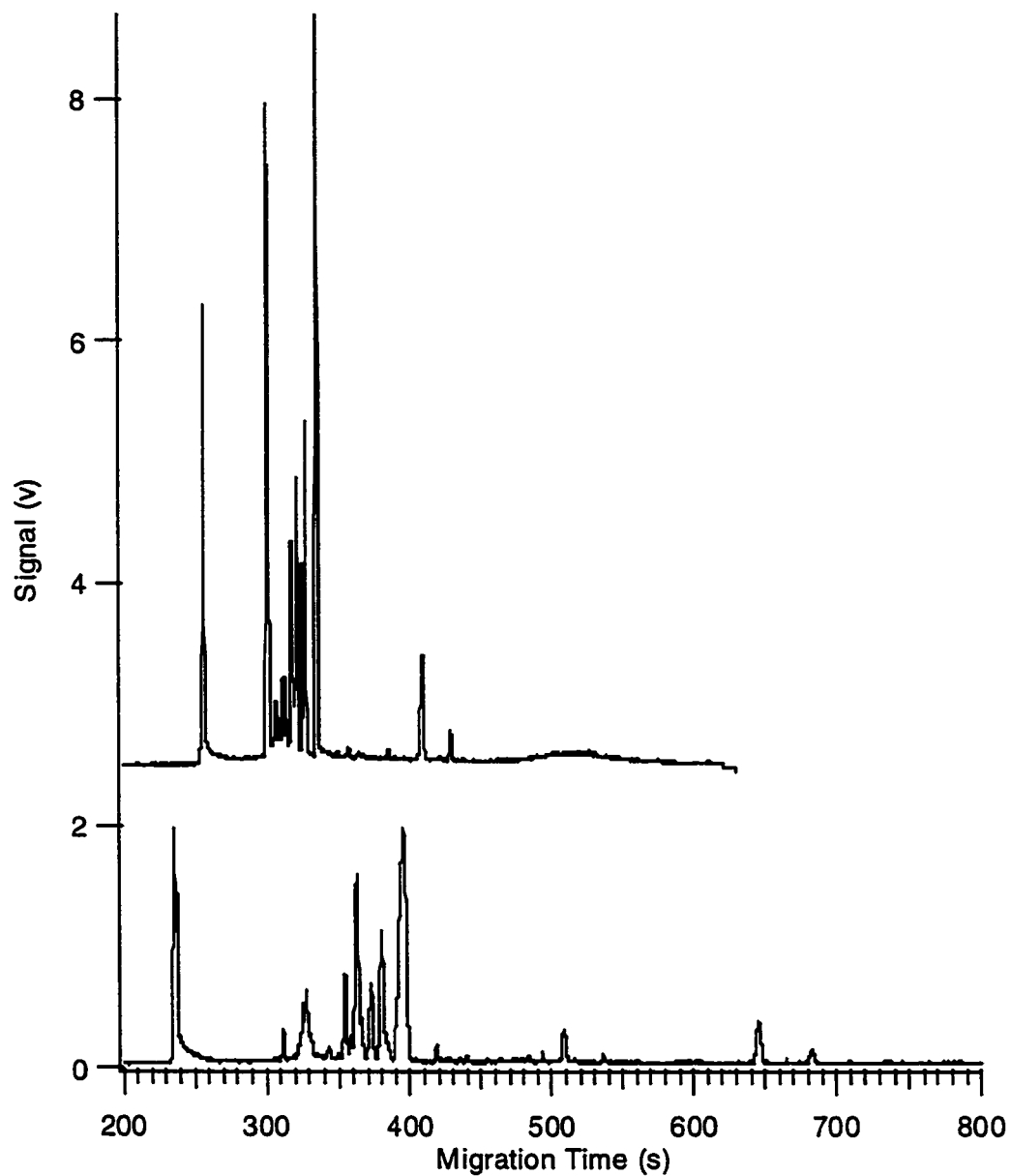


Fig. 5.7 CN<sup>-</sup> effect on fused-silica capillary. The separation buffer was 50 mM phosphate, 11 mM sodium pentasulfate (SPS), at pH 6.8.

a. [CN<sup>-</sup>] = 0.5 mM, b. [CN<sup>-</sup>] = 25 mM

## 5.6 Reference

1. Lee, T. T.; Yeung, E. S. *J. Chromatogr.* **1992**, 595, 319-325
2. Schultz, N. M.; Huang, L.; Kennedy, R. T. *Anal. Chem.* **1995**, 67, 924-929
3. Pinto, D. M.; Arriaga, E. A.; Craig, D.; Angelova, J.; Sharma, N.; Ahmadzadeh, H.; Dovichi, N. J.; Boulet, C. A. *Anal. Chem.* **1997**, 69, 3015
4. Bao, J.; Regnier, F. E. *J. Chromatogr.* **1992**, 608, 217
5. Chang, H.T.; Yueng, E. S. *Anal. Chem.* **1993**, 65, 2947
6. Cai, J.; El Rassi, Z. *J. Liq. Chromatogr.* **1992**, 15, 1179-92
7. Swartz, M. E.; Merion, M. *J. Chromatogr.* **1993**, 632, 209-13
8. Hjerten, S.; Lao, J. L.; Zhang, R. *J. Chromatogr.* **1994**, 676, 409-20
9. Lao, J. L.; Zhang, R.; Hjerten, S. *J. Chromatogr.* **1994**, 676: 421-30 C
10. Swartz, M. E.; Merion, M., *J. Chromatogr.* **1993**, 632, 209-213
11. Weinberger, R., *Practical Capillary Electrophoresis*. Academic Press, New York, **1993**, 238-240
12. Gebauer, P.; Thormann, W.; Bocek, P. *Electrophoresis* **1995**, 16, 2039-2050
13. Zhao, J. Y.; Waldron, K. C.;m
14. Craig, D. B.; Dovichi, N. J. *Anal. Chem.* **1998**, 70, 2493-2494
15. Beale, S. C.; Savage, J. C.; Wiesler, D.; Wiestock, S. M.; Novotny, M. *Anal. Chem.* **1988**, 60, 1765-1769
16. Lee, I. H.; Pinto, D.; Arriaga, E. A.; Zhang, Z; Dovichi, N. J. *Anal. Chem.* **1988**, 70, 4546
17. Beckers, J. *J. Chromatogr.* **1993**, 641, 363-373
18. Dolnik, V.; Cobb, K. A.; Novotny, M. *J. Microcol. Sep.* **1990**, 2, 127
19. Foret, F.; Szoko, E.; Karger, B. L. *Electrophoresis* **1993**, 14: 417-28

20. Vinther, A., Soeberg, H.; Nielsen, L.; Pedersen, J.; Biedermann, K. *Anal. Chem.* **1992**, *64*, 187-191
21. Foret, F.; Krivankova, L.; Bocek, P. *Capillary Zone Electrophoresis*, VCH, Weinheim, **1993**
22. Reinhoud, N. J.; Tjaden, U. R. van der Greef, J. *J. Chromatogr. A* **1994**, *673*, 239-253
23. Beckers, J.L.; Everaerts, F. M. *J. Chromatogr.* **1990**, *508*, 3
24. Gelfi, C.; Curcio, M.; Righetti, P. G.; Sebastiano, R.; Citterio, A.; Ahmadzadeh, H.; Dovichi, N. J. *Electrophoresis* **1998**, *19*, 1677
25. Chrambach, A.; Jovin, T. M.; Svendsen, P. J.; Rodbard, D. in: Catsimpoolas, N. (Ed.), *Methods of Protein Separation*, Plenum Press, New York **1979**, pp. 27-144
26. Wu, S.; Dovichi, N. J. *J. Chromatogr.* **1989**, *480*, 141-155

**Chapter 6: Separation of proteins by sodium dodecyl sulfate-capillary electrophoresis in hydroxypropylcellulose sieving matrix with laser-induced fluorescence detection**

## 6.1. Introduction

Sodium dodecyl sulfate - polyacrylamide gel electrophoresis (SDS-PAGE) has been used for the separation and molecular mass determination of proteins for over 30 years (1, 2). This method provides high resolution for protein separation, especially when combined with isoelectric focusing to analyze complex protein mixtures in two-dimensional (2-D) mode. Another advantage of this method lies in its feasibility for preparing and purifying proteins. This is important for biochemists to study the structure and function of proteins. Although SDS-PAGE is a dominant method for protein separation, it has some limitations. First, it is time-consuming to prepare the gel and perform the separation and detection. Second, the detection for SDS-PAGE is realized by staining in most cases. This detection mode lacks accurate quantitation and full automation, resulting in difficulty in handling and storing the data. Hence, developing a high-resolution capillary electrophoresis (CE) method for separation of SDS-proteins is of great interest since CE has advantages such as on-line detection, rapid separation and full automation. Hjerten first reported the use of polyacrylamide gel for capillary zone electrophoresis (CZE) separation of membrane proteins (3). Later, Cohen et al. reported a cross-linked polyacrylamide capillary gel electrophoresis method for separation of SDS-proteins (4). Recently, various polymer solutions have been employed as the replaceable sieving matrix for CE separation of proteins instead of cross-linked polyacrylamide. This approach simplifies the SDS-CE method since the polymer sieving solutions can easily be prepared and put into the capillary. The polymer solution is also replaceable after each run, which adds flexibility for SDS-CE method. For example, different injection modes, gels, and buffers can be applied. Linear polyacrylamide (LPA) is a commonly used polymer for this purpose (5, 6). Generally, polymer concentrations of 2%-8% are used. However,

LPA has significant UV absorbance, affecting the linear dynamic range and detection limit of UV detector (7). PEO is another important linear polymer for separation of SDS-proteins. This sieving matrix is UV-transparent, which is good for improving UV detection sensitivity. The molecular weight of PEO employed for separation of SDS-proteins is often around 100000 (7, 8, 10). Other reported sieving polymers include dextran and pullulan, which are both slightly branched. Dextran within a very broad molecular weight range from 1270 to 2000000 has been reported for separation of SDS-proteins (7, 9, 10), this polymer is also UV-transparent. In terms of UV detection sensitivity, pullulan is also superior to LPA since its UV absorbance, especially in the low UV wavelength range (below 230 nm), is much lower than LPA. The molecular size of pullulan used for separation of SDS-proteins is 50000-100000 (11, 12). From the existing publications, a polymer size around 100000 is reasonable for separation of SDS-proteins considering the separation performance and ease of preparation.

A UV-detector is often used for CE separation of SDS-proteins.

Unfortunately, this detector lacks detection sensitivity. Another problem involved is that some sieving polymers used for SDS-CE are UV-absorptive (13). Compared with UV detection, laser-induced fluorescence (LIF) offers high detection sensitivity and low background. So it is important to develop LIF detection methods for CE separation of SDS-proteins. To date, there have been only a few publications on developing LIF detection for SDS-CE (14-18).

In this work, a new SDS-CE method was developed for the separation of standard proteins and HT29 cancer cell proteins using hydroxypropylcellulose (HPC) as a replaceable matrix. The proteins were combined with SDS, labeled with FQ,

separated in HPC sieving matrix and then detected by sheath-flow LIF. This work indicates that HPC might be a useful sieving matrix for separation of SDS-proteins.

## **6.2 Experimental**

### **6.2.1 Apparatus**

The CE instrument with a sheath-flow cuvette and LIF detector was built in-house (19). The high voltage was provided by a 0-30kV dc power supply (CZE 1000, Spellman, Plainview, NY, USA). The excitation for the sheath flow cuvette detector was provided by an argon ion laser (Model 2211-15SL, Uniphase, San Jose, CA, USA) operated at 12 mW. The 488 nm laser line was focused ~30  $\mu$ m from the tip of the capillary by using a 6.3 $\times$  objective (Melles Griot, Nepean, ON, Canada). Fluorescence was filtered with a 630DF30 bandpass filter (Omega Optical, Brattleboro, VT, USA), collected with a 60 $\times$ , 0.7 NA microscope objective (MO 0060LWD, Universe Kokagu, Oyster Bay, NY, USA) and then detected with a photomultiplier tube (R1477, Hamamatsu, Middlesex, NJ, USA). Data sampling was accomplished by a 16-bit data acquisition board (NB-MIO16XH-18, National Instruments, Austin, TX, USA) connected to a Macintosh computer.

### **6.2.2 Reagents**

Acrylamide and ammonium persulfate (APS) were purchased from Life Technologies (Burlington, ON, Canada).  $\gamma$ -methacryloxy-propyltrimethoxysilane (MAPS) and *N, N, N', N'*-tetramethylethylenediamine (TEMED) were purchased from Bio-Rad (Richmond, CA, USA). SDS was obtained from BDH (Toronto, ON, Canada). Enzyme grade 4-(2-hydroxyethyl)-1-piperazineethanesulfonic acids



(HEPES) was obtained from Fisher Scientific (Fair Lawn, NJ, USA). HPC (MW=100000) was obtained from Aldrich (Milwaukee, WI, USA).

Tris, tricine, and standard proteins including  $\alpha$ -lactoalbumin (MW=14200), carbonic anhydrase (MW=29000), ovalbumin (MW=45000), bovine serum albumin (MW=66000) and phosphorylase b (MW=97400) were provided by Sigma (St. Louis, MO, USA). FQ and KCN were obtained from Molecular Probes (Eugene, OR, USA). Stock solution of 25 mM KCN was prepared with water. Stock solution of 100 mM FQ was prepared with methanol. 10- $\mu$ L FQ solution was placed into 500- $\mu$ L microcentrifuge tube and the solvent was vacuumed with a Speed Vac (Savant Instrument Inc., Farmingdale, NY, USA). The dried FQ aliquots (100 nmol) were stored at -20°C. These precautions were used to prevent FQ degradation in solutions.

### 6.2.3 Capillary coating

Capillaries were coated as described by Hjerten (20) and Karger and coworkers (21). In brief, fused-silica capillaries of 150- $\mu$ m OD and 50- $\mu$ m ID (Polymicro Technologies, Phoenix, AZ, USA) were flushed sequentially with 0.1 M sodium hydroxide, water and methanol. Then the capillary was filled with a 1:1 mixture of methanol and MAPS after it was purged with nitrogen gas for 30 min. This allowed the inner surface of the capillary to react with the methoxy and silanol groups to form the Si-O-Si-C bond at room temperature. The capillary was then filled with a degassed 4% acrylamide solution overnight containing 0.1% APS and 0.1% TEMED to form a linear polyacrylamide on the capillary wall. Next, the capillary was flushed with water to push excessive polyacrylamide (not attached) out of the capillary. Finally, the capillary was filled with 37% formaldehyde (pH 10) for cross-

linking the polyacrylamide. After 12 hrs, the capillary was flushed with water and both ends were dipped into water for storage.

#### **6.2.4 Sieving buffer**

HPC sieving buffer solution was prepared by dissolving appropriate polymers in the running buffer. Three running buffers, including Tris/tricine, HEPES/NaOH and tricine/NaOH, were used to prepare corresponding sieving buffer solutions. Before use, the polymer solution was degassed for 30 min and centrifuged at 8000 rpm for 5 min. A home-made pressurizing device was used to fill the polymer solution into the capillary. The polymer solution was preconditioned at the running voltage for 20 min before each run.

#### **6.2.5 Sample preparation**

##### *6.2.5.1 Model proteins*

To denature the protein, 5  $\mu\text{L}$  protein solution was mixed with 5  $\mu\text{L}$  5% SDS solution and then heated at 90 °C for 5 min. Thiols such as 2-mercaptoethanol or dithreitol were not included since these nucleophilic thiols may react with FQ and affect the protein labeling. Then 5  $\mu\text{L}$  of the denatured protein solution was derivatized by mixing with 5  $\mu\text{L}$  of 25 mM KCN solution in a 500- $\mu\text{L}$  microcentrifuge tube containing 100 nmol of previously dried FQ. The mixture was incubated for 5 min at 65 °C and then diluted with 40  $\mu\text{L}$  running buffer.

##### *6.2.5.2 Cell extract*

Roughly  $10^6$  HT29 human colon adenocarcinoma cells were washed five times with phosphate-buffered saline (PBS) and resuspended in 40  $\mu\text{L}$  water. Then

the cells were lysed by sonication and the suspension was centrifuged at 1000 rpm (600 g) for 10 min.

Typically, 5  $\mu\text{L}$  of the cell extract supernatant was mixed with 5  $\mu\text{L}$  of 5% SDS and heated at 90  $^{\circ}\text{C}$  for 5 min. Then 5  $\mu\text{L}$  of this solution was added into a 500- $\mu\text{L}$  microcentrifuge tube with 5  $\mu\text{L}$  of 25 mM KCN and 100 nmol of previously dried FQ. The derivatization reaction was then performed at 65 $^{\circ}\text{C}$  for 5 min and stopped by diluting the solution with 40  $\mu\text{L}$  running buffer.

### 6.3 Results and discussion

In CZE, pre-column fluorescent labeling is popularly used for small molecules such as amines or amino acids to improve their detection sensitivity, however there is a considerable limitation when it is used for proteins. In most cases, proteins possess a number of amine reactive groups. After labeling reaction, each protein might have a different number or arrangement of tags. This means that the reaction product will be heterogeneous, resulting in broad or multiple peaks under CZE. This group has reported that the use of submicellar concentrations of SDS in the separation buffer eliminates multiple labeling artifacts in FQ-labeled proteins (19, 22). Recently, I replaced SDS with sodium pentanesulfonate (SPS) as a buffer additive to collapse the multiple-labeling envelope to a single, sharp peak. By using this surfactant at a submicellar concentration, I have succeeded in generating a one-dimensional protein map for a single HT29 cancer cell (23).

In contrast to CZE mode, this multi-labeling problem might not be as serious in SDS-CE. Most proteins bind SDS at a constant mass ratio of 1.4g SDS/g protein. Since the protein has a large molecular weight, individual protein molecules will

combine with a large number of SDS molecules to become highly charged. This charge prevents further heterogeneity in the charge-to-size ratio of individual protein population caused by derivatization. In addition, SDS-CE is a size-based method for protein separation. Attaching labels to the large protein molecule should not dramatically change the size of the protein molecule and therefore its migration velocity (14, 17). Moreover, the separation medium used in SDS-CE always contains submicellar SDS, which is similar to that in SDS-PAGE. The submicellar SDS tends to make multiply labeled product peaks collapse, which improves the high-efficiency separation (19, 22). In this chapter, FQ is used to label SDS-proteins. FQ is a fluorogenic dye, so it can be in high excess without causing a high background signal. This property is very important when labeling proteins at low concentration (19). Since proteins combined with a number of SDS molecules, FQ labeling of the protein lysine moiety might be limited spatially. A large excess of FQ (100 nmol) and elevated temperatures (65 °C) were utilized to improve the reaction efficiency (22).

Cellulose is an important separation medium for separation of biopolymers. For instance, hydroxyethylcellulose (HEC) and hydroxypropylmethyl cellulose (HPMC) are important sieving matrixes for CGE separation of DNA (24). Cellulose derivatives such as cellulose acetate or nitrocellulose are often used in classic electrophoresis methods for separation of proteins (25, 26). Recently, different celluloses were also used as the additives in CZE for separation of proteins. For instance, methylcellulose was used to improve separation of proteins in cerebrospinal fluid (27). HEC, HPC and HPMC were used to improve separation of proteins in cereals (28, 29). HPMC was used to improve resolving histone subtypes (30, 31). In this work, HPC with a molecular weight of 100000 was tested as the sieving polymer for separation of SDS-proteins. The electropherogram for five standard proteins

obtained in Tris/tricine/HPC sieving buffer is presented in Fig. 6.1. These standard proteins have molecular weights from 14000 to 97000 and a calibration curve ( $r=0.9829$ ) is obtained between the molecular weight of these proteins and their peak migration times (Fig. 6.2). The average theoretical plate number for these five proteins is estimated to be 18000. Multiple labeling might have caused the low separation efficiency, although a similar low separation efficiency was reported earlier (14-17). Another possible reason is that some proteins consist of several glycoforms, which may co-migrate and result in low efficiency. The detection limits ( $S/N=3$ ) for these standard proteins are 30 nM for lactoalbumin, 7 nM for carbonic anhydrase, 8 nM for ovalbumin, 4 nM for BSA, and 5 nM for phosphorylase. These data indicate that this method provides better sensitivity than SDS-CE-UV methods (7, 11).

The new SDS-CE method described above was used to separate the proteins in HT29 cell extract. The cells were lysed by sonication, and SDS solution was added to denature the proteins. Finally, the denatured protein sample was mixed with FQ and KCN for fluorescent labeling. Fig. 6.3A shows a typical separation pattern for HT29 cell protein extract obtained in Tris/tricine buffer with sieving polymer HPC. Comparing with the results obtained for standard proteins (Fig. 6.1), it can be seen that some cancer cell proteins are over 100,000 Dalton in size. This is expected since some cell proteins found in membrane or cell cytoskeleton are large, and some proteins may form dimers, trimers, or even tetramers. The results obtained here are similar to that obtained using PEO as the sieving matrix (7). Fig. 6.3B presents the same electropherogram as Fig. 6.3A but with a different scale for fluorescence signal. Clearly, a typical run allows between 25 to 30 peaks to be separated in 20 min, which

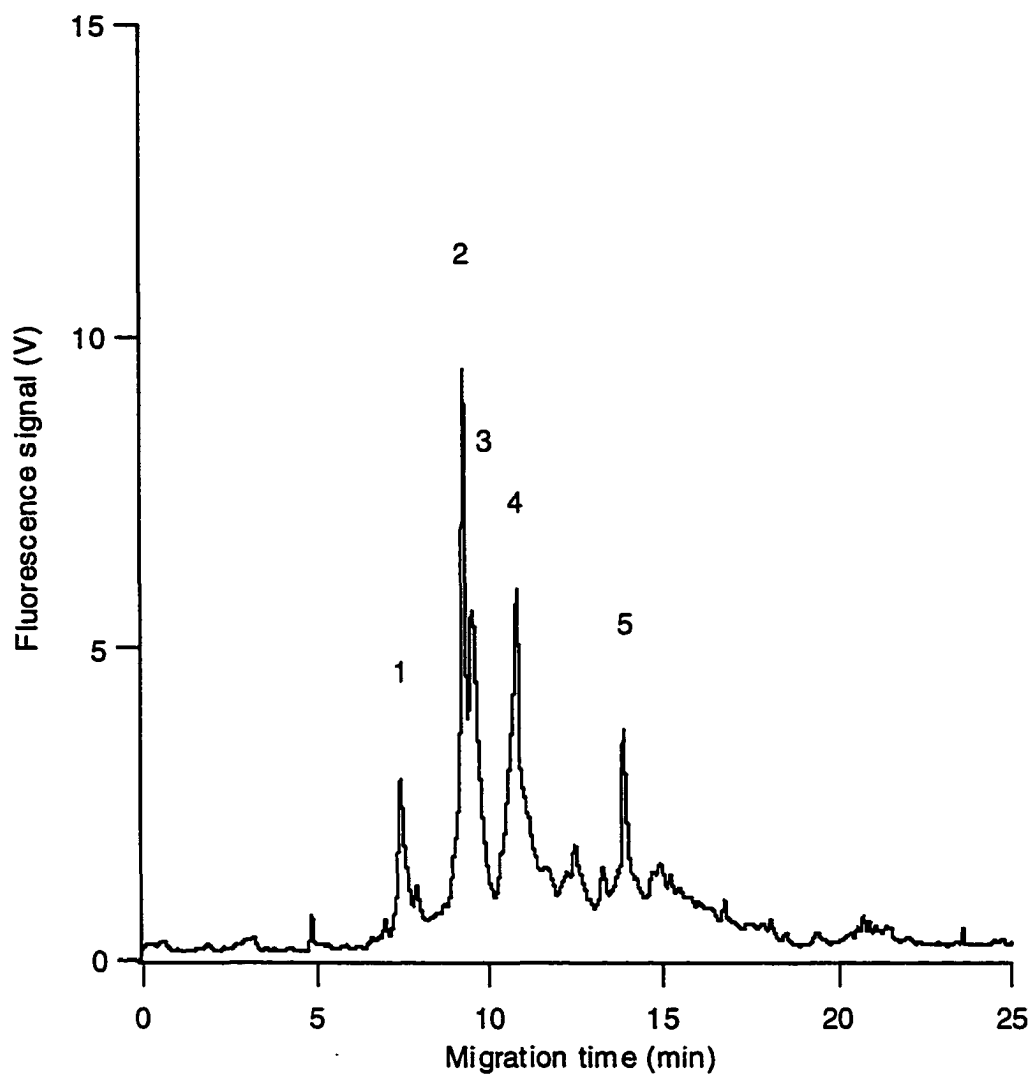


Figure 6.1. Electropherogram of standard proteins using 2% HPC sieving polymer and LIF detection. Conditions: capillary length, 20 cm; running voltage, -300 V/cm; injection, -300 V/cm for 5 s; running buffer, 20 mM Tris-20 mM tricine with 0.1% SDS (pH 8.0); polymer, 2% HPC. Protein peaks: 1,  $\alpha$ -lactoalbumin ( $1.2 \times 10^{-6}$  M); 2, carbonic anhydrase ( $1.0 \times 10^{-6}$  M); 3, ovalbumin ( $5.5 \times 10^{-7}$  M); 4, BSA ( $3.1 \times 10^{-7}$  M); 5, phosphorylase ( $2.1 \times 10^{-7}$  M).

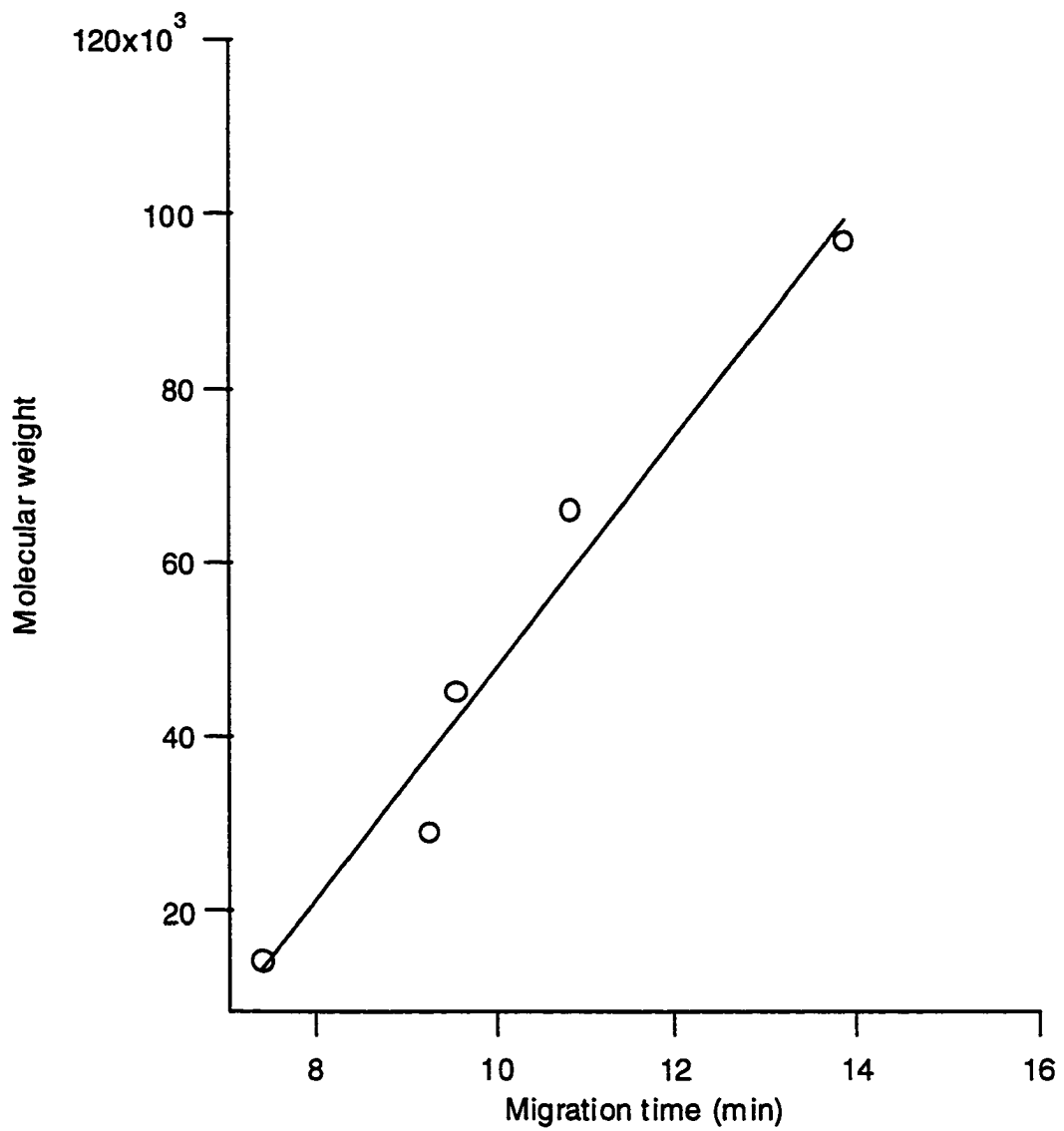


Figure 6.2 Plot of molecular weight vs. migration time of five standard proteins.

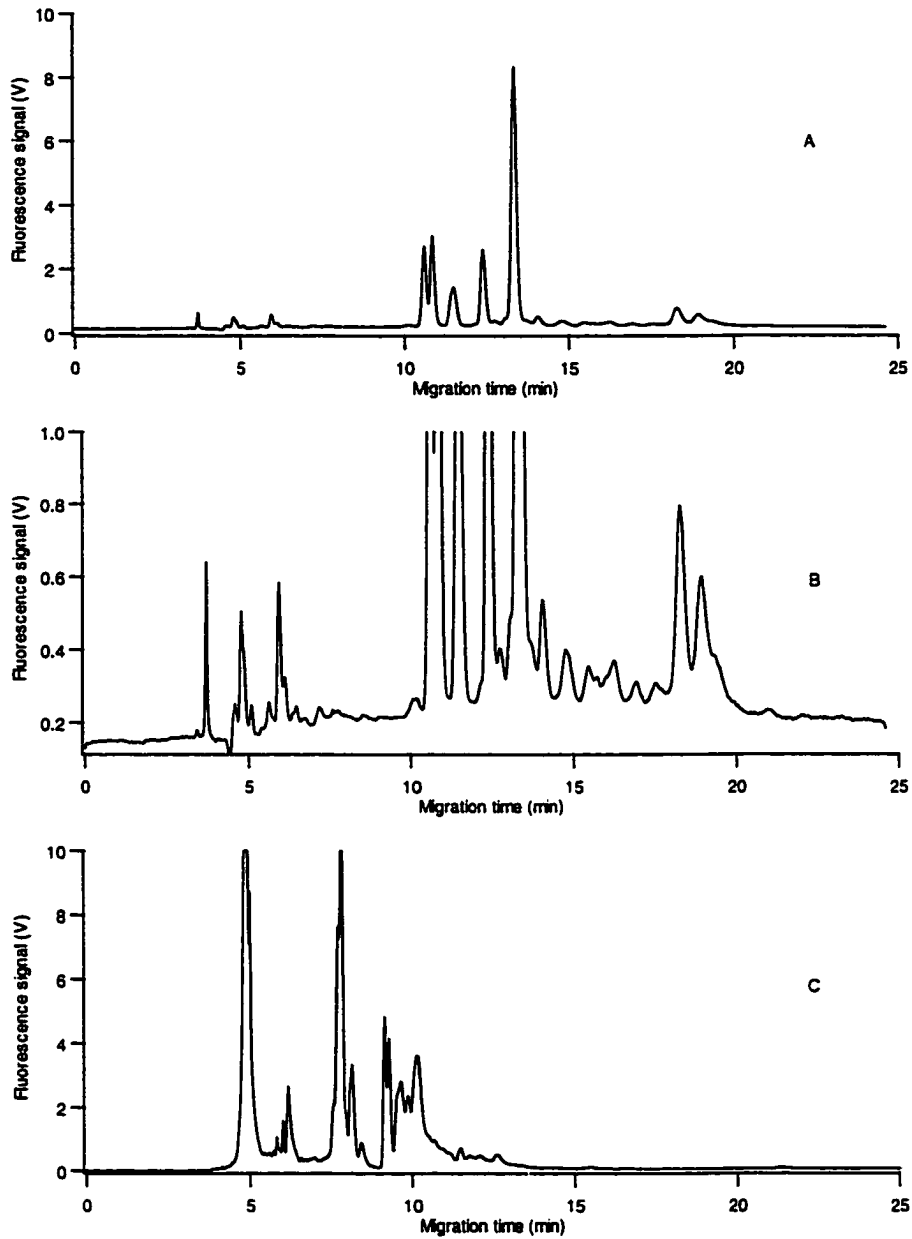


Figure 6.3 Separation of proteins from HT29 cell extract in 20 mM Tris-20 mM tricine-0.1% SDS buffer (pH 8.0) (A) with 2% HPC, (B) with 2% HPC, expanded scale of (A), (C) with no HPC. Other conditions as in Fig. 1.



demonstrate the potential of this method to rapidly analyze complex protein samples. The electropherogram for HT29 cell extract proteins obtained in the same Tris/tricine buffer but without HPC is also shown in Fig. 6.3C. Before separation, the protein extract was mixed with SDS and labeled with FQ. Due to SDS combination, the proteins contained a large number of negative charges. This allowed them to migrate from the injection end to the detection end under the negative high voltage (free solution CE mode). However, it can be seen that the pattern for the cell extract proteins in this case is very different from that obtained in Tris/tricine buffer containing HPC. The SDS-protein complexes migrated very fast under free solution CE mode since they didn't encounter any resistance from the HPC polymer. The separation window under this condition (Fig 6.3C) is only about half of that when HPC is added to the running buffer (Fig. 6.3A). Further, lack of resistance from HPC caused the sample volume injected into the capillary to be more than that when HPC contained in the running buffer.

The effect of buffer composition on the separation of cell extract proteins was also examined. Two other running buffers, 25 mM HEPES/NaOH (pH 8.0) or 40 mM tricine/NaOH (pH 8.0), were used in sieving buffers with the same concentrations of HPC and SDS. Corresponding electropherograms for HT29 cell extract proteins

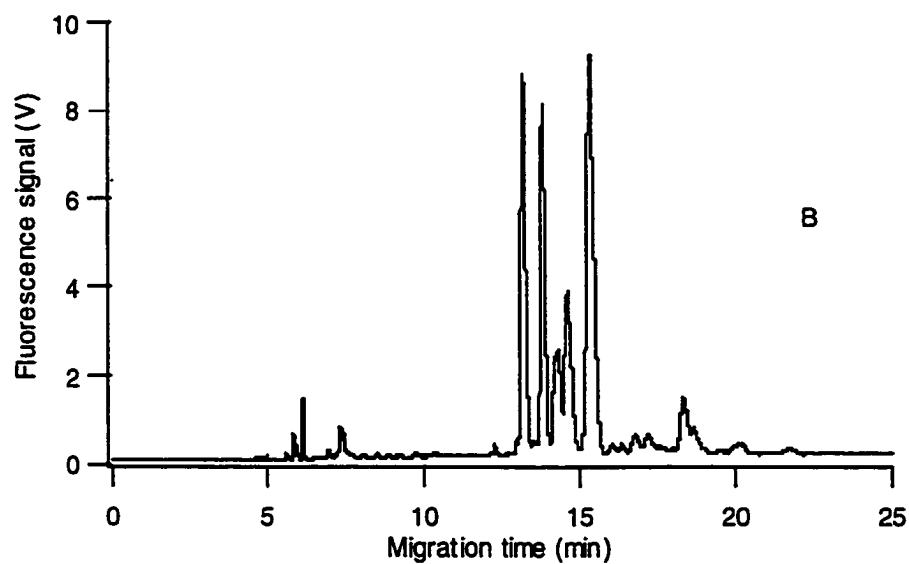
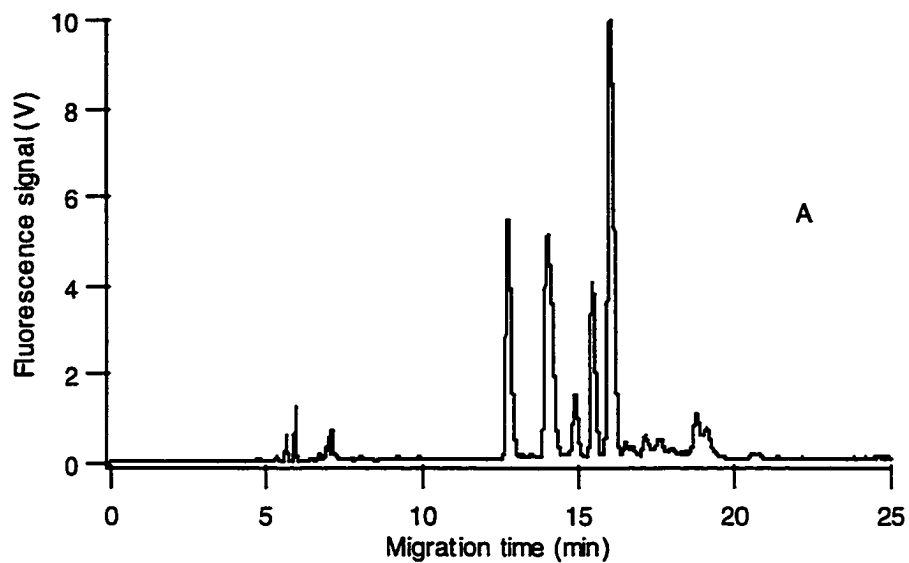


Figure 6.4 Effect of buffer composition on the separation of proteins from HT29 cell extract. Polymer: 2% HPC; Buffer: (A) 25 mM HEPES with 0.1% SDS (pH 8.0); (B) 40 mM tricine with 0.1% SDS (pH 8.0). Other conditions as in Fig. 1.

obtained in these two sieving buffers are shown in Fig. 6.4A and Fig. 6.4B. Compared with the electropherogram shown in Fig. 6.3A obtained in Tris/tricine/HPC sieving buffer, we can see that all three sieving buffers present very similar patterns for cell extract proteins. This is reasonable since all three sieving buffers contain the same polymer HPC. Clearly, sieving polymer plays a critical role in protein separation regardless of which running buffer is used. However, it was observed that Tris/tricine/HPC sieving buffer provided a more stable current in the capillary than HEPES/NaOH/HPC or tricine/NaOH/HPC. Hence, practically, Tris/tricine is a better buffer system for SDS-CE-HPC method.

#### **6.4 Conclusion**

This is the first study of using SDS-CE-LIF with HPC sieving matrix for separation of proteins. This method provides better sensitivity than SDS-CE-UV. Moreover, its analysis speed is fast with separation under 20 min. This method was applied to analysis of proteins from HT29 cancer cells. Nearly 30 peaks are observed for a typical protein extract in a 20-min separation, indicating that this method is promising for separation of complex protein samples.

## 6.5 References

1. Shapiro, A.; Vinuela, E.; Maizel, J. *J. Biochem. Biophys. Res. Commun.* **1967**, 28, 815.
2. Weber, K; Osborn, M *J. Biol. Chem.* **1969**, 244, 4406.
3. Hjerten, S; *J. Chromatogr.* **1983**, 270, 1.
4. Cohen, A. S.; Karger, B. L. *J. Chromatogr.* **1987**, 397, 406.
5. Widhalm, A.; Schwer, C.; Blaas, D.; Kenndler, E. *J. Chromatogr.* **1991**, 549, 446.
6. Manabe, T.; Oota, H.; Mukai, J. *Electrophoresis* **1998**, 19, 2308.
7. Ganzler, K.; Greve, K. S.; Cohen, A. S.; Karger, B. L.; Guttman, A.; Cooke, N. *Anal. Chem.* **1992**, 64, 2665.
8. Benedek, K.; Guttman, A. *J. Chromatogr.* **1994**, 680, 375.
9. Karim, M. R.; Janson, J.; Takagi, T. *Electrophoresis* **1994**, 15, 1531.
10. Guttman, A. ; Horvath, J.; Cooke, N. *Anal. Chem.* **1993**, 65, 199.
11. Nakatani, M.; Shibukawa, A.; Nakagawa, T. *J. Chromatogr.* **1994**, 672, 213.
12. Nakatani, M.; Shibukawa, A.; Nakagawa, T. *Electrophoresis* **1996**, 17, 1210.
13. Takagi, T. *Electrophoresis* **1997**, 18, 2239.
14. Gump, E. L.; Monnig, C. A. *J. Chromatogr.* **1995**, 715, 167
15. Wise, E. T.; Singh, N.; Hogan, B. L. *J. Chromatogr.* **1996**, 746, 109
16. Harvey, M. D.; Bandilla, D.; Banks, P. R. *Electrophoresis* **1998**, 19, 2169.
17. Craig, D. B.; Polakowski, R. M.; Arriaga, E.; Wong, J. C.Y.; Ahmadzadeh, H.; Stathakis, C.; Dovichi, N. J. *Electrophoresis* **1998**, 19, 2175.
18. Hunt, G.; Nashabeh, W. *Anal. Chem.* **1999**, 71, 2390.
19. Pinto, D. M.; Arriaga, E. A.; Craig, D. B.; Angelova, J.; Sharma, N.; Ahmadzadeh, H.; Dovichi, N. J. *Anal. Chem.* **1997**, 69, 3015

20. Hjerten, S. *J. Chromatogr.* **1985**, 347, 191
21. Schmalzing, D.; Piggee, C. A.; Foret, F.; Carrilho, E.; Karger, B. L. *J. Chromatogr.* **1993**, 652, 149.
22. Lee, I. H.; Pinto, D. M.; Arriaga, E. A.; Zhang, Z.; Dovichi, N. J. *Anal. Chem.* **1998**, 70, 4546.
23. Zhang, Z.; Krylov, S.; Arriaga, E. A.; Polakowski, R.; Dovichi, N. J. *Anal. Chem.* **2000**, 72, 318.
24. Dovichi, N. J. *Electrophoresis* **1997**, 18, 2393.
25. Pristoupil, T. I. *Chromatogr. Rev.* **1970**, 12, 109.
26. Chan, H. P. *Cellulose Acetate Electrophoresis*, Ann Arbor, London, **1979**, p.19.
27. Cowdrey, G.; Firth, M.; Firth, G. *Electrophoresis* **1995**, 16, 1922.
28. Righetti, P. G.; Bossi, A.; Olivieri, E.; Gelfi, C. *J. Biochem. Biophys. Methods* **1999**, 40, 1.
29. Bean, S. R.; Lookhart, G. L. *Electrophoresis* **1998**, 19, 3190.
30. Lindner, H.; Helliger, W.; Sarg, B.; Meraner, C. *Electrophoresis* **1995**, 16, 604.
31. Kratzmeier, M.; Albig, W.; Meergans, T.; Doenecke, D. *Biochem. J.* **1999**, 337, 319.

## **Chapter 7: Conclusions and future work**

## 7.1 Conclusions

Analysis of biomolecules from a single cell requires ever increasing sophistication in analytical techniques. Because of the ultra-small quantities, the role of high sensitivity analysis of biomolecules has become increasingly important in biology, medical research, and the biotechnology and pharmaceutical industries. Development and application of micro-scale analytical techniques such as capillary electrophoresis, laser induced fluorescence detection, and crude cell extract and single cell handling and labeling approaches were presented in this thesis in an effort to address a few of the challenging goals of single cell research.

CE is a powerful separation technique well suited to the determination of minute quantities of biomolecules. The versatility of CE is greatly enhanced due to the availability of different separation modes. A description of CE modes and other aspects which related this thesis were presented in Chapter 1.

The method presented in Chapter 2 correlated cell cycle with oligosaccharide metabolic activity in single cells. In this chapter, the combination of metabolic cytometry with image cytometry to correlate oligosaccharide metabolic activity with cell cycle was described. This technique is used to measure DNA ploidy, the uptake of a fluorescent disaccharide, and the amount of metabolic products in a single cell. The cells in the G1 phase did not show any biosynthetic activity in respect to the substrate. Several groups of cells with unique biosynthetic patterns were distinguished within G2/M cells.

This is the first report that combined metabolic- and image-cytometry to correlate production of metabolic products with cell cycle. A complete enzymatic cascade is monitored on a cell-by-cell basis and correlated with cell cycle.

Chapter 3 presents the first one-dimensional protein electropherograms generated from a single somatic cell. This chemical cytometry method reveals the distribution in protein expression between cells, which is hidden by classic protein analysis performed on cell extracts. Cell labeling and handling techniques and instrumentation for single cell analysis are also discussed.

In this chapter, a single HT29 human colon adenocarcinoma cell was introduced into a fused-silica capillary, lysed, and the protein content was fluorescently labeled with the fluorogenic reagent 3-(2-furoyl)quinoline-2-carboxaldehyde. The labeled proteins were separated by capillary electrophoresis in a sub-micellar buffer and detected by laser-induced fluorescence in a post-column sheath-flow cuvette. Several dozen components were resolved. A number of experiments were done to verify that these components were proteins. Most components of the single-cell electropherogram had the same mobility as components present in the 30 kDa to 100 kDa fraction of a protein extract prepared from the cell culture. One component was identified as a ~100 kDa protein by co-injecting the sample with purified protein obtained from a SDS-PAGE gel. Protein expression varied significantly between cells, but the average expression was consistent with that observed from a protein extract prepared from  $10^6$  cells.

A highly sensitive and rapid method for the identification of microorganisms is presented in Chapter 4. It is based on on-capillary electrophoretic concentration and



labeling. The response for selected protein fractions was enhanced through manipulation of sample stacking conditions.

The chapter 5 presents isotachophoretic stacking of proteins, which is induced by using excess labeling reagent as the leading electrolyte. The method combines protein labeling, ITP stacking and submicellar separation in one capillary. The gain in sensitivity is given by effective focusing of labeled proteins into sharp and concentrated ITP zones.

Chapter 4 and 5 introduce the new methods to preconcentrate proteins before and after labeling in a single capillary.

In chapter 6, sodium dodecyl sulfate-capillary electrophoresis (SDS-CE) by using hydroxypropylcellulose (HPC) as the sieving matrix was developed for separation of proteins. Five standard proteins within the molecular weight range of 14000 – 97000 were used to test this method and a calibration curve was obtained between the molecular weight of these proteins and their peak migration times. This method was also applied to the separation of proteins from HT29 human colon adenocarcinoma cell extracts, and, typically, nearly 30 protein components could be resolved in a 20-min separation. Similar separation patterns were observed for the cell extract proteins when three running buffer systems were employed, indicating that buffer composition did not have much influence on the separation based on HPC sieving.

## **7.2 Future work**

Single-cell technique has one disadvantage compared with flow cytometry: analysis of a large amount of cells will be difficult. An automated cell injection will be necessary to perform single-cell analysis in medical applications.

The microscope stage may be equipped with stepper-motor driven micrometers. These micrometers will be controlled with a joystick, so that the operator can scan the image field in precise increments. A computer will record the position of the cell. Once a set of cells has been chosen for analysis, an injection/electrophoresis program will be activated. This program will drive the micrometer so that each cell is moved, in succession, to the center of the field-of-view of the microscope. Each cell that matches the criteria will be injected into the separation capillary. Then the capillary will be moved to a set of buffer reservoirs. Once the separation is complete, the next cell will be moved to the microscope's field-of view. The procedure will be repeated for all of the cells that were specified by the operator.

The automated 2-D format CE system will be extremely important for proteome analysis. Capillary isoelectric focusing will be used as the first dimension of the separation. A single cell will be injected into this capillary and lysed with the nonionic surfactant. Fractions will be fluorescently labeled and separated in a second separation step using capillary SDS-gel electrophoresis.

The technique in this thesis is limited by low throughput; about 15-20 min are required to analyze each cell in 1-D format. The throughput of the instrument can be

improved by simultaneously analyzing 96 cells, each in a separate electrophoresis capillary. The technology will rely on a micromachined cell-capture chip, 96 two-dimensional capillary electrophoresis systems, a micromachined flow manifold, and a 96-capillary laser-induced fluorescence detector. This system will be able to generate 2-D electropherograms from 600 cells/day in a fully automated system. The large number of cells will provide outstanding statistical precision to characterize the tumor and to identify rare but dangerous cells.